8-2011

# The Role of the Androgen Receptor Cofactor p44/WDR77 in Astrocyte Activation

Bryce H. Vincent

**The Role of the Androgen Receptor Cofactor p44/WDR77 in Astrocyte Activation.**

**By**

**Bryce Havird Vincent, B.S.**

APPROVED:

_____
Zhengxin Wang, Ph.D.

Supervisory Professor

_____
Gary E. Gallick, Ph.D.

_____
Douglas Boyd, Ph.D.

_____
Joseph L. Alcorn, Ph.D.

_____
David McConkey, Ph.D.

APPROVED:

_____
Dean, The University of Texas
Graduate School of Biomedical Sciences at Houston

# The Role of the Androgen Receptor Cofactor p44/WDR77 in Astrocyte Activation.

**A**

**DISSERTATION**

Presented to the Faculty of

The University of Texas

Health Science Center at Houston

and

The University of Texas

M.D. Anderson Cancer Center

Graduate School of Biomedical Sciences

In Partial Fulfillment

of the Requirements

for the Degree of

**DOCTOR OF PHILOSOPHY**

by

Bryce Havird Vincent, B.S.

Houston, Texas

August, 2011

## DEDICATION

I would like to dedicate this dissertation

to my parents, Bruce Vincent and Pamela Vincent,

who have been very supportive,

and

my grandparents, LA Benson and Lola Benson,

who have been a great inspiration.

## ACKNOWLEDGEMENTS

I express immense gratitude to my mentor, Dr. Zhengxin Wang, for his support throughout my Ph.D. training. His guidance has helped me become a better scientist. I would also like to thank the Smith Research Foundation for their funding during my training at MD Anderson Cancer Center. I am extremely thankful for the members of my supervisory committees, Drs. Sue-Hwa Lin, Douglas Boyd, Joseph L. Alcorn, and David McConkey, for taking time from their busy schedules to support my scientific development. I also thank the past and present members of the Wang lab, including Shen Gao and Jun Chu, for their support.

**The Role of the Androgen Receptor Cofactor p44/WDR77 in Astrocyte Activation.**

**Publication No._____**

**Bryce Havird Vincent, B.S.**

**Supervisory Professor: Zhengxin Wang, Ph.D.**

Astrogliosis is induced by neuronal damage and is also a pathological feature of the major aging-related neurodegenerative disorders. The mechanisms that control the cascade of astrogliosis have not been well established. In a previous study, we identified a novel androgen receptor (AR)-interacting protein (p44/WDR77) and found that it plays a critical role in the control of proliferation and differentiation of prostate epithelial cells. In the present study, we found that deletion of the p44 gene in the mouse brain caused accelerated aging with dramatic astrogliosis. The p44/WDR77 is expressed in astrocytes and loss of p44/WDR77 expression in astrocytes leads to astrogliosis. Our results reveal a novel role of p44/WDR77 in astrocytes, which may explain the well-documented role of androgens in suppression of astrogliosis.

While many of detailed mechanisms of astrocyte activation remain to be elucidated, a number pathways have been implicated in astrocyte activation including $p21^{Cip1}$ and the NF-κB pathway. Astrocytic activation induced by p44/WDR77 gene deletion was associated with a significant increase of $p21^{Cip1}$ expression and NF-κB activation characterized by p65 nuclear localization. We found that down-regulation of $p21^{Cip1}$ expression inhibited astrocyte activation induced by the p44/WDR77 deletion and was accompanied by a decreased p65 nuclear localization. While $p21^{Cip1}$ role in

astrocyte activation and NF-κB activation is not well understood, studies of other cell cycle regulators have implicated cell cycle control systems as modulators of astrocyte activation, thus $p21^{Cip1}$ could induce secondary effect to induce p65 nuclear localization. However, p65 knockdown completely relieved the inhibition of astrocyte growth induced by the p44/WDR77 deletion, while $p21^{Cip1}$ knockdown only partially recovered this inhibition. Thus, NF-κB activity performs additional regulatory actions not mediated by $p21^{Cip1}$. These analyses imply that p4/WDR77 suppresses astrocyte activation through modulating $p21^{Cip1}$ expression and NF-κB activation.

## Table of Contents

## List of Figures

**Chapter I: Introduction**



**Chapter III: Preliminary Data**



**Chapter V: Aim 1: To identity Brain derived cells expressing p44/WDR77 and Aim 2: To assess effects of p44/WDR77 on Astrocyte activation**

**Chapter VI: Aim 3: To examine the role of p21$^{Cip1}$ in astrocyte activation induced by the loss of p44/WDR77**

**Chapter VII: Aim 4: To examine the role of NF- κB activation in astrocyte activation induced by the loss of p44/WDR77**

**Chapter VIII: Summary and Future Direction**

# List of Tables

## Chapter II: Materials and Methods

# Chapter I: Introduction

**A. Central nervous system (CNS):**

The nervous system is an organ system that exemplifies a masterpiece of biologic function from its molecular and cellular elements to its behavioral and cognitive elements. The extraordinary nervous tissue that innervates the human body was initially described and examined by the ancient Egyptians, Greeks, and Romans (1). However, it was not until the mid-twentieth century, with the advent of electron microscopy, that neuroscientists began to perceive the nervous system as a uniform tissue, flowing continuously together but composed of cellular units (2). Histological research by Italian neuropathologist Camillo Golgi, Spanish neuroanatomist Santiago Ramony Cajal and a cohort of others led to a categorization of a nervous system divided into two broad groups of cells, neurons and neuroglia. These groups of cells forge a neural network that transduces electrophysiological and molecular processes sent throughout the body (2, 3). The innervations and processes of these networks constitute one of three major functional areas: sensory, motor, and associational. The sensory networks incorporate information from both the environment (external) and the body itself (internal). Upon this incorporation the sensory networks then transmit this information on for higher level processing. The motor networks act to direct temporal and spatial muscular contractions, thereby coordinating the grace of movement. Finally the associational networks integrate the processes of the other networks to generate cognitive action. In this way the associational network modes act as hubs for complex cognitive processes forming the foundations for emotions, cognition, and other complex brain functions (3). From an anatomical point of view, neuroscientists have divided the human nervous system into two large systems, peripheral and central. The peripheral nervous system (PNS) arises from sensory and motor ganglia integrated with the motor and sensory neurons. Innervations spread from these ganglia throughout the body. The central

nervous system (CNS), then, is subdivided into two large complex components, the brain and spinal cord (3).

**AI. Structural Subdivision of the CNS:**

The CNS is the neural architecture which incorporates environmental signals- both internal and external perceived by innervating sensory neurons and with a dynamic and unique response. This diverse and dynamic system arises from four principal parts: the spinal cord, hindbrain, midbrain, and forebrain. Amidst the subdivisions of the brain flow four fluid-filled cerebral ventricles, a pair of lateral ventricles and, in the midline, the third and fourth ventricle. The pons, cerebellum and medulla together create the hindbrain or rhombencephalon. The hindbrain with the midbrain or mesencephalon (or midbrain) forge from the tectum, and tegmentum, form the brainstem which joins and is structurally continuous with the spinal cord. The diencephalons with the cerebral hemispheres collectively give rise to the forebrain (4). Together all four of these parts cooperate and coordinate to create a diverse and dynamic system of informational input and processing.

**AI (i). Brainstem:**

The brainstem transduces information to and from the forebrain for a multitude of primary sensory and motor pathways essential to human health and disease. The corticospinal tract is a bundle of primarily motor axons that travels along the brainstem. This tract transducing through medial lemniscus of the brainstem the posterior column-medial lemniscus pathway facilitates vibration sensation and fine touch. Adjacent to these pathways the spinothalamic tract transmits signals stimulated by crude touch, pain, and temperature. From the surface of the brainstem emerge ten of the twelve cranial nerves in humans providing the primary sensory and motor innervation to the

face and neck. Additionally the brainstem is home to an array of nuclei critical to a myriad of vital functions including control of cardiac output, respiration, circadian rhythm and level of consciousness (5-7). Finally and perhaps the most striking structure of the brainstem is the cerebellum, described early by Aristotle and the anatomist Galen (1). While its role has not been completely elucidated, the cerebellum has been implicated in a number of cognitive and emotional functions, such as language and fear regulation (6). However, what has been firmly established is the cerebellum's ability to integrate sensory input with fine motor activity to facilitate graceful coordination, in order to enhance the learning of motor tasks (7). These pathways and structures help facilitate bidirectional communication between the brain and periphery (3).

**AI (ii). Diencephalon:**

The forebrain is comprised of five subdivisions: the subthalamus, hypothalamus, thalamus and epithalamus which together form the diencephalon and the telencephalon or cerebrum (4). While the subthalamus is believed to have functional interconnections with the basal ganglia with implication in mediating skeletal muscle movement, its overall function still remains to be elucidated (8, 9). The epithalamus acts as a conduit between the limbic system and other areas of the neural cortex (10). Located between the cerebral cortex and midbrain in humans the thalamus relays gustatory, auditory, visceral, somatic, and visual systems sensory information to the telencephalon. The thalamus has a multitude of other functional implications including relaying motor signals and modulating circadian function (11, 12). The hypothalamus creates a dynamic interplay between the nervous system and endocrine system that provides regulatory control over an array of homeostatic mechanisms. This interplay is directed by the synthesis and secretion of neurohormones, hypothalamic releasing hormones, which act on the pituitary to stimulate the release of regulatory hormones (13). This

interplay illustrates the diencephalons ability to act as a medium for transmission of information between other biological systems such as the endocrine, and immune systems, and the higher brain functions orchestrated telencephalon or cerebrum (3).

**AI (iii). Telencephalon:**

The most notable features of the cerebrum are the cerebral hemispheres with their gyri, or ridges of folded cortical tissue, surrounded by sulci, the depressions or fissures that separate the gyri. These gyral and sulcal patterns divide the hemispheres into four lobes occipital, temporal, parietal, and frontal-- named after the underlining cranial bones. The precentral and postcentral gyri which contain primary motor cortex and primary somatic sensory cortex respectively are divided by the central sulcus which runs between the frontal and parietal lobes of the cerebral hemispheres. Additional subdivisions of the telencephalon are the basal ganglia, hippocampus and amygdala. The basal ganglia are a collection of interwoven subcortical nuclei embedded deeply within the cerebrum. This interwoven network of subcortical nuclei dynamically connects the cerebral cortex, thalamus and other cortical areas, with functional involvement in motor and cognitive processes. Located inside the medial temporal lobes the hippocampus is a prominent member of the limbic system that has been described as looking like a sea horse. The hippocampus provides a critical role for the process of behavioral inhibition, memory and spatial navigation. The amygdala, a fellow component of the limbic system like the hippocampus, is located within the medial temporal lobes. The amygdala has been shown to conduct key functions in emotional learning and memory (14, 15). These processes further illustrates that the telencephalon or cerebrum with vast diversity and complexity is the origin of the extraordinary process that form what we view as cognition (3). This being said, a much

deeper understanding of its beauty and complexity as it relates to human health and disease lies in the molecular mechanisms of its cellular components (16).

**AII. Cellular Composition of the CNS:**

**AII (i). Neurons:**

There are more than 100 billion neurons that innervate the human brain. These neurons utilize electrical and chemical signaling mechanisms to monitor changes in the environment, process these changes and in doing so facilitate the appropriate responses. A neuron is composed of a cell body or perikaryon, containing the nucleus and cytoplasmic organelles, from which a signaling process or axon extends as axonal branching. Growing out from the perikaryon are varying number of ornate branches or dendrites that form connections with the perikaryons and axons of other neurons. The grey matter of the CNS, which directs sensory or motor stimulus to interneurons, generates a response to the stimulus through chemical synaptic activity arising from neuronal cell bodies. Synaptic activity from the grey matter pulses down the axons, many of which are insulated with myelin sheaths that forge the white matter. Although this fundamental cellular organization is shared among most neurons, they are distinguished by specializations in sizes and shapes which reflect their diverse functions in the networks in which they reside (16).

Elaborate dendritic branching from the perikaryon facilitates the potential diversity of multitudinous signals, by creating a vast area by which afferents can be received. As expected the complexity of the dendritic arbor greatly influences the number of synaptic inputs a given neuron can receive. This complexity is illustrated in nerves cell lacking dendrites, which may have from only one to a few synaptic inputs. The vital ornate branching of dendrites is maintained by a graceful interplay between cytoskeletal elements and adhesion molecules. Additional dendrites are marked by

high numbers of ribosomes, which aid in the integration signals from other neurons. From the dendrites and the perikaryon, electric and chemical signals are transduced down the neuronal axon to other neurons (16).

The synaptic connections between axons and dendrites, or less often between axon and perikaryon, are composed of a presynaptic terminal, in most cases a synaptic cleft, and the postsynaptic specialization of the target cell. The presynaptic terminals arise from distal terminations of the branches of an axon with an elaborate secretory apparatus adjacent to a postsynapic target (16). Extracellular proteins such as S-laminin assemble in the synaptic cleft to influence the binding, diffusion, and degradation of molecules released by from presynaptic terminal (17). With the aid of a complex of cytoskeleton proteins the postsynaptic specialization consolidates and coordinates neurotransmitter receptors to modulate the response to neurotransmitters flowing into the synaptic cleft. These neurotransmitters released by synaptic vesicles in the synaptic cleft, bind to their receptors ignite synaptic activation at the postsynaptic specialization which pulses the signal down the axon to its target cell (16).

A self-regenerating wave of electrical activity know as the action potential which transduces the synapse initiates in a swelling or axon hillock that leaves the perikaryon traveling into the axon to form synaptic connections with other neurons. The synaptic connections made by axons help to mold its morphology and the path it navigates through the nervous system. This is illustrated by the often unmyelinated axons, and the relatively simple morphology of axons that extend from local interneurons or circuit neurons, contrary to the frequently myelinated axons of neurons with connections to a multitude of areas of the nervous system (16). These synapses create a symphony of electrical activity which gives rise to a vast amount of neural communication that directs many of the nervous systems actions critical to human health and disease. However the

neurons which generate these signals are not the components in the formation of human cognition (3).

**AII (ii). Neuroglial cells:**

Neuroglial cells or glia were once regarded as the glue that maintains the architecture of the CNS, but now these cells are appreciated for a broad array of functions (18). These formerly under-appreciated cells comprise ninety percent of the cells in the human brain, greatly outnumbering the neurons (19, 20). Functions for glial cells have been established in a multitude of diverse that vital neural mechanisms. These critical roles are illustrated in neuroglia's abilities to maintain a healthy synaptic environment by modulating ion and neurotransmitters concentrations at or near the synapse (21, 22), enhancing the rate of signal transduction by insulating neurons with myelin (23). Additionally neuroglia provides the bases for immune response in the CNS (24). With such vast implications in every aspect of nervous system function that has only gained recognition within the past few decades, research into the molecular mechanisms of neuroglial cells represents an immense well of information that can aid in care for human health and diseases (18).

The glue or glia of the CNS of adult humans is composed of three major cell types: astrocytes named for their star-like appearance, oligodendrocytes, and microglia (18, 23, 25, 26). Astrocytes have a vast array of functions, many of which will be discussed in greater detail later, but a few of which are the regulation of extracellular concentrations of ions, and transmitters (21 and 22), modulation of cerebral blood flow (27), and enhancement of neuronal and synaptic function (28 and 29). Oligodendrocytes enhance the speed of signal transduction by insulating axons in lipid-rich myelin, leaving unmyelinated areas know as nodes of Ranvier by which the action potentials travel (23). Astrocytes and oligodendrocytes, commonly referred to as

macroglia, unlike microglia are derived from ectodermal tissue, and in particular the neural tube, giving them roles in early neural development (18, 19, 23)

Microglia, arising largely from hematopoietic precursor cells, comprising five to ten percent of the glial population in the human CNS. These cells of hematopoietic origin function, when activated, act as phagocytic scavenger cells that clear cellular debris from areas of injury or infection. This function has led some neuroscientists to view microglia as a subtype macrophage (30, 31). Initiation of microglial activation leads to a cascade of molecular mechanisms that induces the transformation of microglial morphology and physiology that facilitates the elimination of pathogens and the isolation of injured tissue (30, 32). This activational state in microglia is marked by the expression of a multitude of cell surface markers such as complement receptor 3 and toll-like receptor 4, which aids in phagocytosis and pathogen recognition (33, 34). Activated microglia, like their fellow phagocytic scavenger cells macrophages, sensitize and secrete a variety of signaling molecules including cytokines, neurotrophic factors and chemokines, which aid in combat against pathogens and isolation of damaged tissue. Additionally microglia, during activation, function as activators of adjacent astrocytes through the release of pro-inflammatory cytokines tumor necrosis factor-α (TNFα), interleukin-6 (IL-6), and interleukin-1β (IL-1β) (35-37). These along with numerous other signal molecules, in addition to their abilities to facilitate the elimination pathogens and the isolation of injured tissue, allow microglia to direct CNS function and influencing human health and disease (30, 32, 35-37).

**B. Astrocytes:**

Astrocytes, the most abundant glial of all glial cells, were long believed to be only a supportive component of the CNS, and their reactive state viewed merely as a marker for CNS disease (25, 38). This view has greatly changed in the past few

decades with a deep interest being placed on the biological importance of astrocytes under normal and pathologic conditions (39). Active roles for astrocytes in numerous functions essential for proper and healthy activity of the CNS have been established, some of which are providing energy metabolites to neurons, enhancing neuronal survival under stressed conditions, modulating extracellular balance of ions, and synaptic transmission (18, 40-42). Insults to the CNS initiates a series of metabolic and morphological changes in astrocytes commonly referred known as reactive gliosis or astrogliosis (Figure1). The hallmark of this phenomenon is up regulation of glial fibrillary acidic protein (GFAP), which is often accompanied with cell hypertrophy and the release of both pro- or anti-inflammatory signaling molecules (43-47). Reactive astrocytes contribute to scar formation and neuronal death. Astrocytes, under certain circumstances, mediate dystrophic effects within the central nervous system and thereby contribute to a decline in neurological functions (48, 49). A multitude of intercellular and intra-cellular signaling pathways have been implicated to ignite the metamorphosis of astrocytes to the reactive state of astrogliosis as well as guide both their deleterious and beneficial actions in a context depended manor (50). However, the detailed molecular mechanisms that direct the phenomenon known as astrogliosis are incompletely characterized presenting a gap in our understanding of overall CNS pathology (50, 51).

**Figure 1. Morphological changes in astrocytes occur during reactive gliosis or astrogliosis.** A, The sections (lateral 2.00 mm) of mouse cerebral cortex with inactivated astrocytes (panel a) and activatived astrocytes (panel b) stained with anti-GFAP antibody. Some reactive astrocytes are indicated by white arrows. B. Model of the functional and morphological changes that occur during reactive gliosis.

**A.**

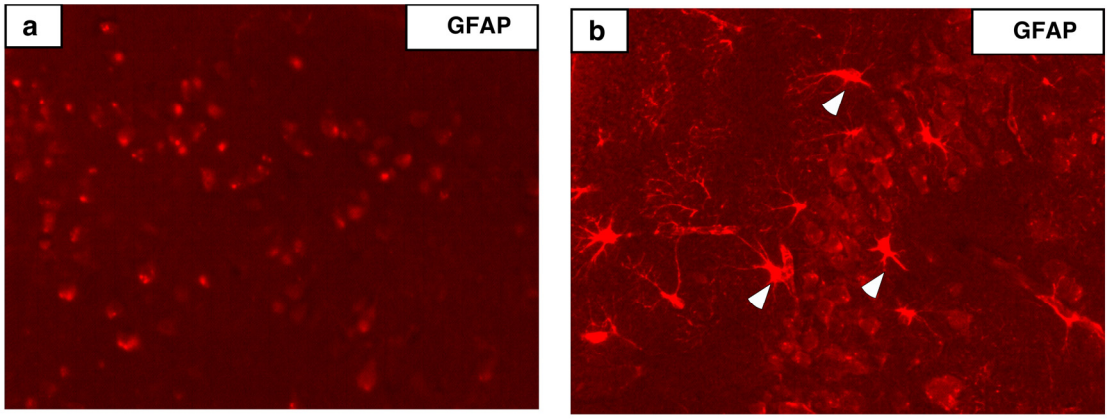


**B.**

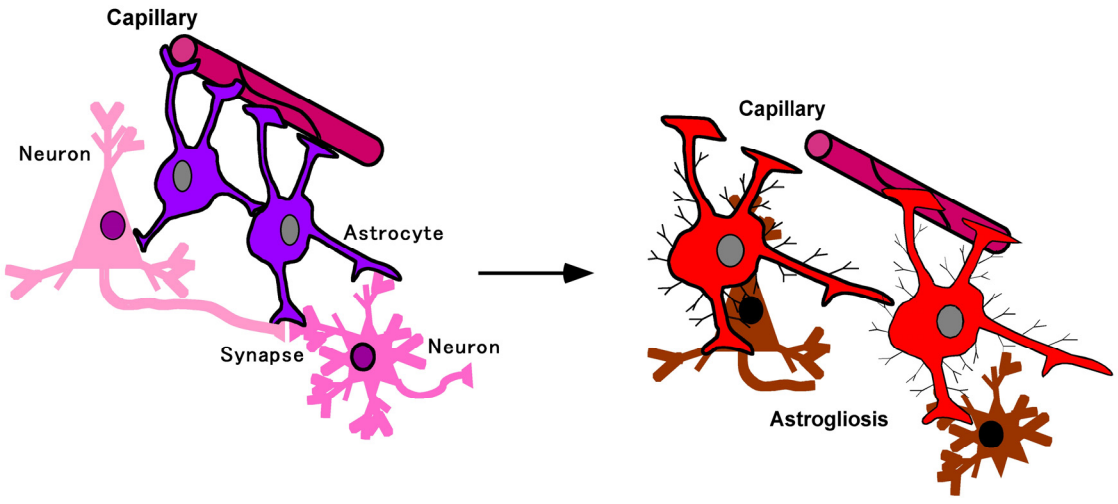

**BI. Astrocyte Classifications:**

**BI (i). Fibrous astrocytes:**

Neuroanatomists described astrocytes as contiguously present through the entire CNS. These contiguously organized cells have long been divided into two major classifications, fibrous and protoplasmic, based on cellular morphologies (52). Fibrous astrocytes of the white matter have many long unbranched processes with a much simpler morphology than protoplasmic astrocytes. This simple morphology is indicative of fibrous astrocytes functions in metabolic support (53). Analysis of the microstructure of fibrous astrocytes has revealed that the end-feet of their processes contact to nodes of Ranvier and like protoplasmic astrocytes they form gap junctions with the processes of adjacent astrocytes (54, 55).

**BI (ii). Protoplasmic astrocytes:**

The most abundant and dynamic glial cells, protoplasmic astrocytes, are highly polarized cells and found throughout the gray matter (52). Protoplasmic astrocytes have a number of stem branches from which a multitude of finely branched processes arise. These fine processes project to envelop vascular walls facilitating astrocytic regulation of neurovascular flow. Additionally the fine processes of protoplasmic astrocytes surround synapses thereby invoking and maintaining microregulation of the synaptic environment (53, 56, 57). This illustrates how the seemly subtle actions of astrocytes can cause dramatic affects in both health and disease states of the CNS.

**BII. Astrocyte Function in the Health CNS:**

**BII (i). Astrocytes in CNS development:**

While astrocytes develop after the formation of neurons in a number of CNS areas, astrocytes have a variety of functions critical to development of the gray and

white matter in the human brain (58). This variety is illustrated in astrocytes creation of a molecular scaffolding that directs neuronal migration and axonal outgrowth during neural development (59). Additionally astrocytes promote synaptogenesis through the delivery of growth factors and molecular signals such as cholesterol that aid in synapse formation (60-62). In the white matter astrocytes form gap junctions composed of connexins with oligodendrocytes which facilitate intercellular ion flow critical for proper myelin development (63). These early actions further show critical and diverse functions carried out by astrocytes as early as CNS development.

**BII (ii). Astrocytes in the neural vascular:**

Astrocytes direct a ballet of bidirectional interplay with cerebral blood vessels and neurons which facilitates microregulation of CNS blood flow meditated by neural activity (64). Consistent with this interplay is a synergistic relationship between the synaptic activity of glutamatergic neurons and vascular flow to the microenvironment. The uptake of glutamate by astrocytes in the synaptic cleft leads to the activation of glutamate receptors on astrocytes and the subsequent release of vascular modulators including nitric oxide, arachidonic acid and prostaglandins (65, 66). These synaptic mechanisms make astrocytes a vital connection between neuronal activity and CNS blood flow (67).

**BII (iii). Astrocytes in CNS homeostasis:**

The homeostatic maintenance of the cellular environment is critical for its function. Processes grow out from astrocytes to engulf a neuron's synaptic area. This action allows astrocytes to conduct a symphony of homeostatic orchestration of fluid, ion and transmitter levels in the synaptic microenvironment (68, 69). Exploiting abundantly expressed aquaporin 4 water channel along the membranes of its endfeet

which interacts directly with microvessels, astrocytes modulate fluid homeostasis in the CNS (70, 71). Astrocytes execute additional regulatory maintenance of pH and ions that forges homeostasis of the CNS through the utilization of monocarboxylic acid transporters, vacuolar-type proton ATPase, bicarbonate transporters and $Na^+/H^+$ exchangers, embedded in their membranes (72). The uptake of neurotransmitters such as glutamate, gamma-aminobutyric acid, and glycine from the synaptic cleft by astrocytes is critical to healthy synaptic function (73, 74). Following this uptake, astrocytes metabolize the transmitters into their inactive forms, which are subsequently recycled back to the synapse for reuse or released into the extracellular space. This further illustrates the elegant way astrocytes govern effects over the intensities of neural communication (42, 75).

**BII (iv). Astrocytes in synaptic regulation:**

The synaptic modulation induced by the multidirectional interplay between astrocytes, neurons and the neural vascular niche extends beyond vascular regulation, homeostatic maintenance and synaptic formation. Astrocytes act to directly modulate signal transduction through the synthesis and secretion of synaptically active gliotransmitters such as glutamate, and gamma-aminobutyric acid (76, 77). Additionally astrocytes can generate and release signal molecules like the cytokine tumor necrosis alpha (TNF$\alpha$) to influence the uniform adjustments in the intensity of synaptic activity made as response to prolonged alterations in the neural electrical activity (78). The synthesis, metabolism and eventual release into the synaptic space of neuromodulatory steroids including testosterone, estradiol, progesterone and metabolites, represents another of the many mechanisms by which astrocytes manipulate synaptic activity. This utilization of metabolic activities shows how astrocytes mediate an additional level of sensitivity and neural modulation to system-wide changes (79).

**BII (v). Astrocytes in metabolic regulation:**

Astrocytes as the primary source of glycogen in the CNS have dynamic interactions with neurons and the vascular system that make them important mediators of energy metabolism in the CNS (18, 80). This astrocyte-neuron interplay is illustrated by glutamatergic neurons at high neural activity eliciting lactate production and release from astrocytes in response in to a loss in function of phosphofructokinase and neuronal glycolysis (81). Consistent with this view, activation of glutamate receptors in astrocytes induces astrocytic uptake of glucose from the vascular system and subsequent release of lactate (82). Astrocytes' contribution of lactate for neuronal metabolic energy extends beyond the uptake of vascular glucose initiated by glutamate. During states of hypoglycemia and high neuronal activity, neural signal molecules such as noradrenaline, invoke glycogenolysis and lactate efflux (83, 84). These and other mechanisms illustrate the vast importance of astrocytes in normal CNS function and the potential grave effects if disruption of these astrocytic functions would have on the CNS and cognitive function (38, 42).

**BIII. Reactive Astrogliosis:**

With such a vast array functions for astrocytes it's not surprising that reactive astrocytes or reactive astrogliosis have primary and secondary affects on the disease pathology of the CNS with direct and even grave implications on patient outcome (39, 50, 85). Growing evidence suggests the phenomenon know as astrogliosis conducts both beneficial and deleterious affects on the CNS depending on the nature and degree of the insult. Despite decades of research and numerous pathological implications the fundamental questions about this phenomenon are just beginning to take shape (50).

Answering even the most basic questions about astrogliosis has become difficult for even the best neurobiologists and neuroanatomists. Immense amount in vitro and in

vivo studies have suggested a definition for reactive astrogliosis. Reactive astrogliosis is a reaction to any affront to the CNS, characterized by an array of biological augmentations. These augmentations are directed with a scaled response indicative of the affront and the cellular environment in which it occurs, illustrated by signaling alterations, progressive cellular hypertrophy, and potential glial scar formation (50, 86, 87). The both advantageous and disastrous affects of the phenomenon known as reactive astrogliosis are invoked through the multiplication of astrocyte function and subsequent secondary actions on the surrounding CNS environment (46, 88, 89). Thus determining the nature of this scaled response and the molecular factors that invoke these changes are critical to our understanding of the CNS and treatment of neurological pathologies.

**BIII (i). Resolvable reactive astrogliosis:**

Moderate or resolvable reactive astrogliosis, as the name implies, can revert to healthy tissue if the initiating affront is cleared. However the lasting effects and nature of the resolution of reactive astrogliosis have yet to be elucidated. This form of reactive astrogliosis can arise from mild non-penetrating and non-contusive trauma, at distal sites of severe trauma, and non-focalized infection (50). Resolvable reactive astrogliosis is marked with cellular hypertrophy and a hallmark increase in GFAP expression (50, 90). This hallmark increase of GFAP expression creates the illusion of astrocytic proliferation in resolvable reactive astrogliosis. Staining for GFAP a cytoskeleton protein widely expressed in the cell bodies of many protoplasmic and fibrous astrocytes, can under estimate the total number of astrocytes in health CNS. Thus with this increase in GFAP expression in resolvable reactive astrogliosis comes increased appearance of astrocytes (91). Perhaps the most distinguishing feature of resolvable reactive astrogliosis from other forms of reactive astrogliosis is the conservation of the non-

overlapping adjoining realms of dense networks of elegantly branched astrocytic processes, in face of cellular hypertrophy (92, 93). This conservatory act is thought to facilitate the resolution of reactive astrogliosis upon the clearance of the initiating affront. That said, even the mechanistic process of this resolution and potentiating effects of the astrogliosis remain elusive (50).

**BIII (ii). Severe reactive astrogliosis:**

Under the assault of inflammatory effects and tissue damage from focalized infection, penetrating or contusive trauma, degenerative disease, autoimmunity and other major attacks to the CNS, astrocytes of the CNS give rise to severe reactive astrogliosis (94-96). Severe reactive astrogliosis is defined by high hypertrophic cell bodies and processes of proliferating astrocytes that have expanded beyond the boundaries of individual astrocytes, blending with other astrocytes to create a blur of astrocytes with strong GFAP expression (92, 50). While knowledge of the mechanisms that induce this proliferation are limited, it is a striking feature demonstrated in CNS dysfunction when considering that the vast majority of astrocytes in healthy CNS are long-living post-mitotic cells (97, 98). This striking and poorly understood process exacerbates the blurring of astrocytic boundaries which are believed to invoke many of the lasting effects seen in severe reactive astrogliosis. This underpins the importance of understanding the molecular mechanism of severe reactive astrogliosis (50).

The loss of astrocytic boundaries in addition to alteration of the cellular architecture of the surrounding tissue, at excessive levels of astrocytic activation guides glial scar formation (94, 99, 100). Inflammatory cytokines such as IL-6 are believed to stimulate proliferation in reactive astrocytes through the up regulation of epidermal growth factor expression (101). These proliferating astrocytes intermingle with other glial cells, fibroblasts and other cells of the surrounding CNS to form glial scars (100,

102). Once formed these glial scars can serve as neuroprotective barriers that isolate infectious pathogens, inflammatory cells and other deleterious agents within the damaged or injected tissue (94, 95, 99). Glial scarring, while beneficial, is far from free of adverse affects illustrated in its ability to hinder axonal regeneration (103). Importantly unlike resolvable reactive astrogliosis the effects of severe astrogliosis are long lasting therefore understanding these functional affects that can influence clinical outcome is critical to treatment of CNS dysfunction (50).

**BIII (iii). Beneficial nature of reactive astrogliosis:**

Reactive astrogliosis has long been viewed as purely deleterious in nature, although this view has transformed over the last twenty years to one of dual nature. It is now known that astrogliosis conducts an array of advantageous functions, many of which are adaptations of astrocytic function during non-pathological conditions (50). This adaptive metamorphosis is demonstrated in the astrocytes' ability to regulate extracellular glutamate levels, and the exploitation of this trait to take up excess glutamate during periods of pathologically generated excitotoxic levels of glutamate (104, 105). Furthermore the dynamic interplay between astrocytes with the vascular system and the homeostasis of the neural extracellular microenvironment allows them to reduce edema follow trauma or stroke as well reduce seizure intensity through ion modulation (71, 106). Astrocytic regulation of the extracellular microenvironment yields additional protective effects through the uptake and degradation of toxic ammonium and amyloid peptides (107, 108). This further demonstrates the extraordinary way astrocytes transform within the framework of their dynamic and poorly understood molecular machinery to perform functions that can shape the outcome of human health during pathological states.

Astrocytes can have beneficial functions during reactive astrogliosis apart from their actions during non-pathological states. This gain is visible in astrocytic secretion and production of molecular protectors in response to an assault. This is demonstrated in the release and production of the master antioxidant glutathione in response to toxic levels of Nitric oxide (109). These and other neuroprotective actions of reactive astrogliosis have altered our approach to CNS pathology. Although a clear mechanistic understanding of reactive astrogliosis inductions of these actions over deleterious ones remain to be elucidated (50).

**BIII (iv). Deleterious nature of reactive astrogliosis:**

While the view of reactive astrogliosis as purely detrimental has changed, it is equally important to remember that reactive astrogliosis is far from purely beneficial. For instance reactive astrogliosis can induce disruption in any a number of essential functions astrocytes carry out, including regulation of neurovascular flow, synaptic homeostasis, and energy metabolism, all which could be disastrous to CNS (42). This deleterious outcome is illustrated in the excitotoxic neurodegeneration occurring through the disruption of neurotransmitter uptake (104, 110). This further demonstrates the essential roles inactive astrocytes play in the biology of the CNS, and the grave effects augmentation and manipulation of astrocyte functions can have on clinical outcome. These grave effects create a genuine need for understanding the molecular processes of reactive astrogliosis.

Just as existing functions can be augmented and new ones gained to yield beneficial effects, they can be altered and gained with disastrous outcomes during reactive astrogliosis. Many of these context-dependent detrimental functions are a reversal of the beneficial effects that can be induced by reactive astrogliosis one example is release of glutamate at potentially toxic levels, rather then uptake and break

down of excitotoxic glutamate (104, 111). This reversal of roles is further exemplified in the augmentation of water channel aquaporin-4 which invokes excessive edema following a stroke (71, 112). This being said the exact nature of reactive astrogliosis during ischemic disease remains unclear (113). Epilepsy, or more broadly stated seizure disorders are not free of this dual nature of reactive astrogliosis which varies with the intensity of the seizures. Reactive astrogliosis invokes its deleterious nature through the augmentation of extracellular levels of potassium in favor of neuronal hyperexcitability and epileptogenesis (114, 115). Additionally, astrocytes can gain the ability to produce and secrete a multitude of deleterious agents not readily seen in health, CNS during reactive astrogliosis such as inflammatory cytokines and noxious levels reactive oxygen species (116-118). During reactive astrogliosis these noxious agents have been shown to influence the development of neuropathology in a context-dependent manner as in the case in the development of neuropathic pain (119). These clinic implications highlights the grave importance of better understanding the induction mechanisms of astrocyte activation and the regulatory actions that take place during this state which could be of value in the treatment of pathologic conditions in the CNS.

**BIII (v). Triggering and signaling events of reactive astrogliosis:**

Reflective of their ability to respond to any affront to the CNS, astrocytes can be activated by a multitude of agents, arising from an array of sources some of which are other cells of the CNS, vascular system and immune cells (50). Microglia and other immune cells induce reactive astrogliosis through the induced expression of cytokines such as IL-6, IL-1 and TNF$\alpha$ exemplify this process (120). Further, immune sensitivity can be invoked through the use of Toll-like receptors on astrocytes (121). Indicative of astrogliosis reactivity to stress, it is not surprising that a multitude of signaling molecules released during states of physiological stress and neurodegeneration including reactive

oxygen species, beta amyloid, and noxious levels of ammonium, can induce reactive astrogliosis (122 -124). Additionally astrocytes the have ability to respond to abnormal neural activity with astrogliosis induction in response to toxic levels of neurotransmitters like glutamate (125). While a vast number of inducers of reactive astrogliosis have been identified, the detailed molecular mechanisms of astrocyte activation are just starting to take shape.

Even with our limited understanding of astrocyte activation, a number of signaling pathways have been implicated in a gene expression profile associated with functional features of reactive astrogliosis (50). Recent studies have suggested that endothelin-1 (ET-1) a key mediator of vascular tone and subsequent activation of the c-Jun/JNK pathway is involved in the poorly understood mechanism of astrocyte proliferation during brain injury induced reactive astrogliosis (126, 127). Signal transducer and activator of transcription 3 (STAT3) was implicated by a conditional deletion study to have a role in astrocyte hypertrophy following spinal cord injury (128). STAT3 function does not end there. STAT3 and Ephrin type-B receptor 2 are implicated in glial scar formation after spinal cord injury (128, 129). STAT3 along with suppressor of cytokine signaling 1 and 3 augmentation of cytokines and chemokines have been suggested to have a mechanistic role in the anti-inflammatory effects induced by activated astrocytes (128, 130). STAT3 and nuclear factor kappa-light-chain-enhancer of activated B cells (NF-κB) influence the hallmark expression of structural proteins GFAP, vimentin, and nestin during astrocyte activation following spinal cord injury (128, 131). Additionally NF-κB is a regulator of immune and inflammatory aspects of astrocyte activation (131). These pathways with an array of others give us some understanding of the mechanisms behind reactive astrogliosis. Nevertheless, these

mechanisms remain poorly understood and respect a gap in our understanding of CNS pathology thereby limiting effective treatment of neurologic disease (50).

**C. NF- κB Involvement in Astrogliosis:**

NF-κB is a transcription factor found in the cytoplasm and nucleus of most cells including astrocytes, with a number of complex roles in both beneficial and deleterious mechanisms during different pathology states in the CNS (132-134). In mammals, the NF-κB family is composed of five members: NF-κB1 (p105/p50), NF-κB2 (p100/p52), RelA (p65), RelB, and c-Rel. These further come together to create at least two major NF-κB pathways. The canonical or classical NF-κB pathway is believed to be the primary NF-κB pathway in astrocyte activation (132, 134). The activation of this pathway can begin with stimulation from a multitude of signal molecules such as TNFα, IL-1, direct pathogen signaling through a Toll-like receptor, and oxygen-free radicals. Activation of a stimulatory cascade invoked by these signaling events leads to the activation of a complex of proteins known as IκB kinase (IKK). IKK phosphorylates serine 32 and serine 36 on IκBα which is bound to the Rel-homology domains of p50 and p65. This binding conceals their nuclear localization signal (NLS), thus acting as in inhibitor of transcriptional activity. Phosphorylation tags IκBα for ubiquitination at positions Lysine 21 and Lysine 22 and subsequent degradation by the 26S proteasome. This degradation frees the NLS of p50 and p65, to facilitate their nuclear localization. Once in the nucleus they form heterodimers with each other and p65 forms homodimers. The homodimers and heterodimers associate with coactivator proteins before binding to response elements in the DNA and inducing gene transcriptional affects (132, 135). This powerful and dynamic transcriptional activity allows NF-κB to

augment the expression of a vast number of genes, which in turn gives it regulatory actions in the induction of activational states of astrocytes (132, 50).

It is not surprising with NF-κB ability to influence over 150 genes including cell cycle regulators, chemokines, cytokines, and neurotrophic factors that it has both protective and deleterious implications in CNS assaults (133, 136, 137). One such gene suggested by recent studies to have involvement in astrocyte activation is the cyclin-dependent kinase inhibitors $p21^{Cip1}$ (138-140). Studies using $p21^{Cip1}$ deficient astrocytes have suggested that $p21^{Cip1}$ expression can increase NF-κB activity in astrocytes (140, 141). Another study in epithelial cells shows an association with $p21^{Cip1}$ over expression with NF-κB activation. There data were strengthened by a decrease in NF-κB induced growth inhibition in $p21Cip1^{-/-}$ epithelial cells (142). These studies allude to a possible bidirectional mechanism where $p21^{Cip1}$ and NF-κB activity is interconnected.

NF-κB has dual effects during pathological states in the CNS with beneficial and deleterious actions. This dichotomy is illustrated in the protective effects on neurons through the release of neurotrophic factors during reactive astrogliosis while inducing the expression of inflammatory cytokines and genes potential inducers of reactive astrogliosis such as $p21^{Cip1}$ (50, 136, 140). The protective nature of NF-κB was described in a recent study that suggested it stimulates of the production and secretion of neurotrophins by astrocytes (143). In another study using transgenic mice expressing a dominant negative (dn) form of the inhibitor of κBα driven by GFAP promoter the loss of NF-κB activity following spinal cord injury resulted in decreased GFAP expression and glial scaring (131). This decrease was accompanied by a reduction in astrocytic production of proinflammatory chemokines and cytokines, such as CXCL10, CCL2 (131). Additionally in a different study using a similar transgenic model astrocytic NF-κB activity was shown to enhance the pathogenesis of experimental autoimmune

encephalomyelitis through the induction of increased cytokine and chemokine response from glial cells (133). These and other studies suggest astrocytic NF-κB plays a role in reactive astrogliosis and neuropathology (50).

**D. Androgen Receptor (AR) Involvement in Astrogliosis:**

Present in a vast array of cells including astrocytes, AR is a nuclear receptor that plays a critical role in the regulation of gene expression in reproduction, development, and metabolism (143-147). AR controls gene expression by acting as a ligand-activated transcription factor of target genes mediated by androgens. Upon binding of androgens to AR there is a release of heat shock proteins, receptor dimerization, and AR binding on androgen-response elements (ARE) located within AR-target genes. During its activation by androgens, AR physically interacts with a medley of cofactors or coregulators that modulate AR transactivation during different physiologic states (148-158). One such physiologic state is astrogliosis (159-162). However the molecular mechanisms underlying this regulatory control remain unclear.

The brain is an important target for androgen (163). Acting on the brain, androgen regulates reproduction and sexual and aggressive behaviors (164, 165). Androgens also prevent neuronal death in neurodegeneration, and decreased androgen levels in plasma increase the risk of development of neurodegenerative diseases in humans (166). During brain development androgen affects, the differentiation of GFAP-positive astrocytes (167-169). In the adult brain, androgens regulate the expression of GFAP in the hippocampus (170). In addition, androgens act as a negative regulator of reactive astrogliosis, illustrated by a reduction GFAP in reactive astrocytes in brains subject to injury and androgen treatment (159-162). These studies suggest that androgens and AR may protect neurons of the CNS through inhibiting astrogliosis

(171). This molecular mechanism of androgen action has yet to be elucidated. The roles of the androgen receptor and its associated proteins represent a critical gap in our understanding of the direct role of astrocytes in all pathologic and non pathologic states of the CNS.

**E. P44/WDR77:**

P44/WDR77 is an AR cofactor that was identified by co-immunoprecipitation with AR from prostate cancer cell line (172). The human p44/WDR77 protein contains 342 amino acid residues and 7 putative WD-40 repeats which facilitate protein–protein interactions (172, 173). Northern blot analysis showed that p44/WDR77 mRNA is expressed in multiple human tissues (172). Prior studies have illustrated that P44/WDR77 is a component of the methylsome complex with protein arginine methyl transferase 5 (PRMT5) (172, 174). PRMT5 is a member of the protein arginine methyltransferase family of coactivators providing support for a role for p44/WDR77 in transcriptional activation (175). Additionally p44/WDR77 shares its protein sequence with the WD45 subunit of the survival motor neuron (SMN) complex, here P44/WDR77 aids in the assembly of the small nuclear ribonucleoprotein (snRNP) complex (174, 176, 177). Interestingly the SMN is only active in the cytoplasm suggesting p44/WDR77 has distinct cytoplasmic and nuclear function (178). This with its role as AR cofactor provides evidence that p44/WDR77 could be involved in a multitude of dynamic mechanisms in various cells at varying differential states.

As an AR cofactor p44/WDR77 (Figure 2) selectively regulates a set of AR-target genes including $p21^{Cip1}$ in the prostate gland and prostate cancer (152, 172, 179). In normal prostate epithelial cells p44/WDR77 localizes to the nucleus, whereas in prostatic intraepithelial neoplasia and prostate cancer p44/WDR77 localizes to the cytoplasm (179). Experimentally induced nuclear localization of p44/WDR77 in prostate

cancer cells inhibited cell growth via G1 cell cycle arrest (179, 180). In addition, the p44/WDR77-null prostate epithelial cells were less differentiated relative to those in the wild-type litermates (181). Thus, the nuclear p44/WDR77 is required for growth inhibition and full differentiation of prostate epithelial cells through selectively modulating expression of a set of AR-target genes. The p44/WDR77 nuclear export might be an essential step that relieves the p44-mediated growth inhibition and resumes proliferation, which is required for prostate tumorigenesis. However, the role of p44/WDR77 in other cell types like astrocytes remains unexplored.

**Figure 2. P44/WDR77 functions as a cofactor for androgen receptor.** Model that illustrates p44/WDR77 ability to physically associate with AR and regulate AR-driven transcriptional activity.

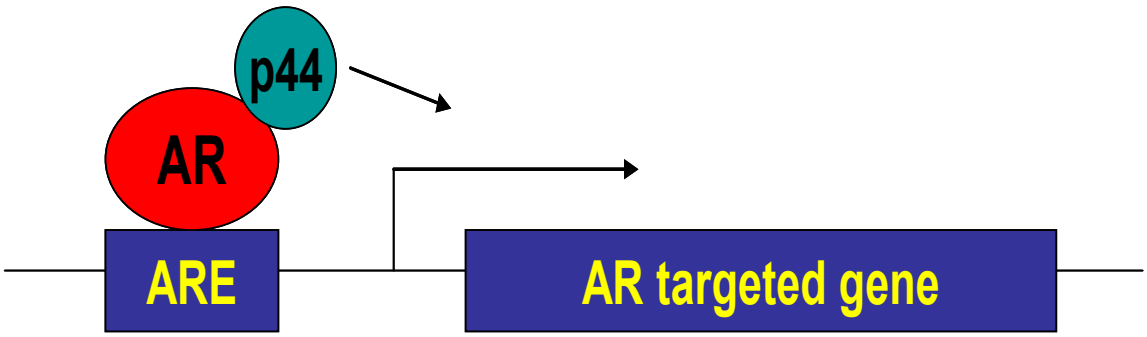

# Chapter II. Materials and Methods

**A. Animals and brain dissection**

The homogenous mice (*p44/*WDR77$^{loxP/loxP}$) and a cross between *p44/*WDR77$^{loxP/loxP}$ (WT) and *PRR2Bi-Cre* mice to generate *p44/*WDR77$^{loxP/loxP}$;Cre (MT) mice were described previously (181, 182). In another line of experiments *ARR2PPbi-Cre* transgenic mouse, were crossed with the mouse line B6;129-Gt(37)26$^{tm1Sor}$ mouse (The Jackson Laboratory, #003309) (183). All mice are on a C57BL genetic background and were handled in accordance with the guidelines published in the NIH Guide for the Care and Use of Laboratory Animals. The Institutional Animal Use and Care Committee at MD Anderson Cancer Center approved experimental procedures. For genotyping, the genomic DNA isolated from mouse-tails was subjected to the polymerase chain reaction (PCR) analysis with 5'GTACCGGTCTGGTGAGCCGAGATC3' and 5'CAGGACGCCAGGTATGGCCGAGGAG3'. Organs were dissected from mice at the age of two months and weighted using an analytic balance. Mice were identified by PCR on tail snips, as previously described (179). Liter mate of different p44/WDR77 genotypes were housed together and fed freely with standard mouse chow over their lifespan in a pathogen-free environment. Mice exhibiting extreme morbidity were sacrificed.

Mice were anesthetized until they no longer displayed a withdrawal reflex in the hind limbs according to procedures approved by the MDACC Animal Research Committee. The animals were intracardially perfused with chilled PBS for approximately two minutes and then with Fresh Formalde (Fisher) for 15 minutes. The animals were decapitated, soft tissue removed, and the skulls were post-fixed in Fresh Formaldehyde for 16 hours at 4$^{o}$C. The brains were removed from post-fixed skulls and sliced into 1 mm sectional pieces. The sliced tissues were put into cassettes, washed with different concentrations of ethanol, and then embedded in paraffin. Sections (4$\mu$m) were cut and

mounted on Super-frost Plus adhesion slides (Fisher) for hematoxylin and eosin (H&E) and immunohistochemical staining.

Dorsal skin sections and cross sections of spleens and skin were fixed in Fresh Formalde for 16 hours at 4$^{o}$C, embedded in paraffin, and stained with haematoxylin and eosin. The heights of the cross sections of spleen and skin were measured under a light microscope. The means of heights from 5 spleens and skins were presented.

**B. Isolation and culture of mouse astrocytes**

A tissue culture system of primary astrocytes was derived from newborn mouse cerebra cortex (184). The newborn mouse pups (n=8-10) were sacrificed in a $CO_2$ chamber. The brains were dissected from mouse skull and transferred to a 60mm Petri dish with ice-cold Hank's Balanced Salt Solution (HBSS). The brainstems, olfactory bulbs and cerebellums were cut off and the two hemispheres were separated. The hemispheres were cleaned out (i.e. remove the hippocampus, basal nuclei, the meninges, and blood vessels) leaving the neocortex. The hemispheres were minced with the small iris scissors and digested with 2ml of collagenase (87.5U/ml) (Worthington Biochemical Corp) and 40μg/ml deoxyribonuclease (Sigma-Aldrich) in low glucose Dulbecco's modified essential media (DMEM) for 30 minutes at 37°C. After centrifugation, cell pellet was dispersed and resuspended in low glucose DMEM supplemented with 10% Bovine Calf Serum (BCS), NaHCO3 500mg/L, and 1% Penicillin-Streptomycin. The cells from each brain was filtered through a 50μm sterile mesh and placed in culture flasks that had been coated with 5μg/ml mouse laminin (Sigma-Aldrich). When the astrocytes were grown confluent (10-14 days) they were ready to be shaken for overnight at 37$^{o}$C (to remove the microglial, oligodendrocytes and neurons) and then 1:4 split. Astrocytes contain characteristic intermediate filaments

(GFAP), which could be readily identified in the cultured cells. The GFAP-positive cells were more than 95% in the cultured cell population.

A confluent plate of astrocytes were harvested and fixed in 4% paraformaldhyde for 20 minutes. The fixed astrocytes were embedded in 0.9% low melting agarose (Sigma-Aldrich). The agarose pellet was embedded in paraffin and sections (4μm) were cut and mounted on Super-frost Plus adhesion slides (Fisher) for immunohistochemistry analysis.

**C. Immortalization of astrocytes**

The Phoenix A packaging cell line was maintained in DMEM supplemented with 10% FBS and transfected with pLXSP:HPV16-E6/E7 using lipofectamine 2000 (Invitrogen) (185). The culture medium was replaced with the fresh low glucose DMEM supplemented with 10% BCS 48 hours post transfection. The virus was collected 12hr later and used to infect the primary astrocytes from WT (*p44/WDR77*$^{loxP/loxP}$) MT (*p44/WDR77*$^{loxp/loxP}$*;Cre*), and *p44/WDR77*$^{+/+}$ mice in the presence of 8μg/ml polybrene (Sigma-Aldrich). Two days after infection, the astrocytes were 1:4 split and selected with 1μg/ml puromycin for three weeks. Total of 8 WT, 20 MT, 8 *p44/WDR77*$^{+/+}$ astrocyte colonies were picked and expanded.

**D. The Cre-mediated deletion of the p44 gene in mouse astrocytes**

Immortalized WT astrocytes (2.5 x $10^5$) were plated on 100mm plate in low glucose DMEM with 10% BCS and 18 hours later, infected with 1.25 x $10^9$ virus particles of adenovirus Ad5-CMV-GFP (Baylor College of Medicine) or Ad5-CMV-Cer-GFP (Baylor College of Medicine). Fresh media was added three days post infection. GFP

expression in the infected astrocytes was examined under a fluorescent microscope and a 100% infection efficiency was achieved (Figure 16). Two adenoviruses used were replication-deficient, and transcription of GFP and Cre cDNAs was under the control of a CMV promoter. Deletion of the p44/WDR77 gene was confirmed using PCR and p44/WDR77 expression was analyzed by immunostaining and Western blot analysis with anti-p44/WDR77 antibody.

**E. Northern blot assay**

Northern blot analysis was performed as previously described (186). The mRNAs were isolated from whole brains of WT (n=5) or MT (n=5) male mice at the age of two months and transferred to a Hybond $N^+$ membrane (Amersham Biosciences). The membrane was hybridized with cDNA probes of p44/WDR77 and β-actin genes.

**F. BrdU labeling**

Mice were injected by intraperitoneal with Bromodeoxyuridine (BrdU) 0.1mg per gram of body weight (Sigma-Aldrich) and skin and spleen were dissected 24 hours later, fixed in Fresh Formalde for 16 hours at 4°C, and embedded in paraffin. Sections (4μm) were cut and mounted on Super-frost Plus adhesion slide for immunostaining the BrdU-labeled cells employing a monoclonal anti-BrdU antibody (BD Pharmingen™). The labeled cells were calculated from three fields of each slide. Three sections from each organ were analyzed to obtain the mean of BrdU positive epithelial cells. The means of the proliferating cells from 5 mice were presented.

Primary WT and MT astrocytes ($1 \times 10^6$) were plated on 100mm plate in low glucose DMEM with 10% BCS and 18 hours later, the cell were incubated at 37°C with

culture medium containing 10μM BrdU. Four hours later the astrocytes were harvested and fixed in 4% paraformaldhyde for 20 minutes. The fixed astrocytes were embedded in 0.9% low melting agarose. The agarose pellet was embedded in paraffin and sections (4μm) were cut and mounted on Super-frost Plus adhesion slides for immunohistochemistry analysis.

**G. β-Galactosidase (β-gal) Staining**

B6;129-Gt(37)26$^{tm1Sor}$ mouse (The Jackson Laboratory, #003309) were crossed with the ARR2PPbi-Cre transgenic mouse. Animals [B6;129-Gt(ROSA)26Sor/J (negative control)] and B6;129-Gt(ROSA)26Sor/J-ARR2PPbi-Cre (F1 heterozygous mice) at two months of age were anaesthetized and perfused with 4% paraformaldehyde. The brains were removed and fixed in 4% paraformaldehyde for 1 hour and sliced sagittal at 0.00 mm plane. The brain slices were fixed with 4% paraformaldehyde overnight and processed for paraffin embedding. The whole brains and tissue section were fixed for 10 minutes with 0.5% Gluteraldehyde in PBS at 4°C and washed three timed with PBS. Specimens were then placed in PBS containing 10 mmol/L K3Fe(CN)6 and 10 mmol/L K4Fe(CN)6 along with the β-gal substrate [5-bromo-4-chloro-3-indolyl-β-D-galactopyranoside (X-gal)] (1 mg/mL). Specimens were incubated at 37°C for eight hours, washed well in tap water, and counterstained with Hematoxylin Solution (Sigma).

**H. Terminal deoxynucleotidyl transferase dUTP nick end labeling (TUNEL) assay**

Animals (n=5, *WT* and n=5, *MT*) at the age of three months were anaesthetized and perfused with 4% paraformaldehyde. The brains are removed and fixed in 4% paraformaldehyde for 1 hour and sliced sagittal at 0.00 (B3), 1.00 (B4), 2.00(B2 and

B4), and 3.00 (B1 and B6) mm planes. The brain slices were fixed with 4% paraformaldehyde overnight and processed for paraffin embedding. Blocks will be sectioned to obtain continuous specimens (4μM each) placed on glass slide. Tissue sections deparaffinized followed the application of 40μg/ml proteinase K (Sigma-Aldrich). The sections were subject to a TUNEL assay utilizing the in situ cell death detection kit (Promega) according to the manufacturer's instructions. TUNEL-positive cells and total cells determined using Hoechst staining (Invitrogen) from each section of WT and MT brains were accounted. The percentage apoptotic cells were calculated. Three sections (500μM apart) from each brain were analyzed. The means of percentage apoptotic cells from 5 brains are presented.

**I. Microscopic observations of living cells**

Living immortalized WT and MT astrocytes were examined with white or green (to observe GFP) light under an Olympus IX71 microscope (Olympus Corp.) and a digital camera (Retiga 1300) interfaced to a computer with PCI software.

**J. Immunohistochemistry**

Immortalized WT and MT astrocytes ($3 \times 10^4$) were plated to 4-well chamber slides (Fisher) in low glucose DMEM with 10% BCS and 18 hours later, they were washed twice with PBS and fixed with cold (-20$^{o}$C) methanol (Sigma-Aldrich). The cells were blocked with 4% fish gel and primary antibodies were applied to the astrocytes sections and incubated overnight at 4$^{o}$C. After washing with PBS immunofluorescent secondary antibodies were applied. The fluorescent signals were observed under a cofocal microscope. The primary antibodies are omitted in negative controls.

Tissue sections deparaffinized and subject to antigen retrieval. Tissue sections were blocked with 3% fish gel and primary antibodies were applied to the tissue sections and incubated overnight. A streptavidin-biotin peroxidase detection system was used according to the manufacturer's instructions (DAKO). For double immunofluorescent staining, secondary antibodies were applied as described in Table 1. The fluorescent signals were observed under a cofocal microscope with a green (to detect the p44/WDR77 protein) or red (to detect GFAP protein) filter. The primary antibodies are omitted in negative controls.

**Table 2:** Antibodies used in Immunohistochemistry

| Primary Antibodies | Company | Dilution | Secondary Antibodies | Dilution |
|---|---|---|---|---|
| antigen-purified p44/WDR77 | described previously (172, 187) | 1:200 | Alexa 488 anti-rabbit IgG | 1:1000 |
| Fluorescent GFAP | Neuromics (CH22102) | 1:1000 | 594 labeled anti-chicken IgG | 1:1000 |
| NEUronal Nuclei (NeuN) | Chemicon (MAB377) | 1:500 | 594 labeled anti-chicken IgG | 1:1000 |
| class III β-tubulin (Tuj1) | Neuromics (CH23005) | 1:400 | 594 labeled anti-chicken IgG | 1:1000 |
| p65 | Santa Cruz Biotechnology (sc-8008) | 1:1000 | Alexa 594 anti-mouse IgG | 1:1000 |
| Non fluorescent GFAP | DAKO (Z0334) | 1:1000 | Peroxidase labeled anti-rabbit IgG | 1:300 |
| BrdU | Beckton Dickinson (347580) | 1:200 | Peroxidase labeled anti-rabbit IgG | 1:300 |

**K. Western blot analysis**

The mouse whole brain was homogenized in 0.5ml passive lysis buffer (Promega) using a dunce. Confluent 100mm plates of astrocytes were collected and lysed in 50μl passive lysis buffer (Promega). After centrifugation at 12,000 rpm, 4$^{o}$C for 12 minutes, the supernants were collected and protein concentrations were measured by the Bradford Reagent (Bio-Rad) with BSA as the standard. Ten micrograms of protein extracts were loaded on 12% sodium dodecyl sulfate (SDS) polyacrylamide gel and subject to electroporation at 175V for one hour. The proteins were transferred to 0.45μm polyvinylidene fluoride (PVDF) membrane (Millipore) using a Semi-Dry Transfer System (Bio-Rad Laboratories) at 6V overnight. The membranes were rinsed in 100% methanol (Sigma-Aldrich) and block for 1 hour in 3% nonfat dry milk in TBST (20 mM Tris-HCl, pH 7.6; 150 mM NaCl; and 0.1% Tween 20). The blots were subject to a two hour incubation with primary antibodies (Table 2) in 3% nonfat dry milk in TBST. After washing with TBST the blot were subjected to 1.5 hours incubation with secondary antibodies (Table 2) in 2% BSA in TBST. The blots were developed utilizing chemiluminescence kit (Amersham Biosciences).

**Table 2:** Antibodies used in Westernblots

| Primary Antibodies | Company | Dilution | Secondary Antibodies | Dilution |
|---|---|---|---|---|
| p44/WDR77 | described previously (172, 187) | 1:5000 | Peroxidase linked anti-rabbit Ig | 1:5000 |
| p65 | Santa Cruz Biotechnology (sc-8008) | 1:1000 | Peroxidase linked anti-mouse Ig | 1:5000 |
| GFAP | DAKO (Z0334) | 1:1000 | Peroxidase linked anti-rabbit Ig | 1:5000 |
| β-Actin | Sigma-Aldrich (029K4838) | 1:2000 | Peroxidase linked anti-rabbit Ig | 1:5000 |
| $p21^{Cip1}$ | Santa Cruz Biotechnology (sc-6246) | 1:1000 | Peroxidase linked anti-rabbit Ig | 1:5000 |

**L. Cell growth assay**

Immortalized WT and MT astrocytes (1 x $10^4$) were plated in each well of 24-well plates in low glucose DMEM with 10% BCS and supplements. Cells will be counted every day with a hematocytometer.

**M. Fluorescence activated cell sorter (FACS) analysis**

Astrocytes were collected 14 days after adenovirus infection, washed with ice-cold phosphate-buffered saline (PBS), and then fixed in 70% ethanol at 4$^o$C for 12 hours. After fixation, astrocytes were washed twice with PBS and incubated in PBS containing 50$\mu$g/ml propidium (PI) (Sigma-Aldrich), 20$\mu$g/ml RNase A (Sigma-Aldrich), 0.1% Tween 20 (Sigma-Aldrich) for 20 minutes. FACScan flow cytometry (Becton Dickinson) was used to measure the propidium–DNA complex. Cells in the sub-G1 population were identified as apoptotic.

**N. Real-Time Quantitative Reverse Transcription PCR (qRT-PCR)**

Total RNAs were isolated from immortalized WT and MT astrocytes and from whole brain tissues using TRIzol regent (Invitrogen). cDNAs were generated from the total RNAs using the Reaction Ready First Strand cDNA Synthesis Kit (Supper-Array Bioscience Corp). The cDNA were subjected to PCR amplification for 40 cycles (30sec at 94°C; 20sec at 55°C; and 30s at 72°C) utilizing a mixture of $RT^2$ real-time SyBRgreen PCR master mix and primers specific to mouse $\beta$-actin (PPM02945A) or $p21^{Cip1}$ (PPMO2910A) purchased from SupperArray Bioscience Corp with the SmartCycler II (Cepheid). The expression levels of the samples were normalized to their $\beta$-actin levels. Quantification and data analysis was generated with the aid of the SmartCycler Software (Cepheid; version 2.0C).

**O. ShRNA knockdown**

Mouse $p21^{Cip1}$ and p65 shRNA constructs and lentivirus production were performed by the Cloning Core Facility at Department of Cancer Biology in MD Anderson Cancer Center, using pLVTHM (addgene) vector. The target sequences used for the nontargeting control and mouse $p21^{Cip1}$ and p65 are TTCTCCGAACGTGTCACGT, TTAGGACTCAACCGTAATA and GAGTTTCAGCAGCTCCTGAAC, respectively. Immortalized WT astrocytes ($2 \times 10^4$) were plated in each well of 6-well plates in low glucose DMEM with 10% BCS and supplements. Twenty-four hours later, the astrocytes were infected with lentivirus in the four groups as follows, (i) non-targeting control virus; (ii) $p21^{Cip1}$ shRNA-expressing virus; (iii) p65 shRNA-expressing virus; (iv) $p21^{Cip1}$shRNA-expressing virus plus p65 shRNA-expressing virus. GFP expression was examined for the infected astrocytes under a fluorescent microscope. This illustrated an 80% infection efficiency. Four days later, the virus was removed and the cells were split for experiments.

**P. Exogenous expression of $p21^{Cip1}$ and p65**

Human $p21^{Cip1}$ and p65 cDNA were subcloned into a lentiviral expression construct OG2 (clonetech) with a CMV promotor. Lentivirus production was performed by the Cloning Core Facility at Department of Cancer Biology in MD Anderson Cancer Center. Immortalized WT astrocytes ($2 \times 10^4$) were plated in each well of 6-well plates in low glucose DMEM with 10% BCS and supplements. Twenty-four hours later, the astrocytes were infected with lentivirus in the four groups as follows, (i) control virus; (ii) $p21^{Cip1}$-expressing virus;(iii) p65-expressing virus; (iv) $p21^{Cip1}$-expressing virus plus p65-expressing virus. The virus was removed 4 days post infection and the cells were split for experiments.

**Q. Quantification and statistical analysis**

The positive cells were counted in three fields of brain regions (three randomly selected non-overlapping 20X fields). Three brain sections (126-mm apart) for each brain block (plane) were counted. Cell counts were thus performed in the same volume of WT control and MT brains. To avoid double counting of the same cells, cell counting was done in brain sections 126 mm apart, which should be larger than most of brain cell diameters. Cell counts were carried out without knowledge of the genotype of mice. Data were analyzed by unpaired Student's *t-test*. In cell counting experiments, the average value of the same counting on three microscopic fields of three brain sections from each brain block (plane) was used for statistical analysis. Differences between experimental groups were considered significant at $P<0.05$. All values represent mean ± S.E.M.

# Chapter III: Preliminary Data

**A. Loss of the p44/WDR77 gene decreased the mouse life span.**

**AI. Rationale:**

AR controls the expression of a vast array of gene involved in reproduction, development, and metabolism (143-147). These regulatory actions are modulated by various cofactors or coregulators which physically interact with AR after ligand activation (148-158). One such cofactor is p44/WDR77 which was identified by co-immunoprecipitation with AR from a prostate cancer cell line (172). Previous studies indicate that p44/WDR77 directs critical functions in prostate tumorigenesis by affecting a subset of AR-target genes in prostate cancer (179, 180). Prostate-specific deletion of the p44/WDR77 gene will provide a better understanding on how p44/WDR77 control growth and differentiation of prostate epithelial cells (188).

**AII. Experimental Design:**

To achieve a prostate-specific deletion of the p44/WDR77 gene, we crossed WT ($p44^{loxP/loxP}$) mice to the *ARR2PPbi-Cre* transgenic line (189), in which the Cre recombinase is expressed under the control of a modified prostate-specific probasin promoter. The promoter ARR2PPbi is a composite of the rat probasin promoter with two androgen responsive elements (ARE) (190). The probasin promoter has been shown to target gene expression to the epithelial cells of the prostate in transgenic mice (191). Studies utilizing ARR2PPbi-Cre mice indicate that the Cre recombinase is highly expressed in every lobe of mouse prostate (192).

The mortality of fifty WT and forty-one MT mice was observed over the course of 300 days postnatal. Mice exhibiting extreme morbidity were sacrificed, and their pathology was examined by a veterinary pathologist at MD Anderson Cancer Center. WT and MT mice were weighed using an analytic balance at 21, 30, 60, 90, and 120

days postnatal to determine their growth rate. To farther examine any morphological differences between WT and MT mice individual organ weights evaluated at two months of age.

**AIII. Results:**

When we crossed WT mice to the ARR2PPbi-Cre transgenic line, we noticed that the MT mice had an unexpected loss in longevity (Figure 3). The median lifespan of the MT mice was dramatically reduced (a median life span: 120 days). Both males and females showed comparable reductions in the life span. Careful examinations of the MT mice by a veterinary pathologist at MD Anderson Cancer Center failed to reveal any obvious pathological defects (data not shown).

**Figure 3. Deletion of the p44/WDR77 gene leads to decreased mouse life span.** Survival data are presented for MT and WT mice. The 50% survival mark was 120 days for MT mice.

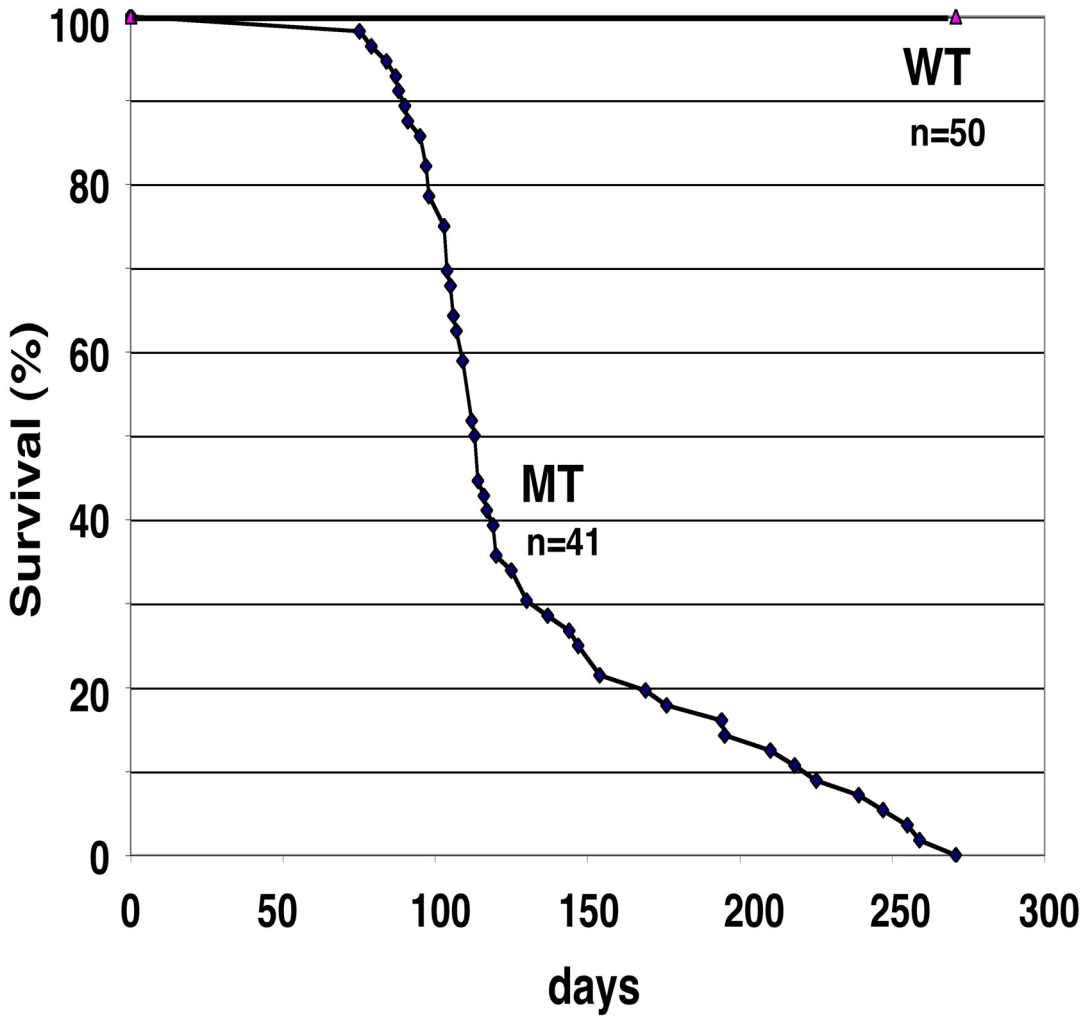

The MT mice appear morphologically identical to their WT littermates when they were born. However, the body weight increase of the MT mouse was less than that of the wild-type littermate by 60 days and stopped after 60 days (Figure 4). By 90 days, virtually all of the MT mice exhibit signs of an absence of vigor. Skin, spleen, liver, uterus, and prostate were significantly reduced in mass in the MT mice than in the age-matched WT littermates (Figure 5).

**Figure 4. Deletion of the p44/WDR77 gene leads to decreased mouse growth rate.**

Comparison of mean body weights of WT and MT mice.

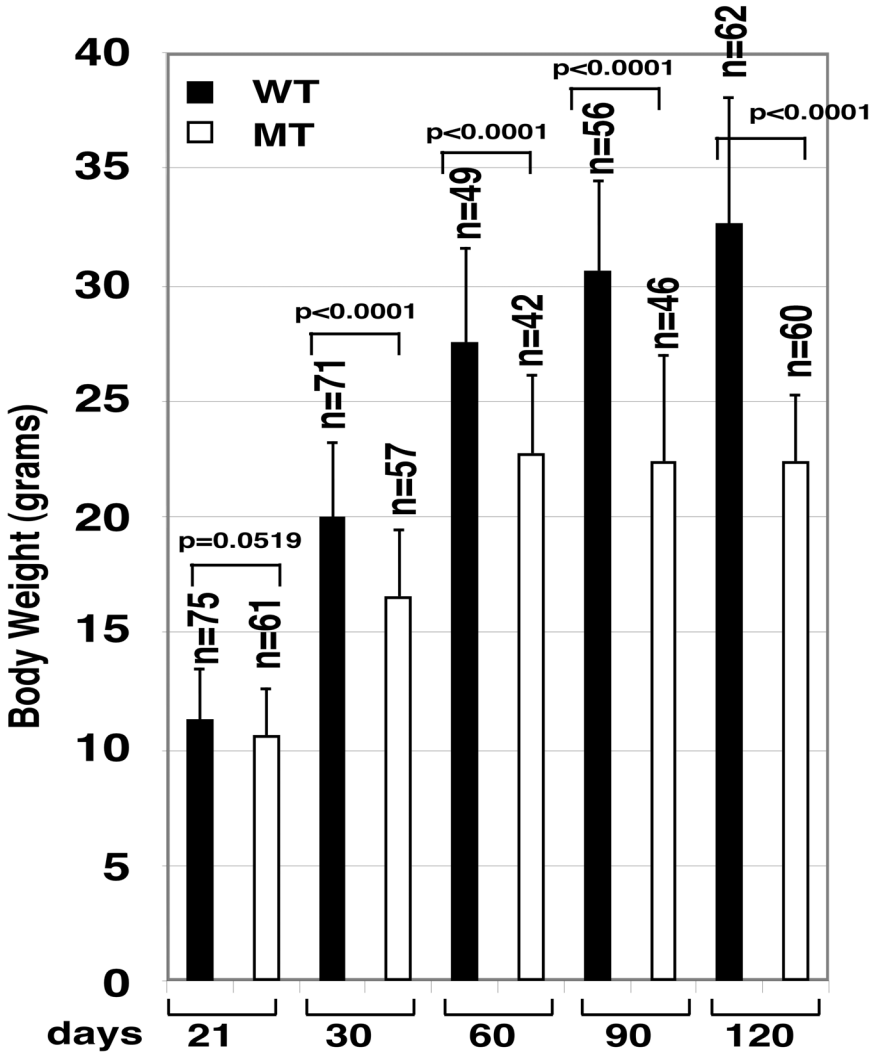

**Figure 5. MT mice exhibit early ageing-related decreases in organ weight.** Comparison of mean organ weights of WT and MT mice. Organs were removed form WT and MT mice at the age of two months and weight.

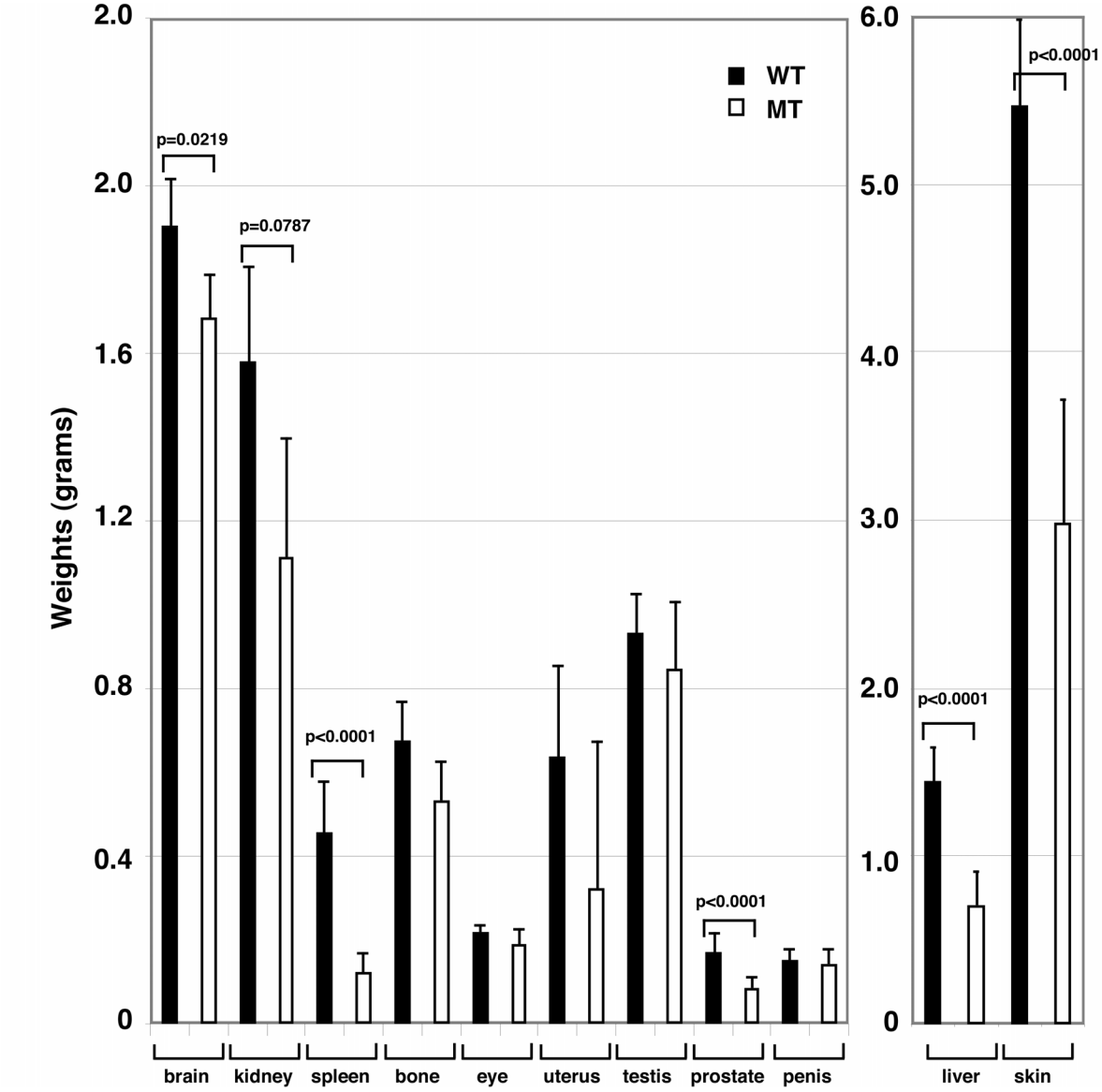

**AIV. Discussion:**

These experiments demonstrated that the deletion of the p44/WDR77 gene driven by ARR2PPbi-Cre leads to a decrease in mouse longevity. This loss of longevity is suggestive of an accelerated aging phenotype associated with the MT mouse and additional support for this phenotype comes from the following observations. First, no obvious pathological defects were detected in the MT mouse. Second, the absence of increase in body weight and lacking vigor was observed in the young MT mice (2 months old). Third and forth, two organs (skin and spleen) in the MT mice show the dramatic aging-related changes. The skin is the largest organ of the body, is significantly affected by the aging process and has been become a marker for aging. Thus the dramatic decrease in the weight of the skin in MT mice presents additional evidence of aging-related changes. This said age-related changes are more complex then a simple decrease in weight. The skin is composed of three layers the epidermis, dermis and subcutaneous tissue. Major components of age-related changes are decreases in adipose thickness and collagen atrophy in these layers (192). The spleen is the largest secondary immune organ in the human body and a multitude of studies have described the effects of aging on lymphocyte function and changes in the distribution of lymphocytes (193-196). Lymphocyte numbers and ability to undergo cell division can decrease with age. This is illustrated by an 80% decrease in lymphocyte numbers and general atrophy in the white pulp of spleens from older rats (197). Further supporting for a decrease in spleen size as a marker of aging comes from studies showing fewer germinal centers in older rodents (198). This being said a closer examination of the skin and spleen in MT mice is needed to confirm aging-related changes. Even still, these observations warrant further studies into what role p44/WDR77 might have in the mammalian aging process.

**B. MT mice exhibit early ageing-related phenotypes.**

**BI. Rationale:**

With the growing population of older adults understanding the mechanisms and nature of aging has become increasingly important. The loss of longevity in MT mice without obvious pathological defects with a striking decrease in spleen and skin size is suggestive of early aging in MT mice. In the skin age-related changes are marked with a decrease in dermal and subcutaneous adipose, accompanied with elasticity of the skin (192). Initial examination of the skin from MT mice showed that it was rigid and stiff when compared to the age-matched WT littermates, suggesting the loss MT skin weight might be due to decreased dermal and subcutaneous adipose. The spleens of aging rodents are marked by a notable decrease in the size of the white pulp indicative of a reduction in the number lymphocytes and lymphocytic cell division (193-197). While the decrease in spleen and skin weight is quite striking an aging phenotype is far more complex and further studies are needed to confirm an aging phenotype of the MT mouse.

**BII. Experimental Design:**

To examine the pathology of the spleen and skin from MT mice more closely we isolated spleens and skin from WT and MT mice at two months of age. Sections taken from fixed tissues underwent staining with Haematoxylin-esosin after which the dermal and spleen thickness and general tissue pathology was evaluated under a microscope.

To examine proliferation in the WT and MT mice, mice were subjected to bromodeoxyuridine (BrdU) pulse (intraperitoneal injection, 100mg/kg) to label proliferating cells. Skin and spleen sections were prepared 24 hours after the pulse and

cells that had incorporation BrdU (i.e. cells in S-phase) were identified by immunohistochemistry with anti-BrdU antibody.

**BIII. Results:**

Histological cross-sections of dorsal skin showed a dramatic reductions in dermal thickness and subcutaneous adipose cells were virtually absent in skin of the 2-month-old MT mouse (Figure 6A, left panels). These differences in mouse skin were confirmed by weighing isolated whole skin from 2-month-old WT and MT mice (Figure 5). Similarly, the spleen sections in 2-month-old MT mice are markedly reduced compared with those in the spleens of age-matched WT mice (Figure 6A, right panels; Figure 6B).

**Figure 6. The reduced thickness of spleen and loss of subcutaneous adipose tissue in the skin of MT mice.** (A) Sections of dorsal skin and spleen of WT and MT mice at the age of two months were stained with Haematoxylin-esosin. (B) The subcutaneous adipose tissue in the WT skin is indicated by a parenthesis on the left. The quantitative data of the length of sections of WT and MT spleens are shown.

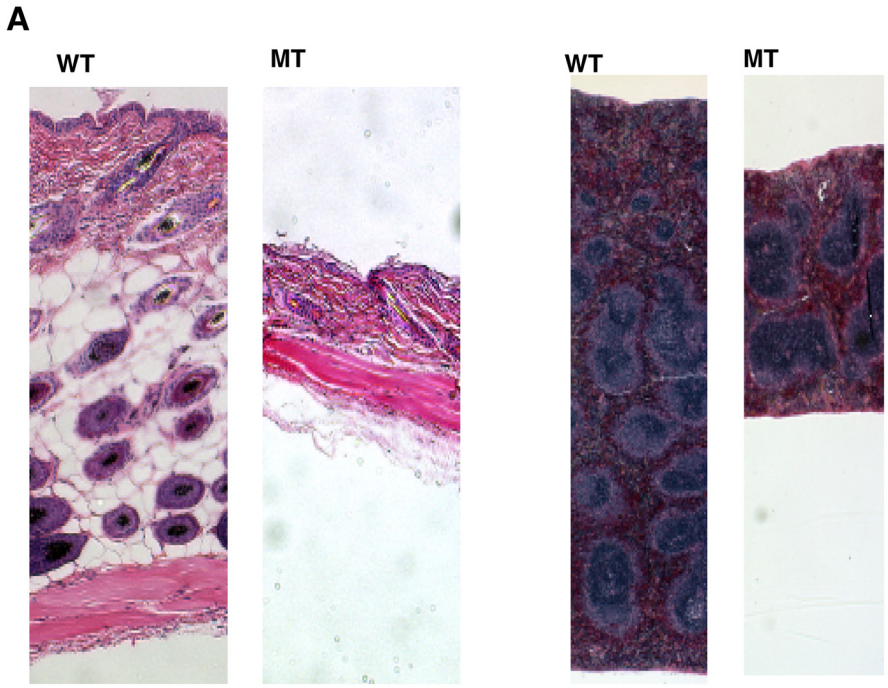


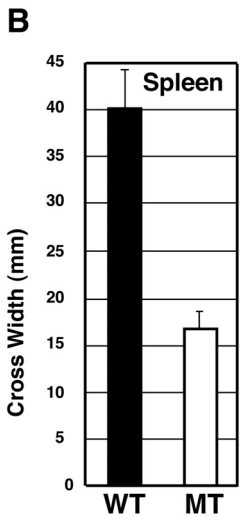

The immunohistochemistry with anti-BrdU antibody in skin and spleen sections taken from WT and MT mice, subjected to BrdU pulse (intraperitoneal injection, 100 mg/kg) showed a decrease of cell of MT mice in S-phase (Figure 7A). BrdU–posituve cells were quantified in skin and spleen sections illustrated that p44/WDR77 deficiency decreased proliferation (BrdU-positive cells) in the skin (from 28 ± 3/per field of view to 5 ± 2/per field of view) and spleen (from 402 ± 41/per field of view to 168 ± 18/per field of view), a finding consistent with the observation that aging decreases cell proliferation in skin and spleen (Figure 7B). Thus, the MT mice display an onset of phenotypes associated with aging.

**Figure 7. The decreased proliferation rate in the skin and spleen of MT mice.** A, B. In vivo proliferation was assessed using the BrdU incorporation assay. Sections of dorsal skin of WT (top) and MT (bottom) mice at the age of 2 months were immunostained with anti-BrdU antibody. The BrdU-positive cells are stained brown (A) and quantitated (B).

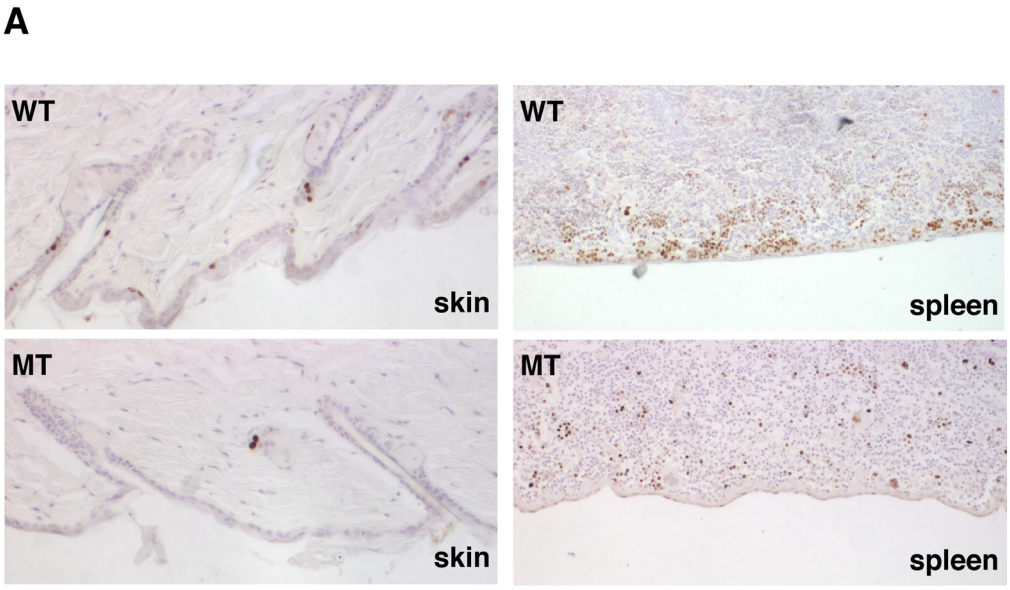


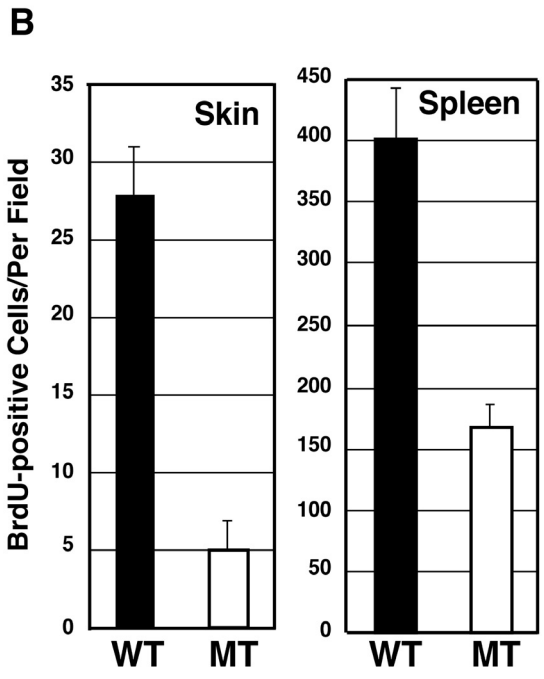

**BIV. Discussion:**

The experiments depicted in Figures 3 through Figure 7 suggest the presence of an accelerated aging phenotype in MT mice. This aging phenotype is supported by the lack of overt pathological defects in the MT mouse and, an ablation of body weight gain after post natal day 60 accompanied with a loss of vigor in MT mice. The phenotype is further demonstrated by a dramatic loss of dermal and subcutaneous adipose associated with fewer dividing cell in MT mice is indicative of an age-related phenotype seen in humans (192). Additionally the decrease in white pulp and the number of germinal centers coupled with a drop in proliferation in spleens from MT mice illustrates a possible age-related phenotype (197, 198). While a broader array of studies are needed to confirm the presence of an accelerated aging phenotype in MT mice, these experiments rationalize the need for additional studies into the roles p44/WDR77 in the regulation of mammalian aging process.

**C. The p44/WDR77 gene was deleted in mouse brain.**

**CI. Rationale:**

To gain a mechanistic understanding for the unexpected loss of longevity in MT mice we endeavored to identify the initiating tissue of this phenotype. Numerous studies have shown that surgical removal of the prostate along with physiologic disruptions in the prostate such as prostate cancer do not induce the aging like phenotype observed in MT mice (199, 200). This prompted the question as to whether the ARR2PPbi-Cre transgenic line is expressing Cre recombinase and inducing p44/WDR77 deletion in cells outside the prostate.

Mice heterozygous or homozygous for the Gt(rosa)26$^{tm1Sor}$ targeted mutation have been useful for identifying tissues expressing Cre recombinase. B6;129-Gt(37)26$^{tm1Sor}$ mice have a neo expression cassette flanked by loxP sites that prevents lacZ gene expression. Upon the induction of Cre recombinase expression the neo expression cassette is removed facilitating lacZ gene expression. This genetic alteration makes these mice an ideal model for the detection of Cre recombinase expression through identification of lacZ expression utilizing beta galactosidase staining (201).

**CII. Experimental Design:**

To investigate whether other tissues in addition to the prostate also express the Cre recombinase in the *ARR2PPbi-Cre* transgenic mouse, the status of p44/WDR77 gene deletion was examined by sensitive PCR analysis. The heart, smooth muscle, skeletal muscle, liver, spleen, lung, kidney, skin, testis, small intestine, large intestine, pancreas, tongue, stomach, bone marrow, lymphnote, prostate, penis, eye, and brain, were isolated from WT and MT at two months of age. DNA was isolated from this panel of tissues and PCR analysis for p44/WDR77 gene deletion.

To confirm the gene deletion p44/WDR77 seen the PCR analysis was due to expression of Cre recombinase expression ARR2PPbi-Cre transgenic mouse, we crossed this mouse line with the B6;129-Gt(37)26$^{tm1Sor}$ mouse (The Jackson Laboratory, #003309). Tissues were isolated from the B6;129-Gt(ROSA)26Sor/J (negative control) and B6;129-Gt(ROSA)26Sor/J-ARR2PPbi-Cre F1 heterozygous mice at two months of age. These tissues and tissue sections taken from where subject to galactosidase staining for the identification of lacZ expression.

Additional studies were conduct to confirm that the Cre recombinase expression and deletion of p44/WDR77 correlated with a decrease in p44/WDR77 mRNA and protein. First, a Northern blot analysis was preformed using RNA isolated from brains from WT and MT mice at two months of age. Second, immunostaining analysis for p44/WDR77 protein was conducted using tissue sections taken brains from WT and MT mice at two months of age.

**CIII. Results:**

PCR analysis showed that the p44/WDR77 gene was deleted, as indicated by excision of the exons 2-5 of the p44/WDR77 gene, in the MT prostate gland but not in the WT prostate gland (Figure 8, lanes 2 and 3). This observation is consistent with expression of the Cre recombinase in the prostate as previously reported (191). The Cre-mediated deletion of the p44/WDR77 gene was also detected in penis, eye, and brain of the MT mouse (Figure 8, lanes 4, 5, 8, 9, 10, and 12). The p44/WDR77 alleles were not deleted in the other tissues (heart, smooth muscle, skeletal muscle, liver, spleen, lung, kidney, skin, testis, small intestine, large intestine, pancreas, tongue, stomach, bone marrow, lymphnote) examined in the MT mice (Figure 8, lanes 6, 7, 12, and 13; data not shown).

**Figure 8. The p44/WDR77 gene was deleted in mouse brain.** PCR analysis of the p44/WDR77 gene deletion in various organs in the MT mouse. Genomic DNA was isolated from organs of WT and MT mice and submitted for the PCR analysis. Excision of the exons 2-5 of the p44/WDR77 gene generated the 220-bp DNA fragment in the PCR reaction. Lanes 1, the 0.1 kb DNA ladders.

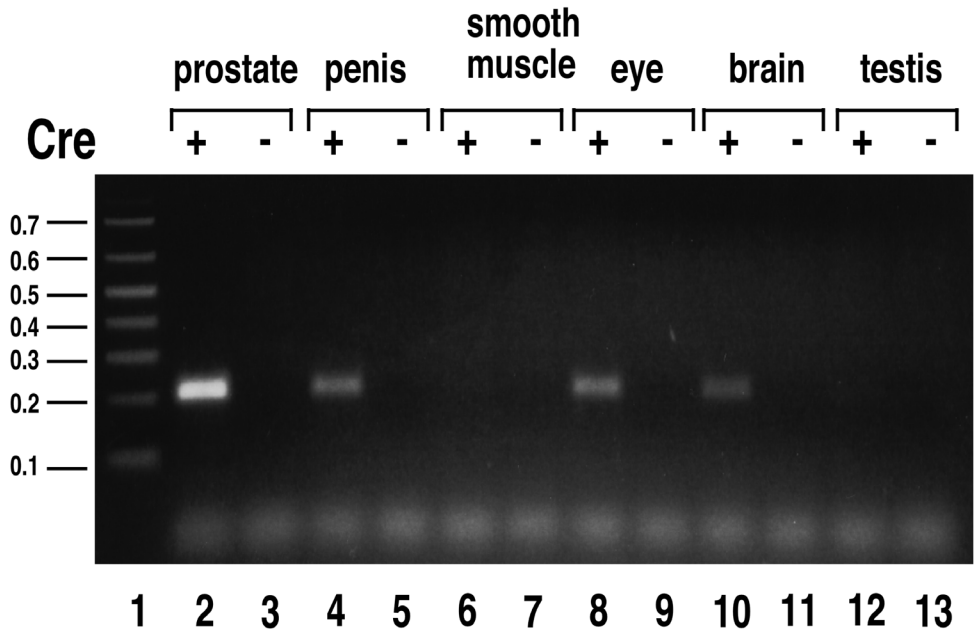

In the experiments utilizing ARR2PPbi-Cre transgenic mouse crossed with the B6;129-Gt(37)26$^{tm1Sor}$ mouse (The Jackson Laboratory, #003309) we found as expected, the prostate stained strongly with beta galactosidase indicative of Cre recombinase expression. The brain also showed clear beta galactosidase staining (Figure 7, middle panel). Sections of the stained brain revealed that some cells were positively stained with beta galactosidase (Figure 9, left and right panels), indicating the Cre recombinase expresses in brain of the ARR2PPbi-Cre transgenic line. Consistent with the PCR analysis, the eye and penis were also found positively stained with β-gal.

**Figure 9. Expression of the Cre recombinase in the brain of the ARR2PPbi-Cre transgenic mouse.** The ARR2PPbi-Cre transgenic mouse was crossed with the B6;129-Gt(ROSA)26Sor/J mouse. Brains were derived from B6;129-Gt(ROSA)26Sor/J (left of middle panel) or B6;129-Gt(ROSA)26Sor/J-ARR2PPbi-Cre (right of middle panel) mice at the age of two months and stained with β-gal (middle panel) and then formalin-fixed and paraffin-embedded. Slides were county stained with Eosin (left and right panels).

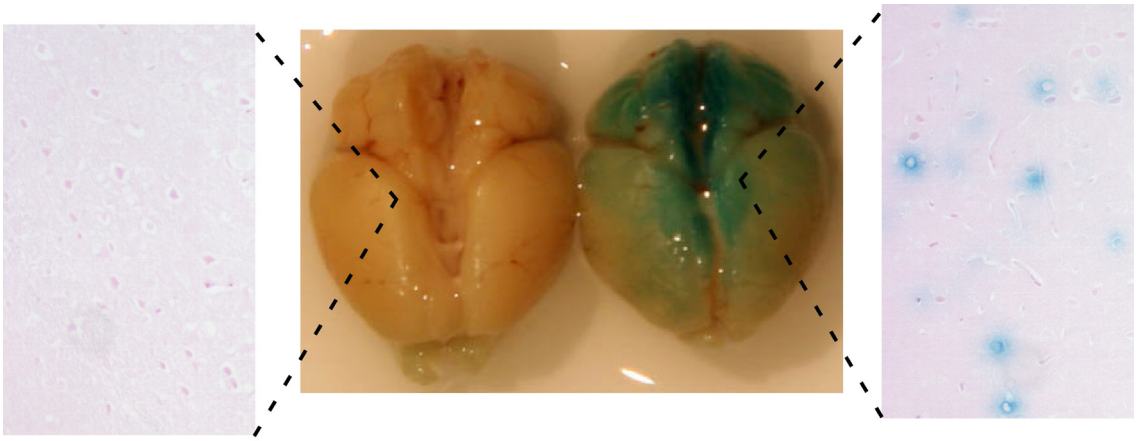

Northern blot analysis shows the Cre-mediated loss of p44/WDR77 mRNA expression in the MT mouse brain (Figure 10A, top panels). Immunostaining analysis demonstrated that p44/WDR77 protein levels were high in the nucleus in brain cells of the WT mouse (Figure 10B, top panel, indicated by arrows). These signals were dramatically reduced in brain cells of the MT mouse (bottom panel). Thus, these analyses indicate that the p44/WDR77 gene was deleted in the MT mouse brain and suggests the observed shorten lifespan in the MT mouse is possibly due to brain-specific deletion of the p44/WDR77 gene.

**Figure 10. Loss of p44/WDR77 gene and protein expression in the MT mouse brain.** A, Northern blot analysis of p44/WDR77 and β-actin mRNAs in the mouse brain. The mRNA was isolated from the brains of five WT (lane 1) or five MT (lane 2) mice at the age of two months, fractionated by electrophoresis, and transferred to a Hybond N+ membrane. The membrane was hybridized with a p44/WDR77 probe (top panel) or β-actin probe (bottom panel). B, Tissues derived from cerebral cortex of WT (top panel) and MT (bottom panel) of mouse brains were immunostained with anti-p44/WDR77 antibody. The nuclear staining of p44/WDR77 in WT mouse brain cells (indicated by arrows) was decreased in the MT mouse brain cells.

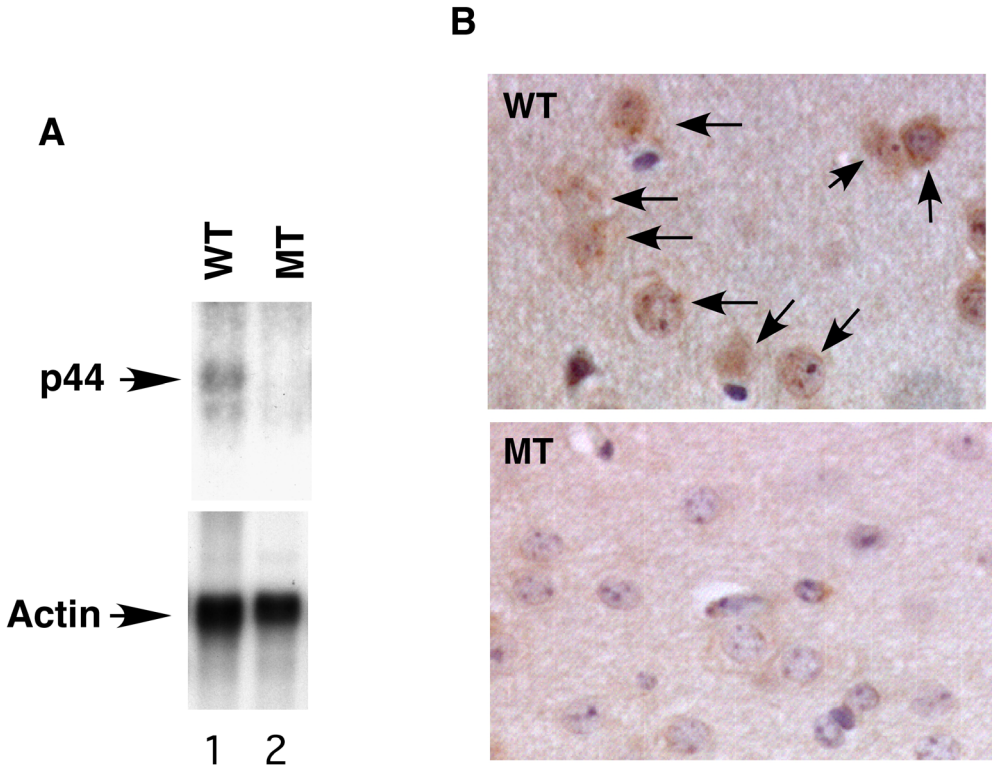

**CIV. Discussion:**

The unexpected short longevity in the MT mouse prompted us to investigate the Cre expression in *ARR2PPbi-Cre* transgenic line and the Cre-mediated deletion of the p44/WDR77 gene in the MT mouse. We found that in addition to prostate, penis, and eye, the brain expresses high levels of Cre and shows the Cre-mediated deletion of the p44/WDR77 gene. Surgical removal of the prostate along with physiologic disruptions in the prostate such as prostate cancer do not induce an accelerated aging like phenotype, suggesting the loss of the p44/WDR77 gene in the prostate is not the source of the aging like phenotype observed in MT mice (199, 200). Similarly while penile cancer can be life threatening and the surgical removal of the penis or penectomy can lead to a difficult recovery, it does not induce the aging like phenotype observed in MT mice (202, 203). Additionally surgical of the removal of the eyes or enucleation is an effective treatment for ocular cancer, and patients who have undergone these treatments do not exhibit the aging like phenotype observed in MT mice (204, 205). Further while ocular disease can elicit neural distress it has not been shown to stimulate the aging like phenotype observed in MT mice (206). While the brain a site of critical endocrine, immune, and system regulation, if disrupted or altered it could generate the phenotype observed in the MT mice (207). Thus, loss of p44/WDR77 expression in the brain is a possible drive of to the observed aging phenotype.

To explore p44/WDR77 role in the brain more deeply we crossed WT with a Nestin-Cre transgentic mice. Nestin is expressed in brain neural progenitors at E8.5 and is down regulated at the end of neurogenesis (208). Nestin-Cre expression has been shown to be an effective means of achieving central nervous system-specific gene deletions (209). A cross of the WT mouse with the mouse expressing Nestin-Cre led to embryonic lethalality, indicating the essential nature of p44/WDR77 in brain

development. The lack of a lethal phenotype in MT is indicative of the fact that only a subpopulation of brain derived cells are expressing Cre recombinase in MT mice. Suggests the loss of p44/WDR77 expression in a subset of cells the brain contributes to the observed aging phenotype. Consistent with these results, we observed in preliminary studies that down-regulation of p44/WDR77 expression was associated with aging in human brains (data not shown).

**D. Deletion of the p44/WDR77 gene induces apoptosis in the brain.**

**DI. Rationale:**

We have observed an unexpected loss in longevity in MT mice accompanied with Cre expression in the prostate, penis, eye and brain. The brain's ability to directly regulate endocrine, immune and neural functions that can invoke metabolic and other system wide changes that can result in an aging phenotype makes it a likely candidate organ for the unexpected loss in longevity seen in MT mice (210-212). The aging brain is associated with increased neurodegeneration, and as excepted increased cell death can result in disruption of neural regulation (213-215). Additionally, previous studies have shown that the loss of the p44/WDR77 gene in the prostate gland increases apoptosis and alters the differentiation of epithelial cells (180, 181). Thus, loss of the p44/WDR77 gene might lead to apoptosis in mouse brain cells.

**DII. Experimental Design:**

To study the in vivo effects of loss of the p44/WDR77 genes on apoptosis in the mouse brain, five brains from WT and MT mice were isolated. The brains were fixed and sagittal sections at 0.00 (B3), 1.00 (B4), 2.00(B2 and B4), and 3.00 (B1 and B6) mm lateral planes were obtained. Slides were made from each section and subjected to TUNEL analysis and TUNEL positive cells were normalized to total (nuclear staining) number of cells per section.

**DIII. Results:**

MT brains showed a significant increase in TUNEL positive cells in every section examined (Figure 11). Consistent with the loss of longevity no difference between males and females were seen. Additionally preliminary studies using double-stained for

TUNEL with MAP2 (staining neurons), suggest the majority of the apoptotic cells in the MT brain sections are neurons. These results suggest p44/WDR77 is important for neuron cell survival and possible neuroprotection.

**Figure 11. Deletion of the p44/WDR77 gene increased apoptosis in MT mice brains.** A, B, Sagittal section at 0.00 (B3), 1.00 (B4), 2.00(B2 and B4), and 3.00 (B1 and B6) mm lateral planes were taken from WT and MT mice brains at the age of 3 months were subjected to Terminal deoxynucleotidyl transferase mediated dUTP nick end labeling (TUNEL) assay (A). The Tunnel-positive cells indicated by white arrows (A) were quantitated (B).

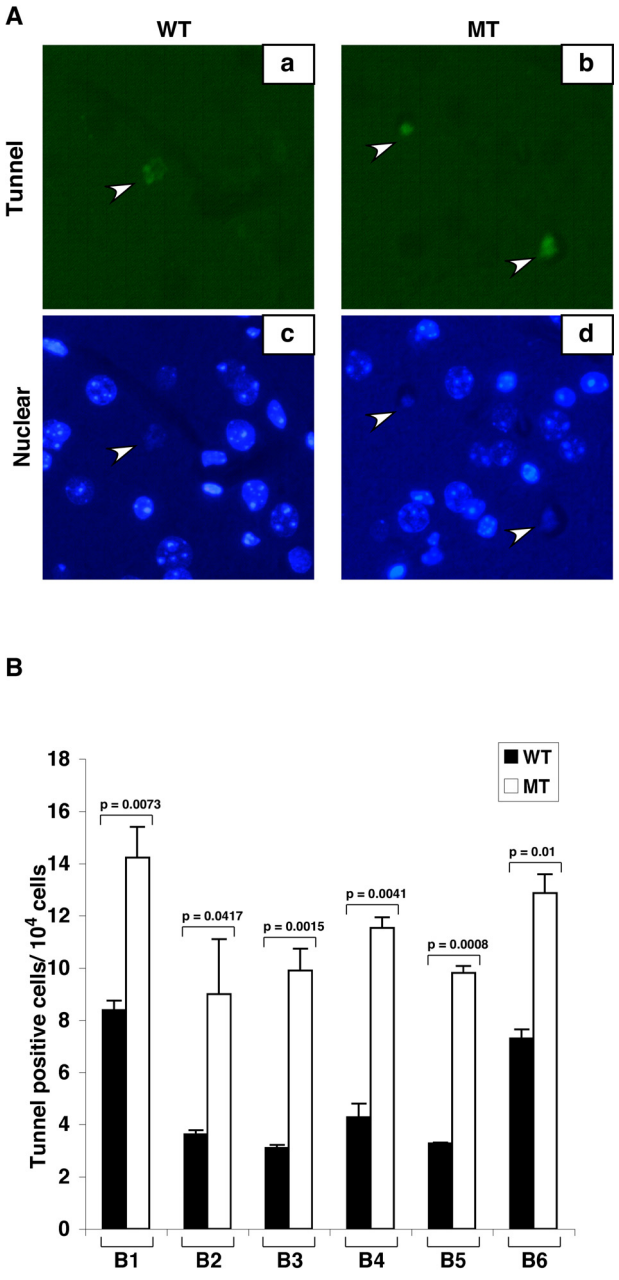

**DIV. Discussion:**

In these experiments we demonstrate that the loss of p44/WDR77 leads to increased cell death in the mouse brain. Additionally preliminary studies suggest that the majority of the apoptotic cells in the MT brain sections are neurons. The known association between aging and increased neural apoptosis and preliminary studies that show a decrease in p44/WDR77 in ageing human brains further strengthens an ageing like phenotype in MT mice (216, 217). A direct effect on neural survival would likely yield a focalized effect on neurons expressing Cre recombinase. The ubiquitous modest increase in apoptosis observed here is suggestive of an indirect glial effect on neural survival.

Previous studies in our lab demonstrated the loss of the p44/WDR77 gene in the prostate gland increases apoptosis and alters the differentiation of epithelial cells (180, 181). These studies suggest that p44/WDR77 has a direct or indirect role in regulating cell survival. Decreased glucocorticoids and androgens have been associated with an increased risk for neurodegenerative diseases (218, 219). Androgens and glucocorticoids down-regulate reactive gliosis after neural injury (220, 221). P44/WDR77 has the ability to act as a cofactor to modulate AR- or glucocorticoid receptor (GR)-dependent gene expression (180). Based on these observations, we anticipate that p44/WDR77 might mediate the suppressive effect of androgen or/and glucocorticoid on astrocyte activation. It is also possible that p44/WDR77 might interact and function with other DNA-binding proteins in astrocytes.

**E. Loss of the p44/WDR77 gene leads to reactive astrocytes in the mouse brain.**

**EI. Rationale:**

We have observed an unexpected sharp reduction in the longevity of MT mice accompanied with Cre expression the brain. Preliminary studies show a decrease in p44/WDR77 in aging human brains, suggesting the loss in longevity is an aging like phenotype in MT mice. Additionally MT mice present with a ubiquitous increase in apoptosis in neuron cells, suggesting an indirect glial effect of p44/WDR77 on neural survival. This implies reactive astrogliosis might play a role in pathology and possibly the pathogenesis of MT mice.

Increased reactive astrogliosis is an aspect of normal brain aging (222, 223). Additionally severe reactive astrogliosis has become a pathological marker of age-related diseases such as Alzheimer, Parkinson, and Huntington (224-226). Molecular alterations that occur during reactive astrogliosis, can have both advantageous and disastrous effects invoked through the multitude of astrocyte function and subsequent secondary actions on the surrounding CNS environment (88, 89). These effects have been shown to directly affect patient outcome (39, 50, 85, 225). Thus a better molecular understanding of reactive astrogliosis could strengthen our quality of patient care.

**EII. Experimental Design:**

To examine reactive astrogliosis in MT mice we immunohistochemically stained brain tissues from WT and MT mice with p44/WDR77 and GFAP. Brains from WT and MT mice were isolated at 2 months of age. The brains were fixed and sectioned at lateral 2.00mm. The sections were first stained with a p44/WDR77 antibody to assess p44/WDR77 expression in astrocytes. The sections were then subjected to a stain for

GFAP. Astrocytes exhibiting strong GFAP expression and other morphologic features of reactive astrocytes were quantitated.

**EIII. Results:**

The p44/WDR77-positive signals in many astrocytes largely disappeared in the MT mouse brain (Figure 12A, panel b versus panel a). In WT mouse brain, only a few astrocytes (with strong GFAP staining and in spiny shapes) were reactive (Figure 12A, panel c, indicated by white arrows). In contrast, in MT mouse brain, more reactive astrocytes were noticed throughout the cerebral cortex (panel d, some are indicated by white arrows.). The cerebral cortex at the 2.00mm lateral plane in the MT mouse brain contained 1,560 ± 166 reactive astrocytes (Figure 12B). But the reactive astrocytes in the WT mouse brain were much less (280 ± 31 reactive astrocytes in the cerebral cortex at the 2.00 mm lateral plane). It is noticed that none of the reactive astrocytes expressed p44/WDR77 (Fig. 12A, panel f). Thus, loss of p44 expression in mouse brain leads to reactive gliosis.

**Figure 12. Loss of the p44/WDR77 gene leads to reactive astrocytes in the mouse brain**. A, Reactive astrocytes were observed in the MT mouse brain. The sections (lateral 2.00 mm) of cerebral cortex were derived from WT (left panels) or MT (right panels) brain and stained with anti-p44/WDR77 (top panels) or anti-GFAP (middle panels) antibodies. The p44/WDR77 staining was merged with the GFAP staining (bottom panels). Some reactive astrocytes are indicated by white arrows. B, The quantitative data of reactive astrocytes in WT and MT brains are shown.

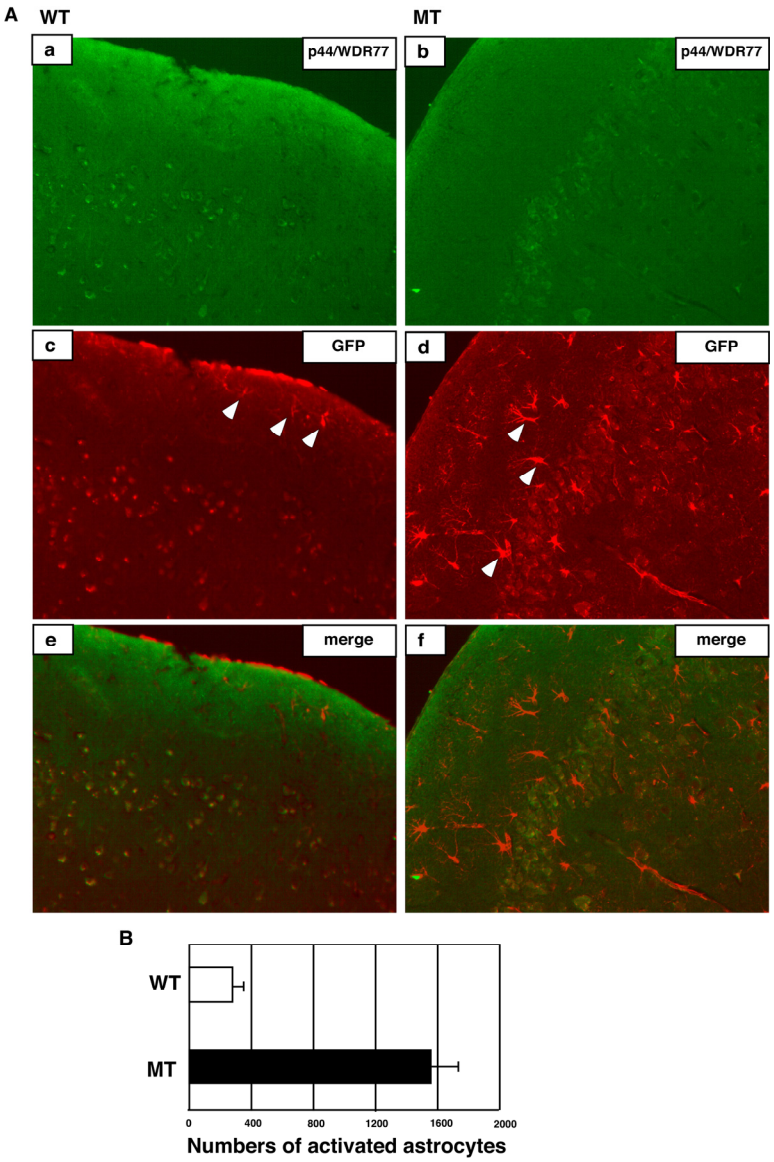

**EIV. Discussion:**

These experiments revealed the expression of p44/WDR77 in astrocytes in the mouse brain and its expression was significant decreased in the MT mouse brain. Astrogliosis was only observed in astrocytes that had lost p44/WDR77 expression. While the significant increase in astrogliosis in the MT mouse brain could be the result of some other factor making the microenvironment unfavorable for neurons and astrocytes, the lack of p44/WDR77 expression in activated astrocytes suggests a role for p44/WDR77 in astrocytes activity.

Previous studies in our lab have shown that prostate epithelial cells from MT are less differentiated relative to those in the wild-type litermates (181), suggesting p44/WDR77 plays a role in cellular differentiation and possibly astrocyte activation. While many of the detailed mechanisms of astrocyte activation remain to be elucidated, a number of pathways have been implicated in astrocyte activation (50). The effects of some of these pathways can be seen in studies that demonstrate decreased glucocorticoids and androgens are associated with an increased risk for neurodegenerative diseases. Androgen and glucocorticoid down-regulate reactive gliosis after neural injury (227-229). P44/WDR77 has the ability to act as a cofactor to modulate AR- or glucocorticoid receptor (GR)-dependent gene expression (180). Based on these observations, we anticipate that p44/WDR77 might mediate the suppressive effect of androgen or/and glucocorticoid on astrocyte activation. It is also possible that p44/WDR77 might interact and function with other DNA-binding proteins in astrocytes.

# Chapter IV: Hypothesis and Aims

**Rationale:**

Astrocytes have numerous critical functions in the CNS. Additionally reactive astrogliosis has been shown to influence the clinical outcome in every form of CNS pathology. Despite decades of research on activated astrocytes and clinical implications in CNS insults the fundamental mechanisms about this phenomenon are just beginning to take shape (50).

Preliminary data demonstrated increased levels of reactive astrogliosis and cellular apoptosis in the brains of MT mice. The ubiquitous modest increase in CNS apoptosis observed in MT is suggestive of an indirect astrocyte effect on neural survival. Recent studies have suggested that the AR-target gene $p21^{Cip1}$ directly effects astrocytes activation (140, 141, 152, 172). This finding correlates with increased $p21^{Cip1}$ expression in MT mice brains illustrated in our whole brains gene array from MT and WT mice. $P21^{Cip1}$ has been implicated as a positive modulator of NF-κB, a potent inflammatory transcription factor (132, 140, 141), suggesting the loss of p44/WDR77 in astrocytes might lead to deleterious effects on the CNS through the up regulation of $p21^{Cip1}$ expression and subsequence NF-κB activation (131, 140, 141). P44/WDR77's ability to regulate astrocyte activation through NF-κB and $p21^{Cip1}$ remains unexplored and represents a means to better understanding of and treatment of neurological pathologies (50).

**Hypothesis:**

Deletion of the *p44/*WDR77 gene induces astrocyte activation.

**Aims:**

Aim 1: To identity brain derived cells expressing p44/WDR77

Aim 2: To assess effects of p44/WDR77 on astrocyte activation

Aim 3: To examine roles of $p21^{Cip1}$ in astrocyte activation induced by the loss of p44/WDR77.

Aim 4: To examine roles of NF-κB activation in astrocyte activation induced by the loss of p44/WDR77.

# Chapter V:

# Aim 1: To identity Brain-derived cells expressing p44/WDR77

# and

# Aim 2: To assess effects of p44/WDR77 on Astrocyte activation

**A. Astrocytes in the brain express the p44/WDR77 protein.**

**AI. Rationale:**

Astrocytes mediate numerous critical functions in the CNS. Additionally reactive astrogliosis has been shown to influence the clinical outcome in every form of CNS pathology (50). These clinical observations highlight the need to understand the nature and molecular mechanisms of action that induce astrocyte activation and reactive astrogliosis.

Increased levels of reactive astrogliosis and cellular apoptosis are evident in the brains of MT mice. To gain a mechanistic understanding for the unexpected induction of reactive astrogliosis and any roles of p44/WDR77 in the MT mouse brain we endeavored to learn the initiating cell type of this phenotype. The presence of p44/WDR77 in inactivated astrocytes along with its absence in activated astrocytes is suggestive of a direct involvement in astrocyte activation. Additionally the ubiquitous modest increase in CNS apoptosis observed in MT is suggestive of an indirect glial effect on neural survival. When endeavoring to understand what mechanistic steps are responsible for p44/WDR77-induced reactive astrogliosis the first question is what cell types in brain are expressing p44/WDR77.

**AII. Experimental Design:**

To determine which cell types in the mouse brain express the p44/WDR77 protein we double-immunostained stained brain tissues from WT mice with p44/WDR77-antibody and one of the two cellular markers NeuN (neurons) and GFAP (astrocytes). Brains from WT were isolated at 2 months of age. The brains were fixed and sectioned at lateral 2.00 mm. The sections were first stained with p44/WDR77-antibody. The next day the sections were subjected to a second stain for GFAP to

examine p44/WDR77 expression in astrocytes or NeuN to examine p44/WDR77 expression in neurons. Cells expressing p44/WDR77 and one of the two markers were quantitated per field of view under 20X magnification.

**AIII. Results:**

Population of the p44/WDR77 positive cells co-localized with GFAP staining (Figure 13), indicating that p44/WDR77 is expressed in astrocytes. Further immunostaining analysis with an anti-NeuN antibody indicated revealed that GFAP negative cell (indicated by white arrows) that stained positive for p44/WDR77 are neurons (Figure 14). Similar analysis indicates that p44/WDR77 is expressed in astrocytes of human brain tissues (Chemicon, TMA3001-4) data not shown.

**Figure 13. P44/WDR77 expression in astrocytes of mouse brain.** A, B, Tissues were derived from cerebral cortex of the WT mouse brain were double-immunostained for p44/WDR77 (A) and GFAP (B). C, The GFAP staining signals are merged with p44/WDR77 staining.

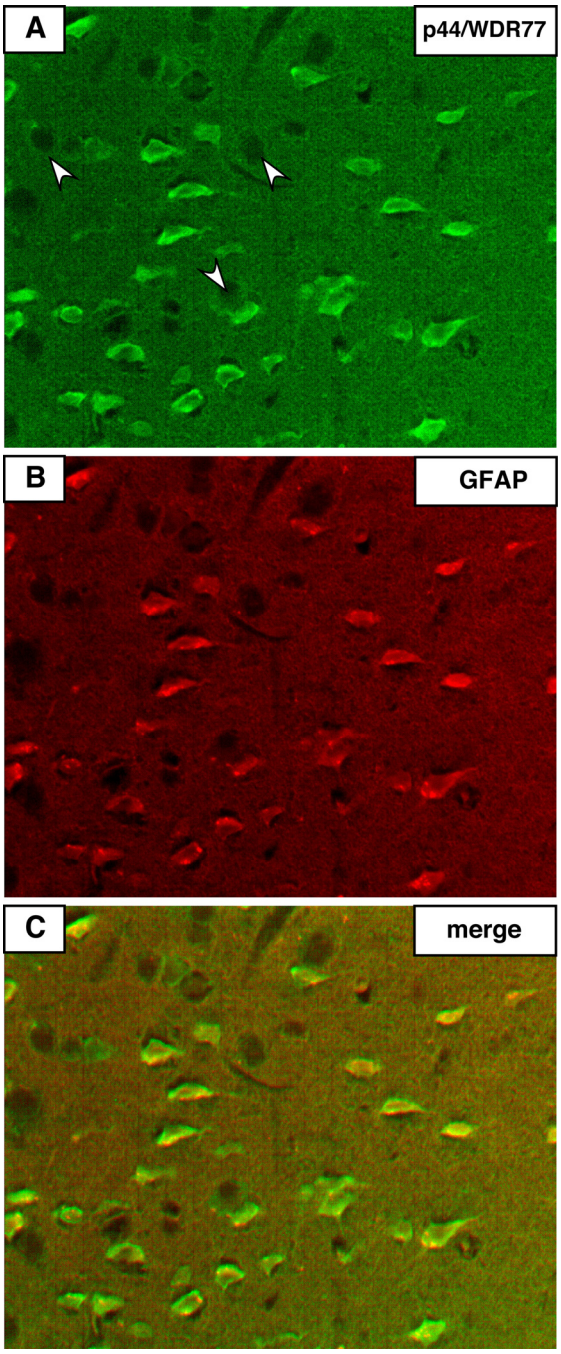

**Figure 14. P44/WDR77 expression Neurons of mouse brain.** A, B, Tissues were derived from cerebral cortex of the WT mouse brain were double-immunostained for p44/WDR77 (A) and NeuN (B). C, The NeuN staining signals are merged with p44/WDR77 staining.

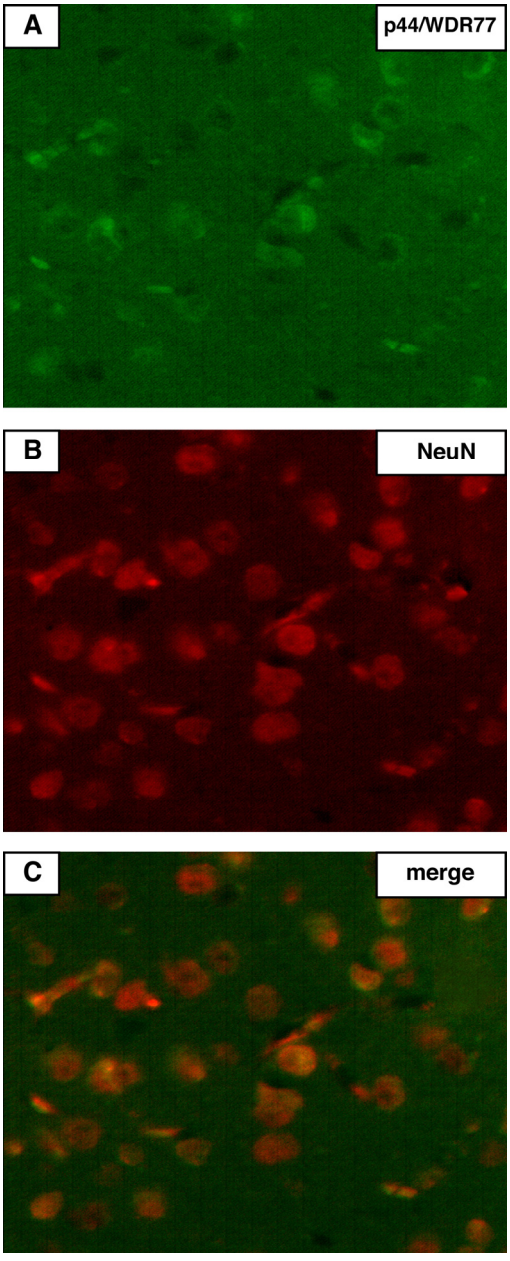

**AIV. Discussion:**

These experiments revealed by immunostaining astrocytes and some neurons express p44/WDR77 in the mouse brain. With such broad level of expression of p44/WDR77 in NeuN positive neurons a dramatic increase in neural apoptosis would be excepted if the loss of p44/WDR77 was the primary cause for the increased apoptosis, contrary to the modest increase in CNS apoptosis seen in MT mice. Thus the ubiquitous modest increase in CNS apoptosis observed in MT suggests p44/WDR77 has an indirect effect on neural survival in brains of MT mice. However there are multitudes of ways where seemly subtle changes in neurons pathophysiology such as alteration in glutamate production could result in toxic environments which in turn generate both increased apoptosis and reactive astrogliosis (50, 104, 111). However many of these alterations would result in a focalized effect around the toxic environment, unlike the ubiquitous one that presents in the brains of MT mice (50). Despite these finding, it is not clear whether the loss of p44/WDR77 expression in astrocytes and/or in some neurons leads directly to the observed reactive astrogliosis.

**B. Loss of p44/WDR77 expression leads to increased GFAP expression in astrocytes.**

**BI. Rationale:**

Astrocytes, the most abundant cell type in the brain, were long believed to merely be a supportive component of the CNS and their activation was seen as a disease marker in the CNS (25, 38). Now, however they are appreciated for having critical roles in the health CNS, with both advantageous and disastrous effects during pathological states (39, 50). Even as their vast importance comes to light, many of the molecular mechanism that initiates the changes in astrocytes to induce advantageous or disastrous effects remain unclear (50).

The loss of p44/WDR77 mediated by ARR2PPbi-Cre induces increased levels of reactive astrogliosis in the brains of MT mice. We found that p44/WDR77 is expressed in inactivated astrocytes while astrocytes in an activated state do not express p44/WDR77. This result coupled with an ubiquitous modest increase in CNS apoptosis in MT mice, implies that p44/WDR77 plays a direct role in astrocyte activation. However this view is complicated by the presences of p44/WDR77 in NeuN positive neurons even with the lack of focalized astrogliosis and apoptosis in the brains of MT mice. This rationalizes a need to study MT and WT astrocytes in an environment independent of the effects of other cell types.

**BII. Experimental Design:**

To study MT and WT astrocytes independently of other brain-derived cells, primary astrocytes were isolated from newborn mouse cerebra cortex (184). These primary cells were grown in the tissue culture for five days, after which they were

transferred to chamber slides for immunostaining with anti-GFAP antibodies to confirm a pure population of astrocytes.

To confirm the deletion of p44/WDR77 in primary MT astrocytes cells they were fixed in paraformaldhyde and embedded in low melting agarose (Sigma-Aldrich) and paraffin. Section taken from the cell block underwent staining with anti-p44/WDR77 antibodies.

To assess astrocyte activation in WT and MT primary astrocytes cell lysates were prepared after five days of culture. These lysates were subjected to Western blot analysis with anti-p44/WDR77 and anti-GFAP antibodies.

**BIII. Results:**

Primary MT astrocytes could rarely be maintained in culture for more then 5 to 7 days; in fact many of the astrocytes isolated from MT mice did not survive past the first day of culture. This result is contrary to primary WT astrocytes which could be maintained in tissue culture for over two weeks.

The immunohistochemistry staining of primary astrocytes with anti-GFAP antibodies revealed that more than 95% of the cell culture population was GFAP-positive cells (Figure 15A). While immunohistochemistry staining of primary WT astrocytes with anti-p44/WDR77 antibodies revealed that 100% of the astrocytes expressed p44/WDR77, only 50% of the primary astrocytes from MT mice expressed p44/WDR77 (Figure 16 A, B).

Western blot assays using lysates from primary astrocytes demonstrated a significantly decreased expression of p44/WDR77 in astrocytes from MT mouse brain (Figure 15B, top panel, lane 2 versus lane 1). This decrease in p44/WDR77 expression correlated with an increase in GFAP expression (Figure 15B, bottom panel, lane 2

versus lane 1), suggesting that loss of the p44/WDR77 gene leads to astrocyte activation.

**Figure 15. P44/WDR77 expression in primary astrocytes.** A, GFAP staining (green) of primary astrocytes in the tissue culture. The nucleus was staining with DAPI. B, Lost of p44/WDR77 expression in astrocytes isolated from the MT mouse brain. The whole cell lysates (20 μg protein) were made from astrocytes isolated from the WT (lane 1) and MT (lane 2) mice. Western blot analysis was performed with anti-p44/WDR77 (top), anti-GFAP (middle), or anti-actin (bottom) antibody.

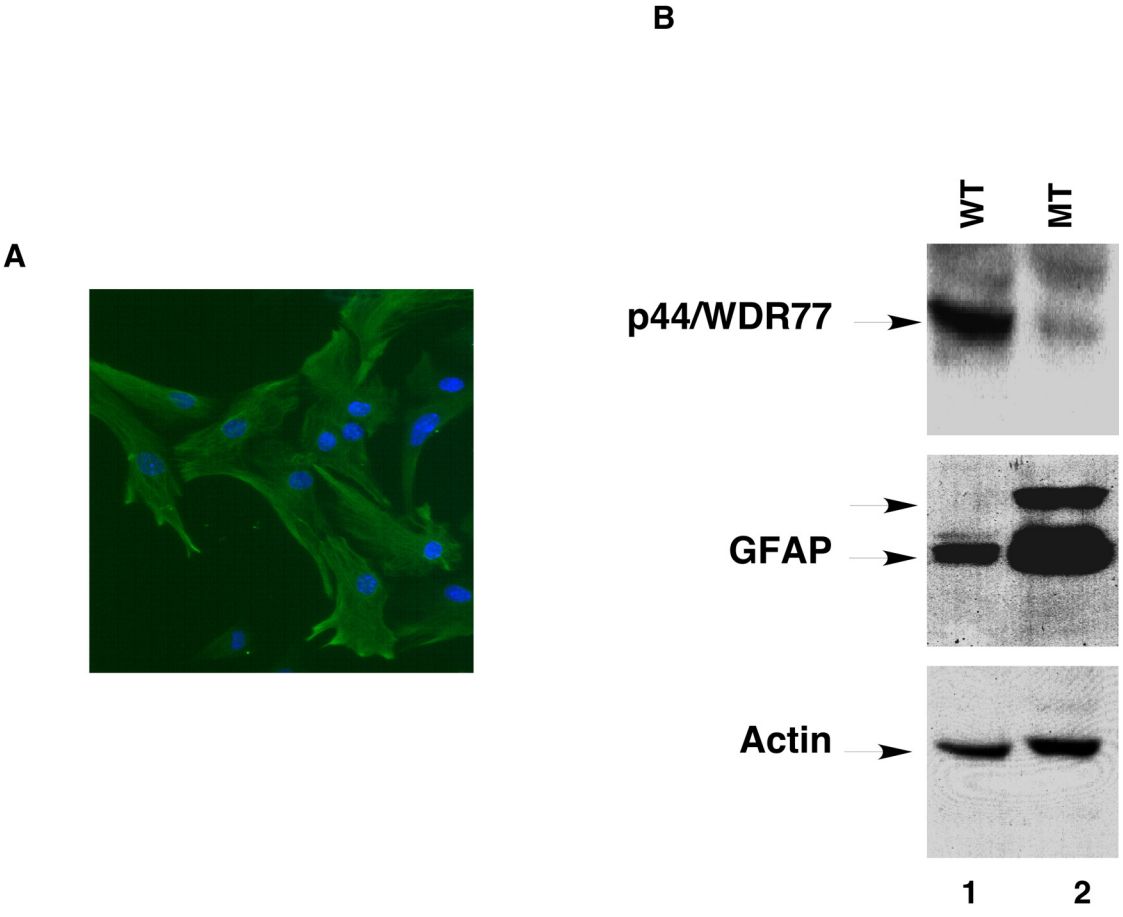

**Figure 16. Some MT primary astrocytes express P44/WDR77.** A, Primary astrocytes were isolated from MT and WT mice and stained for nuclear staining (a and d) and p44/WDR77 (b and e). Arrows indicate p44/WDR77 negative cells (c). The p44/WDR77 staining signals are merged with nuclear staining (c and f). B, The quantitative data of p44/WDR77 protein expression in WT and MT astrocytes are shown.

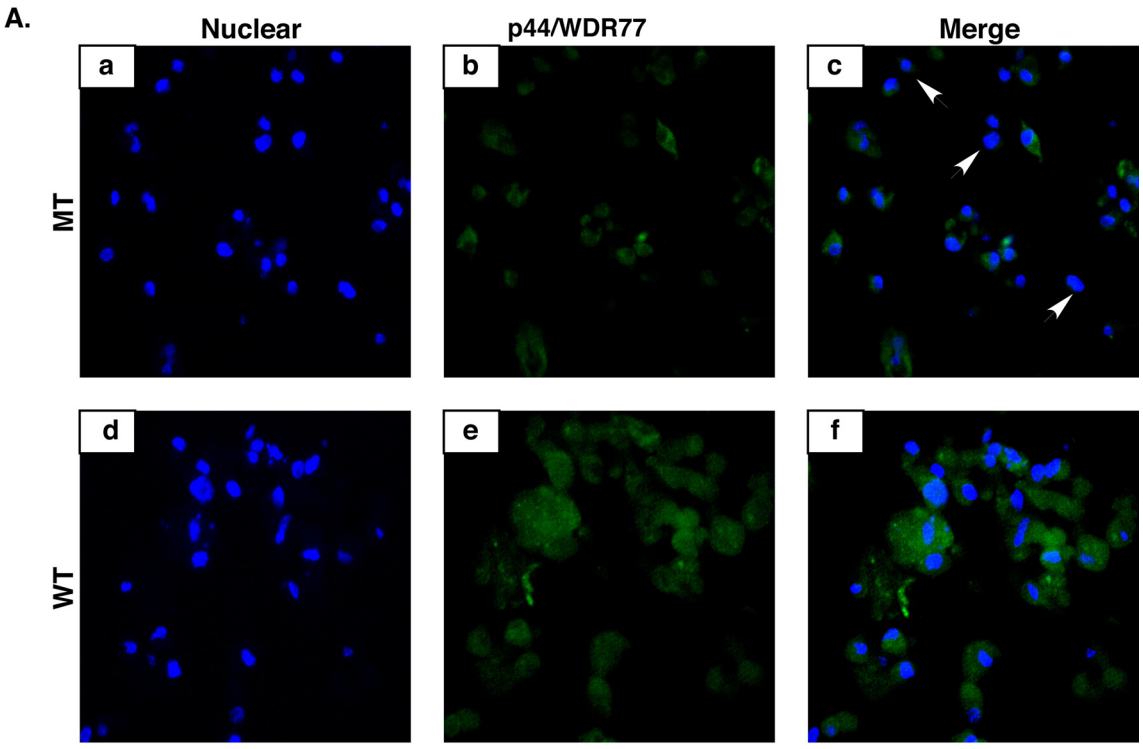

**BIV. Discussion:**

The experiments depicted in Figure 12 demonstrated a significant increase in astrogliosis in the MT mouse brain, prompting us to investigate the role of p44/WDR77 in astrocytes. In vitro culture of primary astrocytes revealed a dramatic decrease in the survival of MT astrocytes, not seen in the brains of the adult MT mice. This discrepancy could be due to changes that occur from being in the culture; however this is unlikely to be the only cause for this loss of survival when considering the survival of WT astrocytes was unaffected in culture. Additional factors such as the lack of vascular clearance of toxic molecules being secreted from highly activated astrocytes could be contributing to this loss of survival (50). The possibility of the accumulation of toxic molecules induced by astrocyte activation was strengthened by increase in GFAP protein expression and inductive astrocytes activation correlated with a decrease in p44/WDR77 in MT astrocytes. Additional support for this toxic effect comes from the large number of MT astrocytes expressing p44/WDR77; suggesting p44/WDR77-null astrocyte can influence the survival of adjacent p44/WDR77 positive astrocytes. Thus, the mixed expression of p44/WDR77 in primary MT astrocytes complicates our understanding of the direct effects of the loss of p44/WDR77 on astrocyte function. While the mechanisms of action remain unclear the striking difference in GFAP protein expression and survival seen between WT and MT primary astrocytes illustrates that p44/WDR77 has a critical role in astrocyte activity.

**C. Primary astrocytes isolated from MT mice brains have increased levels of apoptosis and cell division.**

**CI. Rationale:**

Increased levels of reactive astrogliosis in the brains of MT mice, accompanied by up regulated GFAP expression associated with decreased p44/WDR77 in primary astrocyte suggest the loss of p44/WDR77 in astrocytes induces astrocyte activation. Considering the role of astrocytes in CNS physiology, p44/WDR77's involvement in the their induction of activation as well as p44/WDR77's known roles in the prostate prompts a deeper study into p44/WDR77 functions in astrocytic cellular proliferation and death (50, 179). This importance is compounded by our limited understanding of the mechanisms that induce proliferation in astrocytes, and the roles proliferating astrocytes have during severe reactive astrogliosis at blurring the boundaries between individual astrocytes and glial scaring (92, 50).

**CII. Experimental Design:**

To examine the effect of p44/WDR77 deletion on astrocyte proliferation, primary astrocytes were isolated from the brains of one day WT and MT mice. After 4 days culture the astrocytes were plated on a 100mm cell culture plate. 18 hours later the cell were pulsed with BrdU (10$\mu$M) for 4 hours, followed by fixation and embedding in low melting agarose (Sigma-Aldrich). The sections were cut from these agarose pellets after being embedded in paraffin. Cells in S-phase cells in these sections were identified and quantitated by immunohistochemistry with anti-BrdU antibody.

To study the in vitro effects of loss of the p44/WDR77 genes on apoptosis in astrocytes, primary astrocytes were isolated from the brains of one day WT and MT mice. Following 5 days of the culture, astrocytes were fixed in paraformaldhyde and

embedded in low melting agarose (Sigma-Aldrich) and paraffin. Section taken from the fixed-cell block was submitted to TUNEL analysis.

**CIII. Results:**

The immunohistochemistry with anti-BrdU antibody showed an increase of proliferative cells in MT astrocytes compared to the WT astrocytes (Figure 17). BrdU–positive cells were quantified in WT and MT astrocytes and p44/WDR77 deficiency increased proliferation (BrdU-positive cells) in astrocytes (from 8 ± 3/per 100 cells to 16 ± 2/per 100 cells), a finding consistent with increased GFAP expression that suggest astrocyte activation (Figure 17).

**Figure 17. Increased proliferation in MT astrocytes.** BrdU-positive cells from MT and WT astrocytes were quantitated

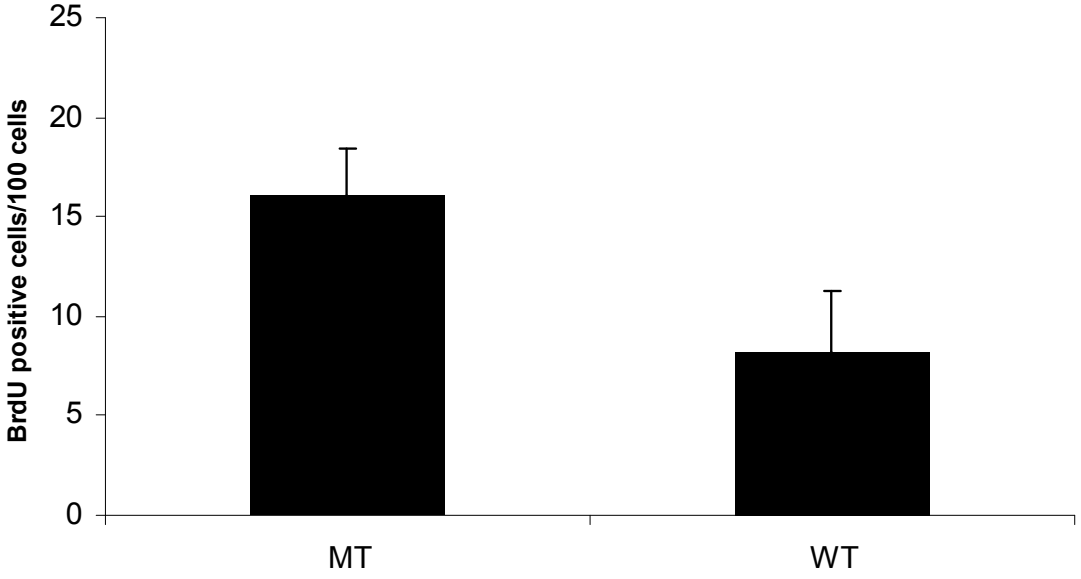

TUNEL analysis of WT and MT astrocytes revealed an increase in apoptotic MT astrocytes (Figure 18). TUNEL–positive cells were quantified in WT and MT astrocytes demonstrated that p44/WDR77 deficiency increased apoptosis (TUNEL-positive cells) in astrocytes (from 5 ± 1/per 100 cells to 11 ± 1/per 100 cells) with a p value of less than 0.05 by student test, a finding consistent with the poor survival of survival observed in primary culture of MT astrocytes (Figure 18).

**Figure 18. The increased apoptosis in MT astrocytes.** TUNEL-positive cells from MT and WT astrocytes were quantitated.

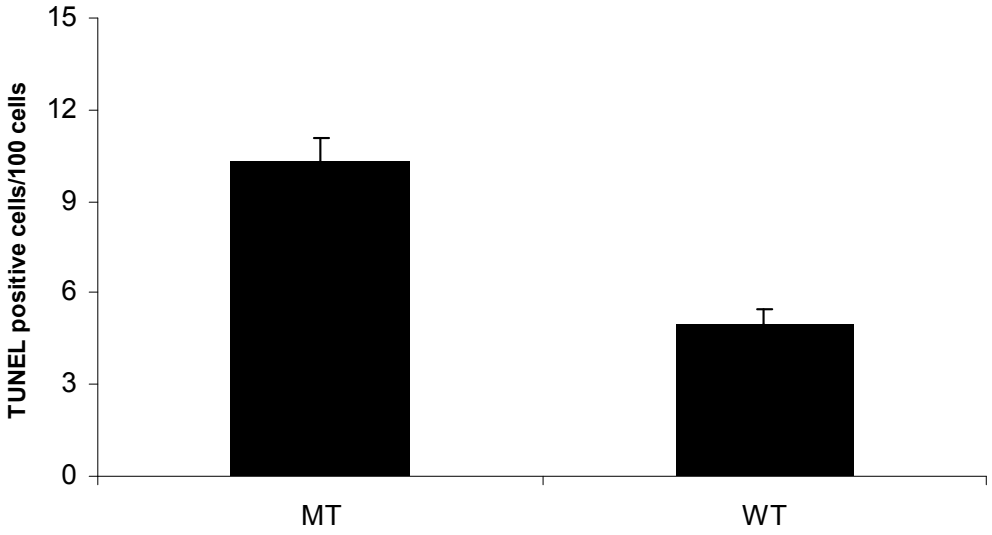

**CIV. Discussion:**

These experiments demonstrate that the loss of p44/WDR77 in astrocytes leads to increased cell death and cell division. These results are consistent with prior studies in our lab that demonstrated the loss of the p44/WDR77 gene in the prostate gland increases proliferation and apoptosis and alters the differentiation of epithelial cells (180, 181). Additionally these finding with the results from experiments depicted in Figures 12 through Figure 15 and studies by others that illustrate some state of astrocytes activation induce astrocyte proliferation and apoptosis, suggest that the loss p44/WDR77 leads to astrocytes activations. While our understanding of astrocyte proliferation and survival during activational states still remain unclear, p44/WDR77 could be directing regulatory actions through the androgen regulated genes endothelin-1 and $p21^{Cip1}$ (152, 172, 179, 230). The lack of a dramatic increase in astrocyte apoptosis in the brains of MT mice complicates our understanding of the direct affects the loss of p44/WDR77 to has on astrocyte proliferation and apoptosis. The lack of a significant increase in astrocyte apoptosis in the brains of MT mice might be explained by changes induced by cell culture or the mice with exhibiting high Cre recombinase are dying prior to TUNEL analysis of the whole brain. Even still the mix expression of p44/WDR77 in primary MT astrocytes further complicates the interpretation and raising the questions as to whether the increased proliferation and apoptosis observed in these experiments are secondary effects arising from changing in the secretion of signaling molecules being released from 44p/WDR77 deficient astrocytes, acting on WT astrocytes or a direct affect by 44p/WDR77 on astrocyte function.

**D. Loss of the *p44* gene increased apoptosis and decreased proliferation of astrocytes.**

**DI. Rationale:**

During severe reactive astrogliosis proliferating astrocytes fuse with other glial cells, fibroblast and the cellular architecture of the surround CNS to give birth to glial scars (100, 102). While glial scars can act as neuroprotective barriers that isolate deleterious agents, they are permanent markers of CNS severe reactive astrogliosis that hinder axonal regeneration and patient recovery (94, 95, 99, 103). The experiments illustrated in Figures 12 through Figure 15 suggest that the loss p44/WDR77 leads to astrocyte activations. Additionally primary MT astrocytes showed increased levels of cell growth and death (Figures 17 and 18), suggesting p44/WDR77 has a role in regulating the poorly understood pathways of astrocyte apoptosis and proliferation (50). These findings were complicated by mixed expression of p44/WDR77 in primary MT astrocytes. These limitations rationalize a need to study astrocytic functions in a system containing a pure population of p44/WDR77 deficient astrocytes.

**DII. Experimental Design:**

To further study p44/WDR77 function, astrocytes were isolated from *p44/WDR77*$^{loxP/loxP}$ mouse brains and immortalized with a vector expressing E6/E7 (185). E6 protein interacts with p53 resulting in its degradation through the ubiquitin pathway, and E7 associates with Rb disrupting the interaction between Rb and E2F transcription factors, efficiently immortalizing cells (231, 232). Eight cell lines were obtained and all immortalized astrocytes express E6/E7. Two immortalized astrocyte cell lines (E3.1 and E3.2) were infected with either adenovirus Ad-CMV-GFP or Ad-CMV-Cre–GFP to generate 4 cell lines (WT: E3.1 GFP, E3.2 GFP, MT: E3.1 Cre, E3.2

Cre). GFP expression was examined in the infected astrocytes under a fluorescent microscope. PCR analysis was used to confirm the deletion of the p44/WDR77 gene, as indicated by excision of the exons 2-5 of the p44/WDR77 gene, in the MT astrocytes but not in the WT astrocytes (Figure 18B inset). Nine days after infection MT and WT astrocytes were immunostained for p44/WDR77. After p44/WDR77 deletion was confirmed, astrocytes in culture were examined under 10X magnification from 9 day to 12 day after adenovirus infection to assess the effects of the loss of the p44/WDR44 gene on astrocytes structure.

Then to examine the growth of MT astrocytes, cells were seeded to a 24-well plate and counted everyday from day 9 to day 13 post adenovirus infection. Twelve days after adenovirus infection, astrocytes were subjected to cytometric analysis of the cellular DNA content to further explore p44/WDR77 role in astrocyte growth and apoptosis.

**DIII. Results:**

Examination of GFP expression in the infected astrocytes revealed 100% infection efficiency three days post infection (Figure 19).

**Figure 19. The Cre recombinase-mediated deletion of the p44/WDR77 gene in astrocytes.** A, Diagram illustrates the procedure of astrocyte immortalization and p44/WDR77 gene deletion. B, GFP expression in the adenovirus-infected WT and MT astrocytes

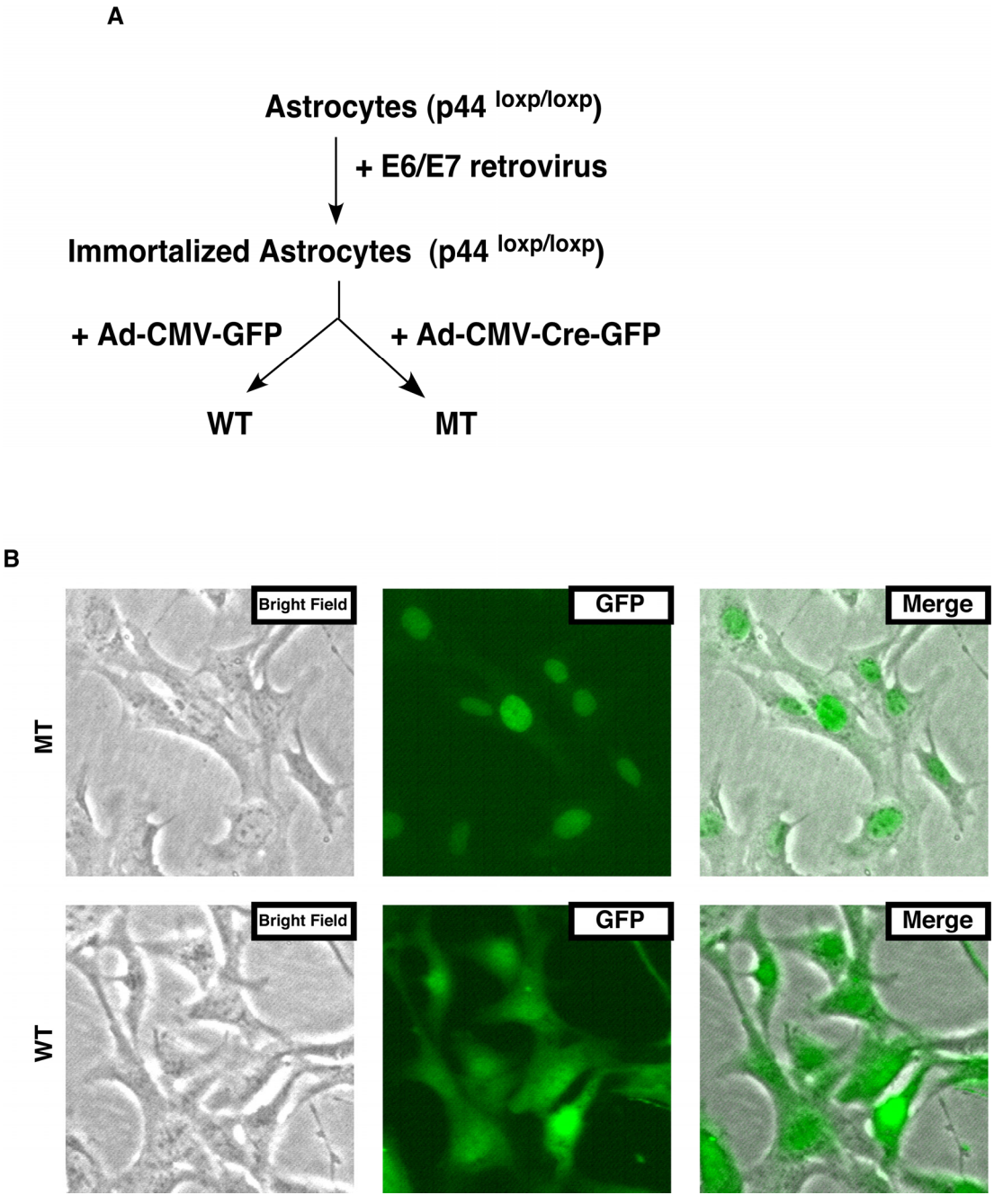

The immunohistochemistry with anti-p44/WDR77 antibody illustrated significant decreases in the levels of the p44/WDR77 protein in MT astrocytes 7 days post infection. The p44/WDR77 signals in MT astrocytes were reduced to the level of the negative control (Figure 20B lower insert) 9 days post infection (Figure 20B). In contrast, p44/WDR77 expression in the WT astrocytes did not change upon adenovirus (Ad-CMV-GFP) infection (Figure 20E).

**Figure 20. Deletion of the p44/WDR77 gene in astrocytes.** A-F, Astrocytes were infected with Ad-CMV-GFP (WT) or Ad-CMV-Cre-GFP (MT) and stained for nucleus (A and D) and p44/WDR77 (B and E). The p44/WDR77 staining signals are merged with nuclear staining (C and F). The lower left corner of A-C depicts staining of WT without the p44/WDR77 antibody. The upper right corner of B depicts PCR analysis of the *p44/WDR77* deletion in WT and MT astrocytes.

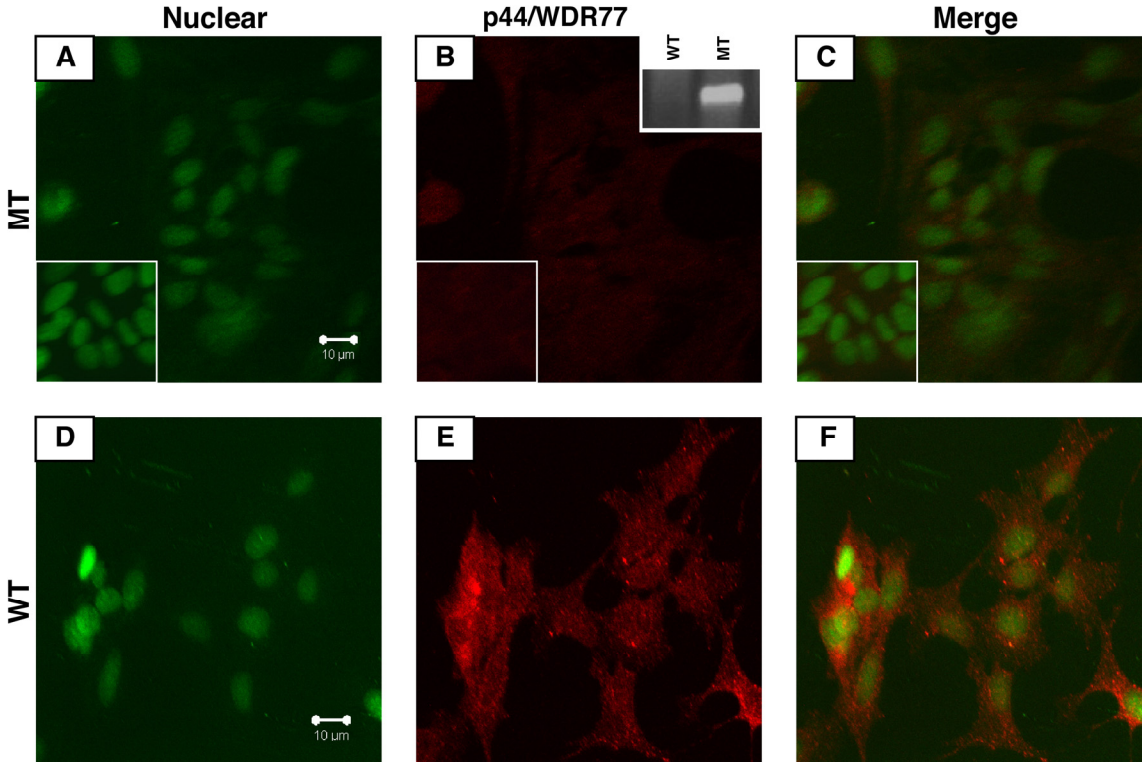

The MT (E3.1 Cre, E3.2 Cre) astrocytes presented with a noticeable increase in the number of multinuclear cells (72%) (Some are indicated by black arrows), hypertrophy of cell nuclei and cytoplasmic regions (90%) (White arrows indicate some.) (Figure 21A, B, E, F). In contrast, the WT (E3.1 GFP, E3.2 GFP) astrocytes present with normal cellular structure (Figure 21C, D, G and H). When the WT cells were approaching 100% confluency (on day 11), cells were split and continued to grow (Figure 19H). However, the MT astrocytes showed a steady decline in cellular density and never approached 100% confluency (Figure 21 E, F).

**Figure 21. Loss of the p44/WDR77 gene alters the cellular structure of astrocytes.** A-H, WT and MT astrocytes were observed 9 (A and C), 10 (B and D), 11 (D and G), and 12 (F and H) days after adenovirus infection. The upper left corners depict an enlarged region from panels indicated by black boxes.

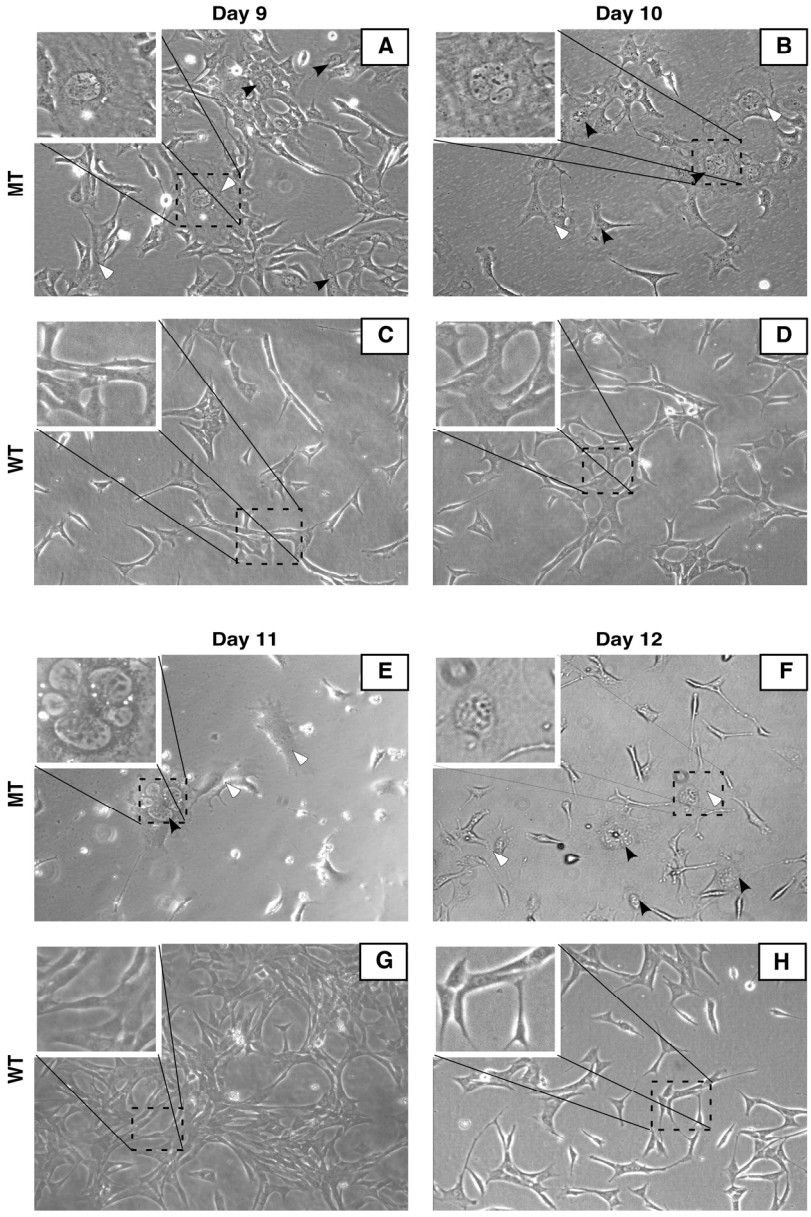

In the growth analysis WT (E3.1 GFP and E3.2 GFP) astrocytes cells continued to increase in cell number until day 12 when they reach confluency (Figure 22). The doubling times for E3.1 GFP and E3.2 GFP are 24 hours and 22 hours, respectively. In contrast, the MT (E3.1 Cre and E3.2 Cre) astrocytes presented with only a sight increase in cell number over the course of 5 days (Figure 22).

**Figure 22. Deletion of the p44/WDR77 gene inhibits growth.** Growth curves of WT (E3.1 GFP, E3.2 GFP) or MT (E3.1 Cre, E3.2 Cre) astrocytes.

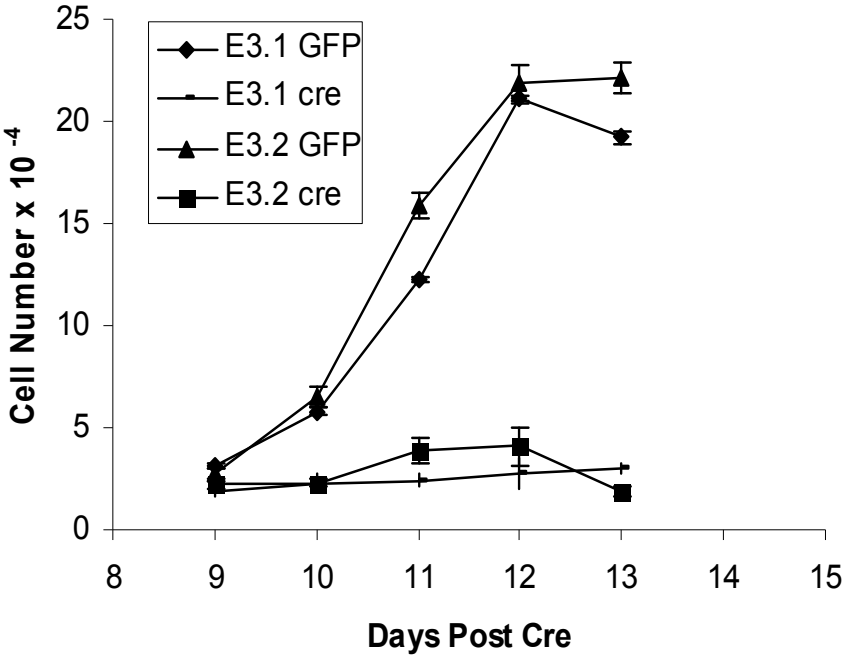

The Cytometric analysis of the cellular DNA content revealed that the WT astrocytes were composed of 54.75% G1, 19.33% G2, and 25.93% S cells. However, the MT astrocytes were composed of 53.81% G1, 24.17% G2, and 22.02% S cells, indicating a slight G2 cell cycle arresting and less cell division (S phase) in the MT astrocytes. This analysis further demonstrated that the sub-G1 apoptotic peaks for MT cells were 41% of the total cell population (Figure 23B). A sharp increase over the 8% sub-G1 apoptotic peaks for WT cells (Figure 23B).

**Figure 23. Deletion of the p44/WDR77 gene inhibits growth and induces apoptosis in astrocytes.** A,B. Flow cytometry data with the sub-G1 area gated for apoptosis of WT (A) and MT (B) astrocytes 12 days post adenovirus infection.

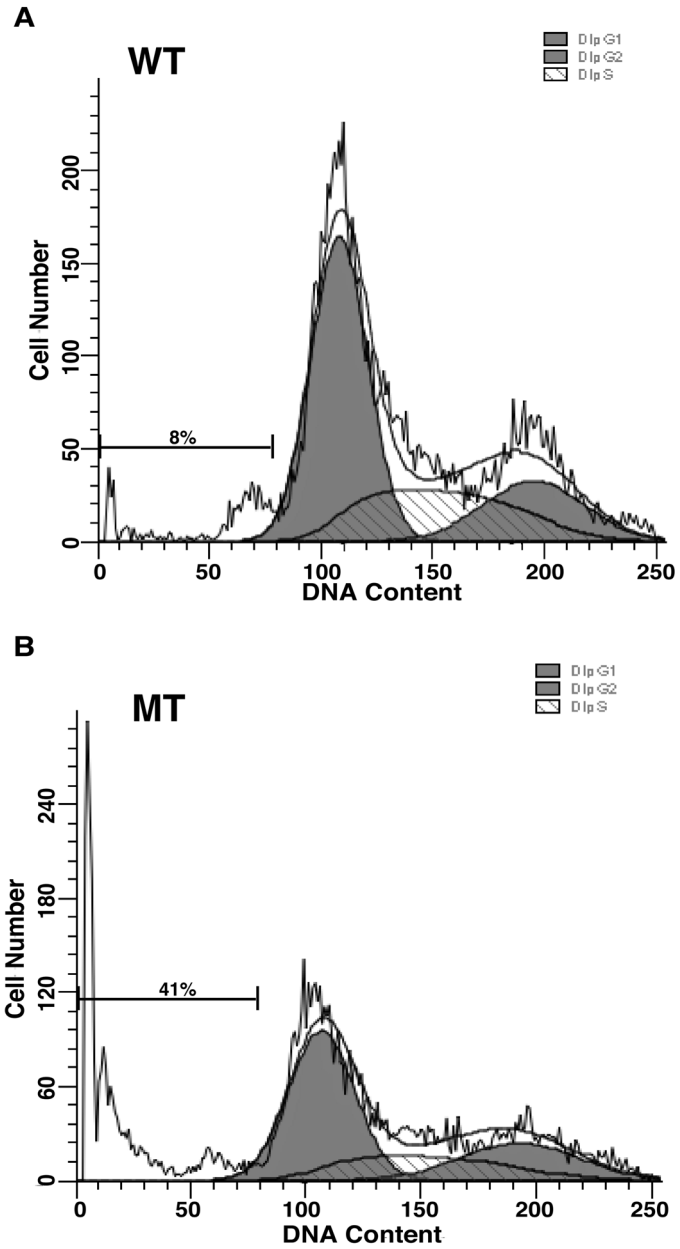

**DIV. Discussion:**

P44/WDR77 expression was confirmed in the cultured astrocytes by immunostaining and PCR. Furthermore, we demonstrated p44/WRD77 is required for growth of astrocytes and loss of p44/WDR77 expression led to dramatic changes in the cell structure which are characteristics of astrogliosis. This is consistent with our findings in primary MT astrocytes that exhibit increase apoptosis and changes in cytoskeleton proteins indicative of astrogliosis. The discrepancies between the experiments illustrated in Figure 17, which present a moderate increase in proliferation in MT astrocytes versus the dramatic decrease depicted in these experiments suggest the increased levels of proliferation in Figure 17 are a result of secondary effects arising from changes in the secretion of signaling molecules being released from p44/WDR77 deficient astrocytes act paracrine fashion on WT astrocytes. A direct role for p44/WDR77 in astrocyte proliferation and apoptosis, are strengthened by previous studies that showed that the deletion of the p44/WDR77 gene in the prostate gland increased proliferation and apoptosis and altered the differentiation of epithelial cells (180, 181). Together these results suggest, that p44/WDR77 has a multitude of critical roles in the regulation of different cellular environments.

MT astrocytes presented with a high percentage of multinuclear cells, hypertrophy of cell nuclei and cytoplasmic regions. These structural changes in MT astrocytes were accompanied with a state of near complete cessation. The abnormal nuclear and cellular morphology, and cell cycle variations seen in MT astrocyte are comparable to the altered cellular phenotype of mouse embryo fibroblast metaphases deficient in pituitary tumor transforming gene (PTTG) (233). This is consistent with gene array data from WT and MT brains, which illustrates strong alteration in PTTG expression in MT brains. PTTG modulates cell transformation, DNA repair, gene regulation, and mitosis in part through its involvement in the initiation of sister-chromatin

separation during the anaphase (233). In the CNS, PTTG has been implicated as important cell cycle regulator in neurogenesis and astrocytes (234, 235). P44/WDR77 role as an AR cofactor coupled with the ability of AR to regulate PTTG gene expression (236) suggests a possible mechanism for the observed phenotype. However, the loss of PTTG expression did not result in the termination differentiation and cell death (233). P44/WDR77 must target other genes which mediate some astrocyte functions.

**E. Deletion of the p44/WDR77 gene leads to astrocytes activation.**

**EI. Rationale:**

Hallmark of reactive astrogliosis are up regulation of GFAP, cellular hypertrophy, and pro- or anti-inflammatory effects on the surrounding CNS tissue with primary and secondary affects on the disease pathology of the CNS with direct and even life threating implications in patient outcome (39, 50, 85). Answering even the most basic questions about astrogliosis has proven to be a challenge for even the best neurobiologists and neuroanatomists, therefore creating a need for a greater understanding of the underlining mechanisms in astrocyte activation (50).

Increased astrogliosis seen in the brains in MT, along with changes in cellular structure of MT astrocytes have suggested a role for p44/WDR77 in astrocyte activation. Initial studies of GFAP expression in MT astrocytes were conducted with astrocytes exhibiting varied expression of p44/WDR77. The studies of proliferation were conducted with astrocytes with varied expression of p44/WDR77 complicating our interpretation of the direct effects of p44/WDR77.

**EII. Experimental Design:**

To further study p44/WDR77's role in astrocyte activation E6/E7 immortalized astrocytes were infected with either Ad-CMV-GFP (WT) or Ad-CMV-Cre–GFP (MT). PCR analysis was used confirmed the deletion of the p44/WDR77 gene, as indicated by excision of the exons 2-5 of the p44/WDR77 gene, in the MT astrocytes but not in the WT astrocytes (Figure 20B insert). Nine days after infection MT and WT astrocytes were immunostained for GFAP.

**EIII. Results:**

Previous studies demonstrated that immortalized astrocytes express low levels of GFAP and show cellular structure of nonreactive astrocytes (237). Consistent with these observations, WT immortalized astrocytes exhibited low levels GFAP and cellular structure of nonreactive astrocytes (Figure 24E). Upon loss of p44/WDR77 expression (9 days post infection), the MT astrocytes expressed much higher levels of GFAP (Figure 22B), suggestive of astrocyte reactivity. The hypertrophy of cell nuclei and the thin processes protruding the cell body were evident in the MT astrocytes (Figure 24A-F), which are characteristics of astrocyte activation (50). These observations are consistent with the primary astrocytes isolated from the MT mouse brains expressing much higher levels of GFAP expression than those isolated from the WT mouse brains (Figure 15B, middle panel, lanes 2 versus lane 1).

**Figure 24. Deletion of the p44/WDR77 gene in astrocytes leads to increased GFAP expression.** A-F, WT and MT astrocytes were stained for nucleus (A and D) and GFAP (B and E). The GFAP staining signals are merged with nuclear staining (D and F).

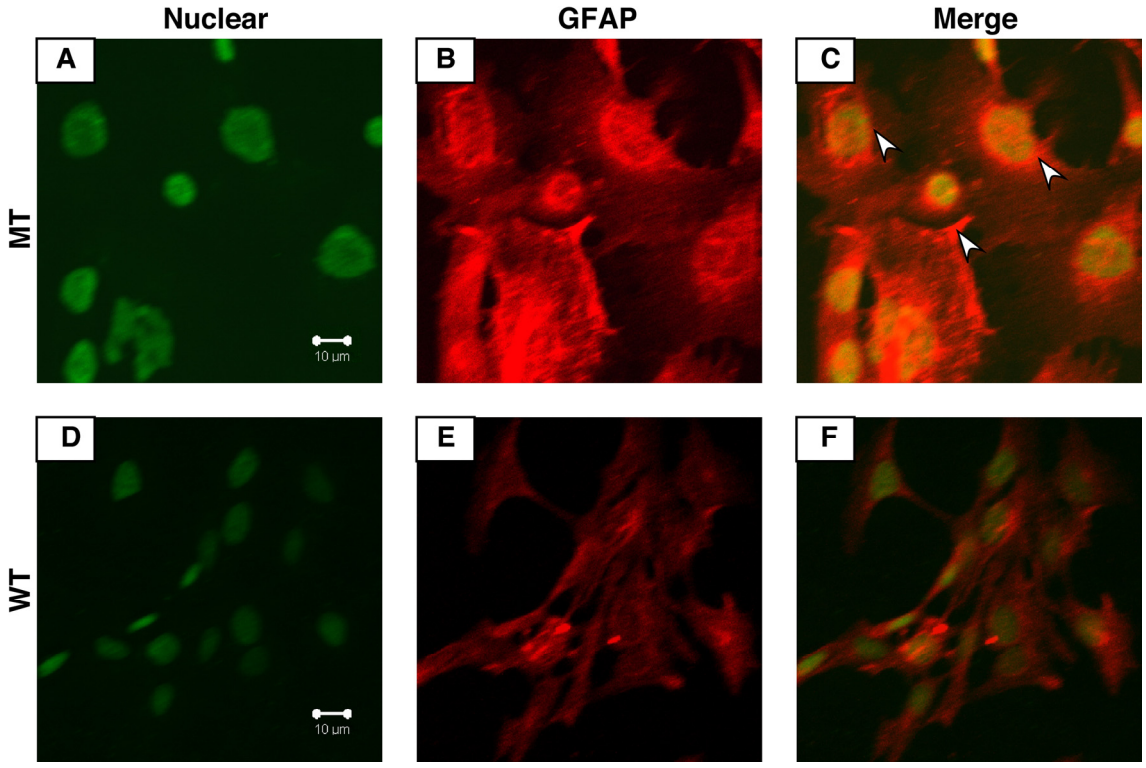

**EIV. Discussion:**

The significant increase in astrogliosis in the MT mouse brain led us to investigate the role of p44/WDR77 in astrocytes. Expression of p44/WDR77 in astrocytes was revealed by immunostaining in the mouse brain and its expression was decreased in the MT mouse brain. Astrogliosis was only observed in astrocytes that had lost p44/WDR77 expression. Furthermore, we demonstrated p44/WRD77 is required for growth of astrocytes and loss of p44/WDR77 expression led to dramatic changes in the cell structure and increased expression of GFAP, which are characteristics of astrogliosis. Thus, p44/WDR77 prevents astrogliosis in the brain.

While the mechanisms of astrocyte activation still remain quite unclear, there are a number of pathways by which p44/WDR77 could drive astrocytes into an activational state (50). P44/WDR77's ability to act as a cofactor to modulate AR- or GR transcriptional activity may be one mechanism (180). GR is a potent repressor of NF-κB activity, which has been implicated in the regulation of astrocyte activation, thus presenting a possible mechanism of action for p44/WDR77 (132-134, 238). Additionally a more recent study suggested that p21 plays a role in astrocyte activation (140, 141). It has been demonstrated that AR and p44/WDR77 target the p21 promoter (152, 172), consistent with the whole brain gene array that demonstrated a significant increase in p21 expression in the MT mouse brain as well as in the p44-null astrocytes.

# Chapter VI:

# Aim 3: To examine the role of $p21^{Cip1}$ in astrocyte activation induced by the loss of p44/WDR77.

**A. $p21^{Cip1}$ is over expressed in activated astrocytes induced by the loss of p44/WDR77.**

**AI. Rationale:**

Despite decades of research on activated astrocytes and pathological implications of CNS insult the fundamental mechanism underlying this phenomenon is just beginning to take shape (50). The studies depicted in Figures 12 – 24 illustrate that the deletion of the p44/WDR77 gene in astrocytes induces astrogliosis characterized by a vast increase in GFAP, along with other morphological and physiological changes indicative of astrocyte activation (50), suggesting that p44/WDR77 has a role in the induction of astrocyte activation.

P44/WDR77's known modulation of AR functions may be one means by which it exerts its control over astrocytes activation. This possibility is illustrated by androgens' ability to down-regulate reactive gliosis after neural injury (227, 228). Recent studies have suggested that the $p21^{Cip1}$ directly affects astrocyte activation induced by LPS (140, 141, 152, 172). This finding correlates with a 4 fold increase $p21^{Cip1}$ expression in MT mice brains found in our gene array of whole brains from MT and WT mice.

**AII. Experimental Design:**

To examine $p21^{Cip1}$ expression in mice brains, total RNA was isolated from whole brains of MT and WT mice at 3 months of age. The RNA was subjected to Northern blot analysis for $p21^{Cip1}$.

To assess $p21^{Cip1}$ expression in astrocytes, immortalized astrocytes were infected with either Ad-CMV-GFP or Ad-CMV-Cre–GFP. Seven days after infection total RNAs were isolated and subjected to qRT-PCR with primers for $p21^{Cip1}$.

**AIII. Results:**

Correlating with DNA microarray data the northern blot analysis showed that Cre-mediated deletion of p44/WDR77 increased (5 fold) expression of $p21^{Cip1}$ mRNA in the MT mouse brain (Figure 25, lanes 3 and 4). The up regulation of p21 gene is not through the p53 pathway since expression of the other p53-target genes (Gadd45A and RGS16) did not change in the MT mouse brain (lanes 5-8). The qRT-PCR analysis revealed a 4.5-fold increase in $p21^{Cip1}$ mRNA expression in MT astrocytes than that in WT astrocytes.

**Figure 25. Deletion of the p44/WDR77 gene increases $p21^{Cip1}$ RNA expression in astrocytes.** A, Northern blot analysis of $p21^{Cip1}$ and β-actin mRNAs in the mouse brain. The mRNA was isolated from the brains of five MT (lanes 1, 3, 5, 7, 9) or five WT (lanes 2, 4, 6, 8, 10) mice at the age of three months, fractionated by electrophoresis, and transferred to a Hybond N+ membrane. The membrane was hybridized with a p44, $p21^{Cip1}$, Gadd45A, RGS16, or β-actin probe.

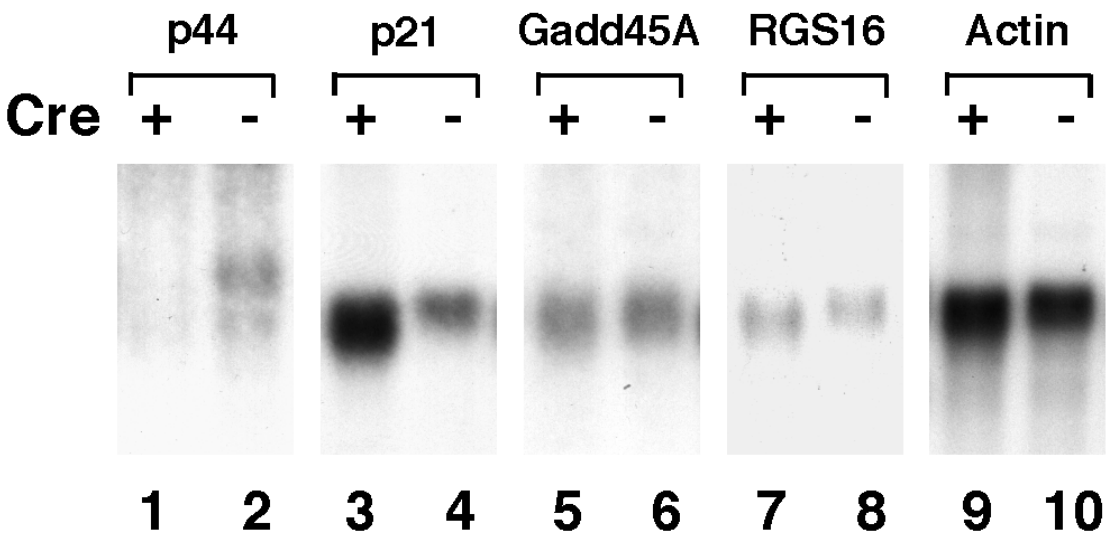

**AIV. Discussion:**

To explore p44/WDR77 mechanistic roles in astrocyte activation we examined $p21^{Cip1}$ RNA expression in MT mouse brains. We found that $p21^{Cip1}$ RNA expression was up regulated in MT mouse brains. The interpretation of this finding is complicated by potential indirect activation secondary to induced neural growth factors and cytokines which can in turn directly affect the activity and expression of cell cycle regulators such as $p21^{Cip1}$ (239-242, 50). To overcome some these complications we examined $p21^{Cip1}$ RNA expression in MT astrocytes. Similar to the northern blot and DNA microarray analysis we found an increase in $p21^{Cip1}$ RNA expression in MT astrocytes. Consistent with regulation of $p21^{Cip1}$ expression by AR (152), we found a reduction in androgen-mediated up regulation of $p21^{Cip1}$ expression in MT astrocytes, suggesting that p44/WDR77 can influence astrocyte activation by enhancing AR-driven repression of $p21^{Cip1}$ gene. However this does not prelude secondary effects on $p21^{Cip1}$ expression that occur during astrocyte activation. Such is the case with NF-κB, a powerful inflammatory transcription factor, which has long been implicated in astrocyte activation which can control $p21^{Cip1}$ in a p53 dependent and independent manner (50, 136).

**B. Over expression of $p21^{Cip1}$ contributes to the decrease in astrocyte growth induced by deletion p44/WDR77.**

**BI. Rationale:**

Cell growth and the progression through the cell cycle are orchestrated by the harmonized interaction of cyclin/cyclin-dependent kinases (CDK) complexes. $P21^{Cip1}$ is a powerful CDK inhibitor (CKI). Through protein-protein interactions with cyclin-CDK2 or -CDK4 complexes $p21^{Cip1}$ directly inhibits their activity, and in doing so acts as a regulator of cell cycle progression at $G_1$ (243, 244). We found that $p21^{Cip1}$ expression is up regulated in astrocyte activation induced by deletion of the p44/WDR77 gene (Figure 25). Given the well known function of $p21^{Cip1}$ in cell growth control and the striking decrease in astrocyte growth in p44/WDR77-null astrocytes (Figure 22), further exploration of the interaction between these two molecules represents a mean to add to the elucidation of the molecular mechanisms in astrocyte activation.

**BII. Experimental Design:**

To determine the role of $p21^{Cip1}$ in astrocyte growth during astrocytes activation induced by the loss of p44/WDR77, $p21^{Cip1}$ expression was silenced by shRNA in WT astrocytes infected with lentivirus expressing a nontargeting sequence or $p21^{Cip1}$ shRNA. To assess the infection efficiency GFP expression was examined in the astrocytes under a fluorescent microscope. Four days later the infected astrocytes were infected with either Ad-CMV-GFP or Ad-CMV-Cre–GFP to generate 4 cell lines (WT: Control shRNA-GFP, $p21^{Cip1}$ shRNA-GFP, MT: Control shRNA-Cre, $p21^{Cip1}$ shRNA-Cre) (Figure 26A). Then cell growth of these lines was examined by plating the cells in a 24-well plate and counting everyday from day 9 to day 13 post adenovirus infection.

To further explore $p21^{Cip1}$ roles in astrocyte growth, WT astrocytes were infected with lentivirus expressing human $p21^{Cip1}$ (Figure 26B). Then the cell growth of these lines was examined by seeding the cells to a 24-well plate and cells were counted daily from day 9 to day 13 post infection.

**Figure 26. Experimental design for $p21^{Cip1}$silencing and over-expressing and p44/WDR77 gene deletion in astrocytes.** A, Diagram illustrates of $p21^{Cip1}$ silencing in astrocytes. B, Diagram illustrates $p21^{Cip1}$ over-expression in astrocytes.

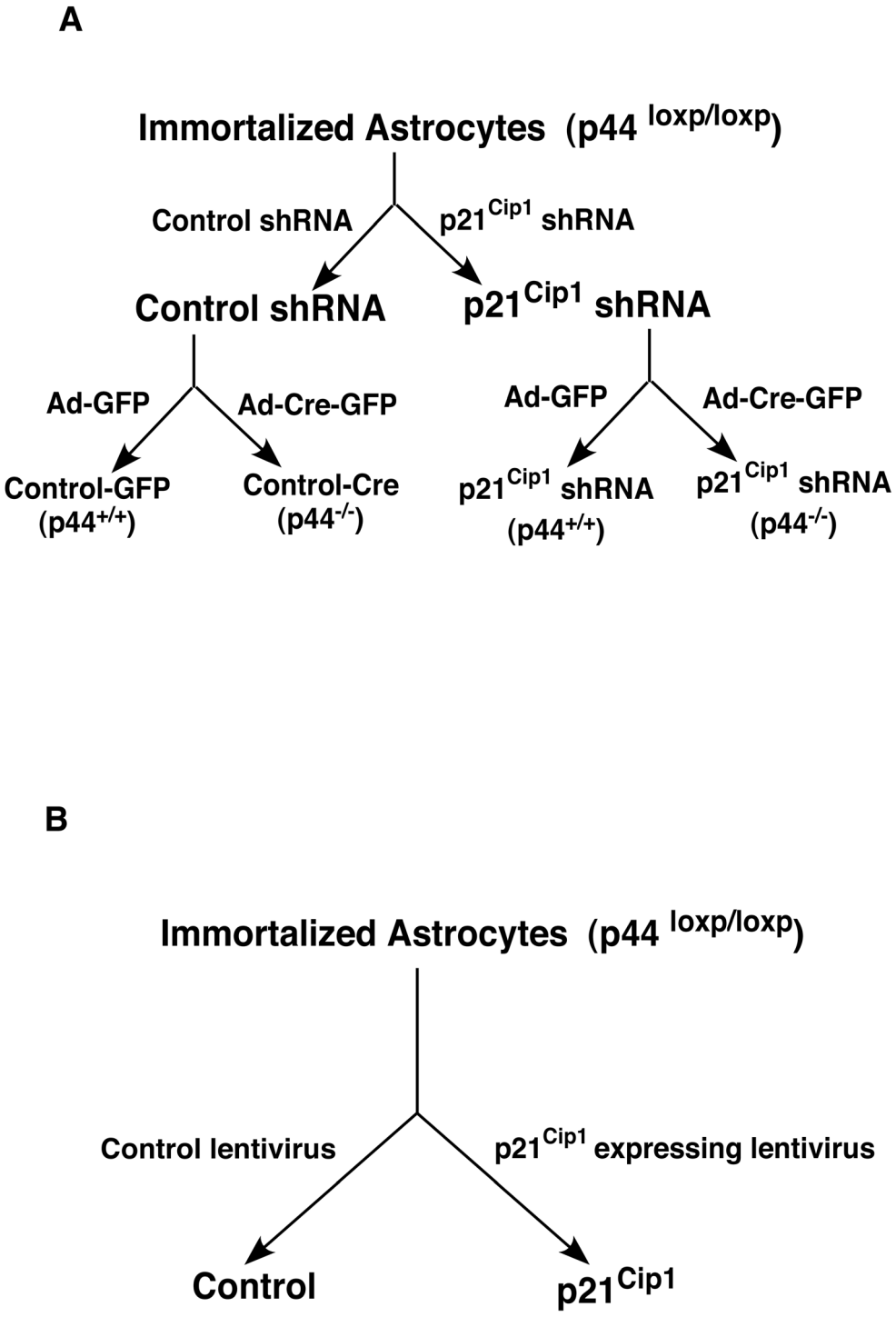

To confirm knockdown and over expression of $p21^{Cip1}$ whole cell lysates were prepared 7 days after adenovirus infection, and subjected to Western blot analysis with anti-$p21^{Cip1}$ or anti-β-actin antibody.

**BIII. Results:**

Examination of lentivirus infection revealed 90% infection efficiency three days after infection (Figure 27).

**Figure 27. Lentivirus infection of astrocytes.** A, Diagram illustrates the procedure of silencing $p21^{Cip1}$ expression in astrocytes. B, GFP expression in astrocytes infected with lentivirus expressing the Control shRNA or $p21^{Cip1}$ shRNA.

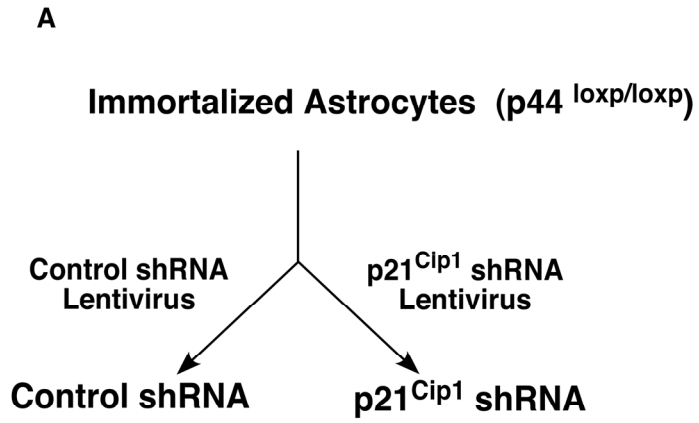


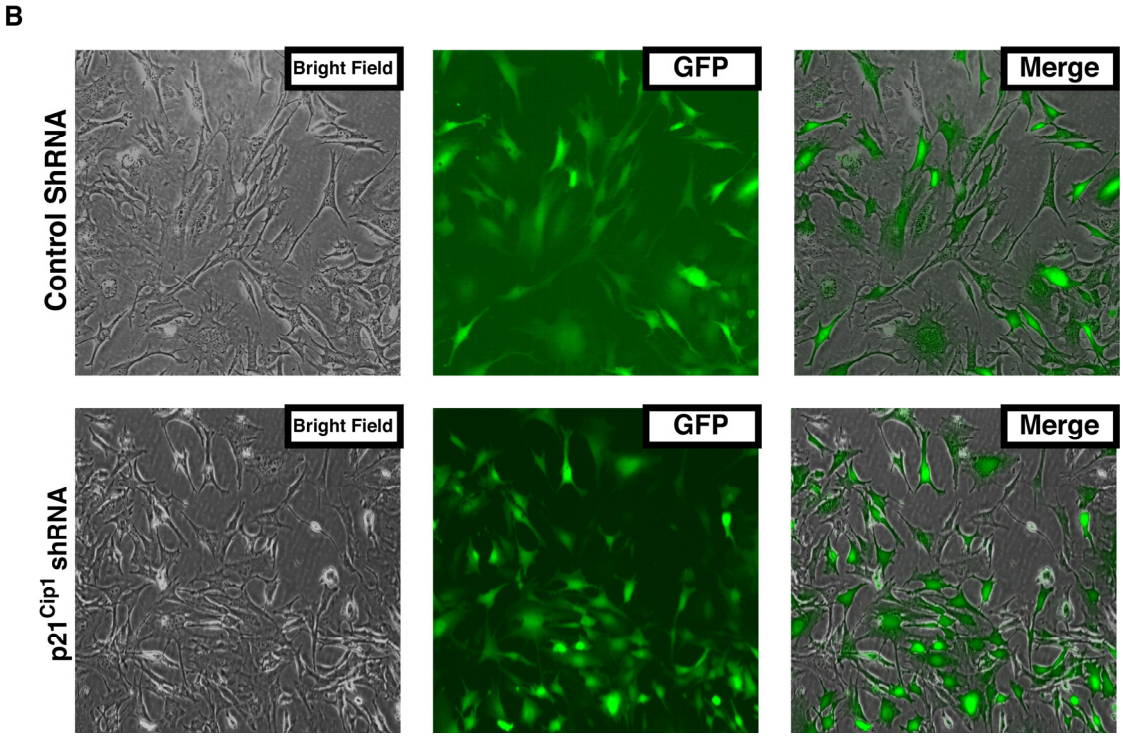

Consistent with qRT-PCR the Western blot analysis revealed a 4 fold increased expression of $p21^{Cip1}$ associated with the loss of p44/WDR77 (Figure 28A, top panel, lane 5 versus lane 1), while no detectable difference in $p21^{Cip1}$ expression was found in Control-GFP and $p21^{Cip1}$ shRNA-GFP astrocytes (Figure 26A, top panel, lane 2 versus lane 1). In contrast, $p21^{Cip1}$ shRNA expression significantly reduced expression of $p21^{Cip1}$ in astrocytes after gene deletion of the p44/WDR77 gene (Figure 28A, top panel, lane 6 versus lane 5).

In the growth analysis p44/WDR77 WT (Control and $p21^{Cip1}$ shRNA expressing) astrocytes continued to increase in cell number until day 12 when they reach confluency. The doubling times for Control-GFP, $p21^{Cip1}$ shRNA-GFP are 26 and 22 hours, respectively. However, silencing of $p21^{Cip1}$ expression (p21Cip1 shRNA-Cre) partially restored the growth of p44/WDR77-null astrocytes (Control-Cre). $P21^{Cip1}$ shRNA-Cre astrocytes had a doubling time of 31 hours and didn't reach confluency during the five days assayed. The p44/WDR77-null (Control-Cre) astrocytes showed only a sight increase in cell number over the course of 5 days (Figure 28B).

**Figure 28. Down regulation of p21$^{Cip1}$ expression partially restores growth of p44/WDR77 deficient astrocytes.** A, The whole cell lysates (20 μg protein) were made from WT astrocytes: the Control-GFP, p21$^{Cip1}$ shRNA-GFP, p65 shRNA-GFP, p21$^{Cip1}$ shRNA + p65 shRNA-GFP (lanes 1-4) and MT astrocytes: Control-Cre, p21$^{Cip1}$ shRNA-Cre, p65 shRNA-Cre, p21$^{Cip1}$ shRNA + p65 shRNA-Cre (lanes 5-8). Western blot analysis was performed with anti-p21$^{Cip1}$ (first panel), anti-p65 (second panel), anti-GFAP (third panel), or anti-actin (fourth panel) antibody. B, Grow curves of WT (Control-GFP, p21$^{Cip1}$ shRNA-GFP) and MT (Control-Cre, p21$^{Cip1}$ shRNA-Cre) astrocytes.

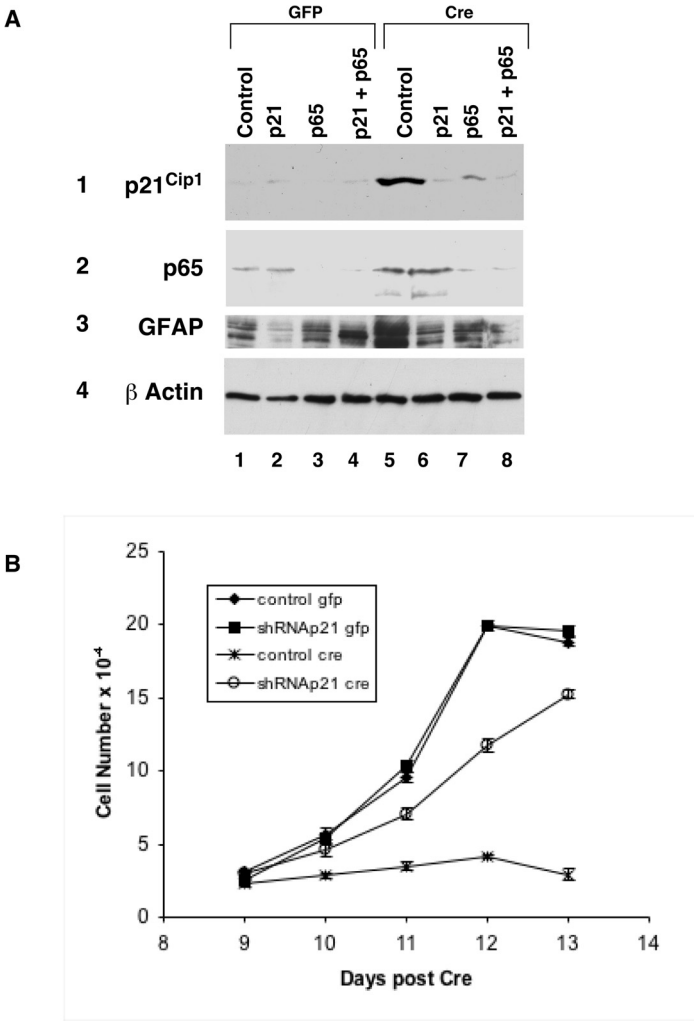

Western blot analysis of confirmed expression of human $p21^{Cip1}$ in $p21^{Cip1}$-expressing astrocytes (Figure 29A top panel, lane 2 versus lane 1).

Human $p21^{Cip1}$ expression decreased growth of astrocytes (Figure 29B). The doubling times for Control and $p21^{Cip1}$-expressing are 24 and 30 hours, respectively.

**Figure 29. P21$^{Cip1}$ over expression decreases growth of astrocytes**. A, The whole cell lysates (20 μg proteins per sample) were made from Control (lane 1), p21$^{Cip1}$ over expression (lane2), p65 over expression (lane3), p21$^{Cip1}$ + p65 over expression (lane4) astrocytes. Western blot analysis was performed with anti-p21$^{Cip1}$ (first panel), anti-p65 (middle panel) or anti-actin (bottom panel). Arrows on the right indicate endogenous mouse p21$^{Cip1}$ and exotic human p21$^{Cip1}$, respectively. B, Grow curves of Control, p21$^{Cip1}$ over expression, and p44/WDR77-null astrocytes.

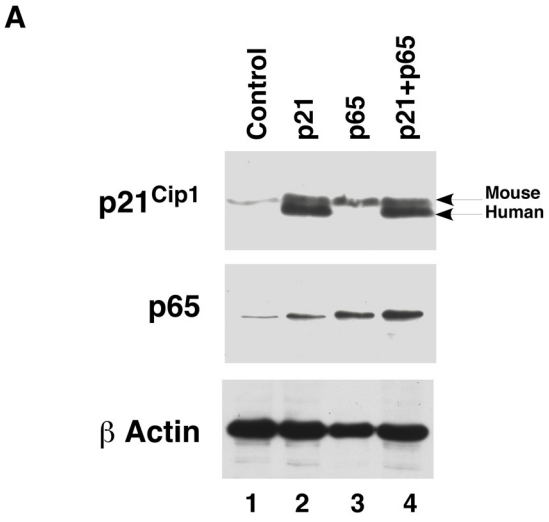


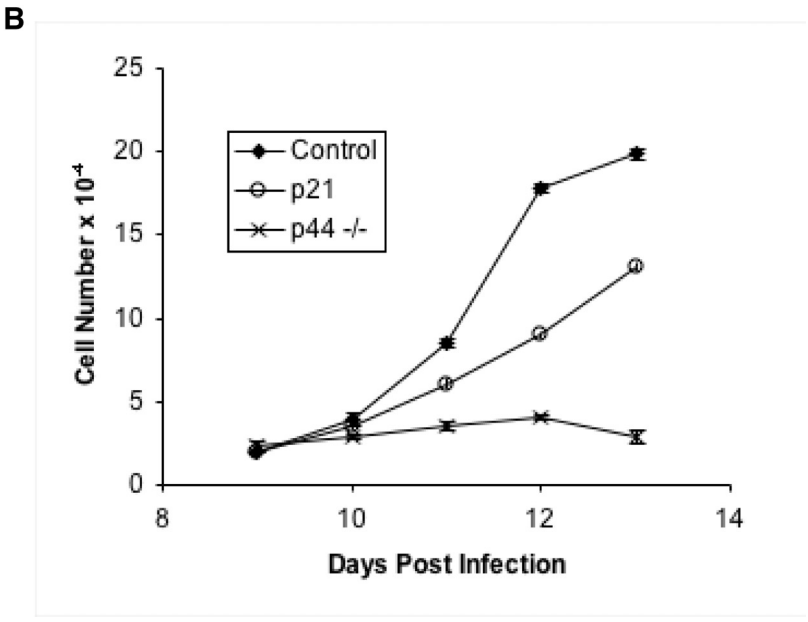

**BIV. Discussion:**

Previous experiments illustrated that the deletion of the p44/WDR77 gene induced a dramatic decrease in growth in astrocytes (Figure 22). While the $p21^{Cip1}$ shRNA did not appear to affect the low levels of $p21^{Cip1}$ expression in the WT astrocytes, the $p21^{Cip1}$ shRNA was effective at knocking down the high levels of $p21^{Cip1}$ expression in the p44/WDR77-null astrocytes and partially restored growth of p44/WDR77-null astrocytes (Control-Cre). These experiments demonstrate that the up regulation of $p21^{Cip1}$ is partially responsible for the dramatic decrease in growth of astrocytes induced by loss of p44/WDR77. Furthermore we confirmed the ability of $p21^{Cip1}$ to directly decrease astrocyte growth through the over expression of human $p21^{Cip1}$ which is functional conserved to mice (244, 245). These findings suggest that p44/WDR77 regulates astrocyte proliferation through decreasing $p21^{Cip1}$ expression. This is consistent with the well established role of $p21^{Cip1}$ as a potent regulator of cell growth and cell cycle (243, 244).

## C. $P21^{Cip1}$ over-expression is essential for astrocyte activation induced by p44/WDR77 gene deletion.

### CI. Rationale:

The fundamental molecular mechanism that guide the induction of reactive astrogliosis and how they affect astrocytic function, are just beginning to come to light (50). Prior experiments in this study (Figure 12 – 24) illustrated that deletion of p44/WDR77 gene in astrocytes induces astrogliosis characterized by the hallmark increase in GFAP. We found that the loss of p44/WDR77 in astrocytes generated a 4 to 5 fold increase in $p21^{Cip1}$ expression (Figure 28B). This finding coupled with recent studies that demonstrated over-expression of $p21^{Cip1}$ is associated with astrocyte activation (140, 141) suggests p44/WDR77 might be influencing astrocyte activation through the regulation of $p21^{Cip1}$.

### CII. Experimental design:

To examine $p21^{Cip1}$ roles in astrocyte activation induced by the loss of p44/WDR77, $p44/WDR77^{loxP/loxP}$ astrocytes were infected with lentivirus expressing a nontargeting control or $p21^{Cip1}$ shRNA (Figure 27A). Four days later the control and p21 shRNA-expressing astrocytes were infected with either Ad-CMV-GFP or Ad-CMV-Cre–GFP to generate 4 cell lines (WT: Control-GFP, $p21^{Cip1}$ shRNA-GFP, MT: Control-Cre, $p21^{Cip1}$ shRNA-Cre) (Figure 26A). Nine days after infection, astrocytes were immunostained for GFAP. Cell lysates were also prepared from astrocytes seven days after adenovirus infection and subjected to Western blot analysis with anti-GFAP antibody.

To further explore $p21^{Cip1}$ roles in astrocyte activation, WT astrocytes were infected with the control lentivirus or lentivirus expressing the human $p21^{Cip1}$. Nine days post virus infection astrocytes were subject to immunostaining for GFAP.

**CIII. Results:**

Comparable with earlier findings, p44/WDR77 WT (Control-GFP, $p21^{Cip1}$ shRNA-GFP) astrocytes exhibited low levels of GFAP and resembled nonreactive astrocytes (Figure 30B, H). Upon the loss of p44/WDR77 expression (9 days post Ad-Cre-GFP infection), the p44/WDR77-null (Control-Cre) astrocytes expressed much higher levels of GFAP with cellular and nuclear hypertrophy (Figure 28E), indicative of astrocyte reactivity while $p21^{Cip1}$-silenced ($p21^{Cip1}$ shRNA-Cre) astrocytes, despite the loss of p44/WDR77, showed low levels GFAP and cellular structure of nonreactive astrocytes (Figure 30K). This finding was confirmed in the Western blot analysis which illustrates a hallmark increase of GFAP in Control-Cre astrocytes while the $p21^{Cip1}$ shRNA-Cre astrocytes maintain basil level of GFAP expression (Figure 28A, third panel, lane 5 and 6).

**Figure 30. Down regulation of p21$^{Cip1}$ expression inhibits astrocyte activation induced by deletion of p44/WDR77 gene.** A-F, WT (Control-GFP) and MT (Control-Cre) astrocytes were stained for nucleus (A and D) and GFAP (B and E). The GFAP staining signals are merged with nuclear staining (D and F). G-L, WT (p21$^{Cip1}$ shRNA-GFP) and MT (p21$^{Cip1}$ shRNA-Cre) astrocytes were stained for nucleus (G and J) and GFAP (H and K). The GFAP staining signals are merged with nuclear staining (I and L).

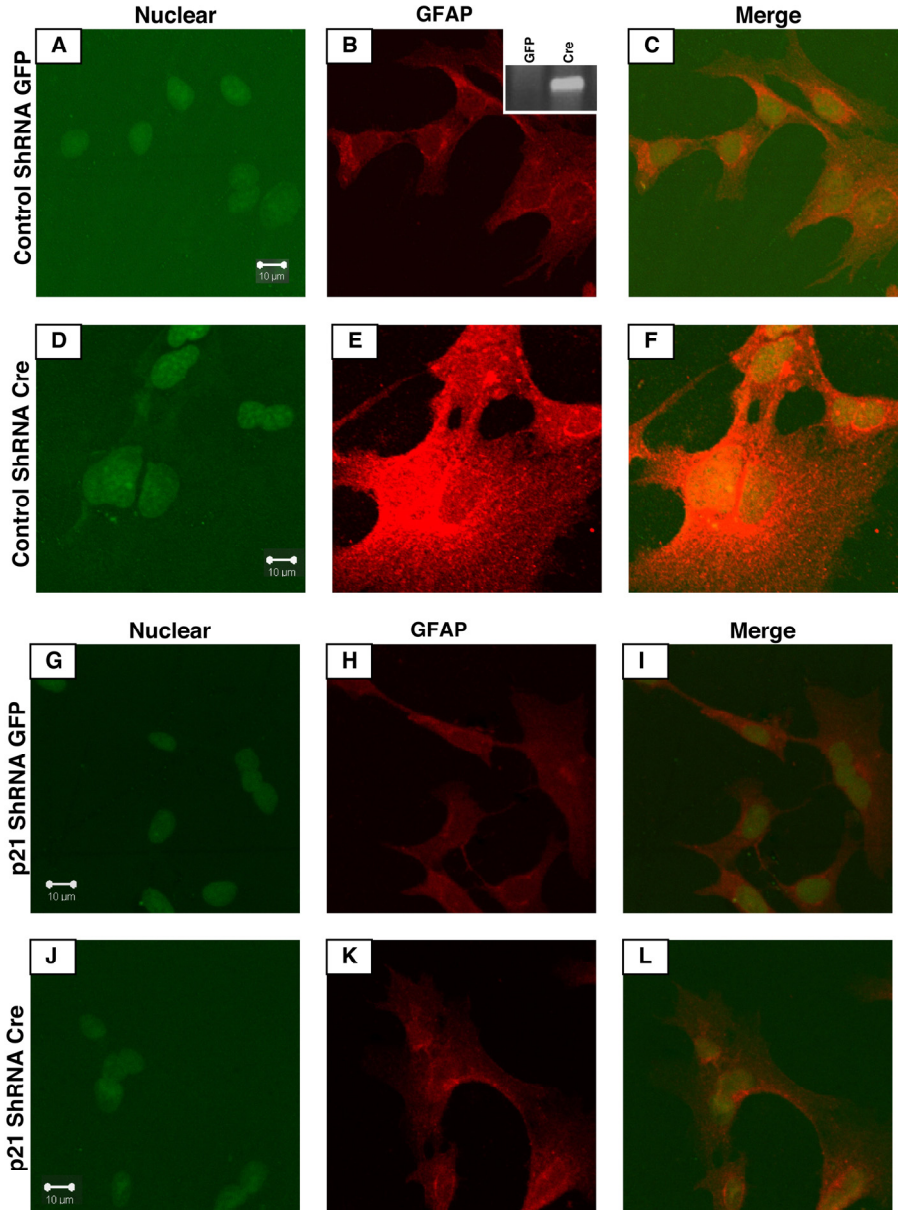

Consistent with prior studies (140, 141) that suggest $p21^{Cip1}$ is involved in astrocyte activation, we found that $p21^{Cip1}$ over expression moderately increased GFAP expression and induce cellular structure of activated astrocytes (Figure 31E), while the control astrocyte maintained low levels GFAP and cellular structure of nonreactive astrocytes (Figure 31B).

**Figure 31. P21$^{Cip1}$ over expression leads to increased GFAP expression in astrocytes.** A-F, Control and p21$^{Cip1}$ over expression astrocytes were stained for nucleus (A and D) and GFAP (B and E). The GFAP staining signals are merged with nuclear staining (D and F).

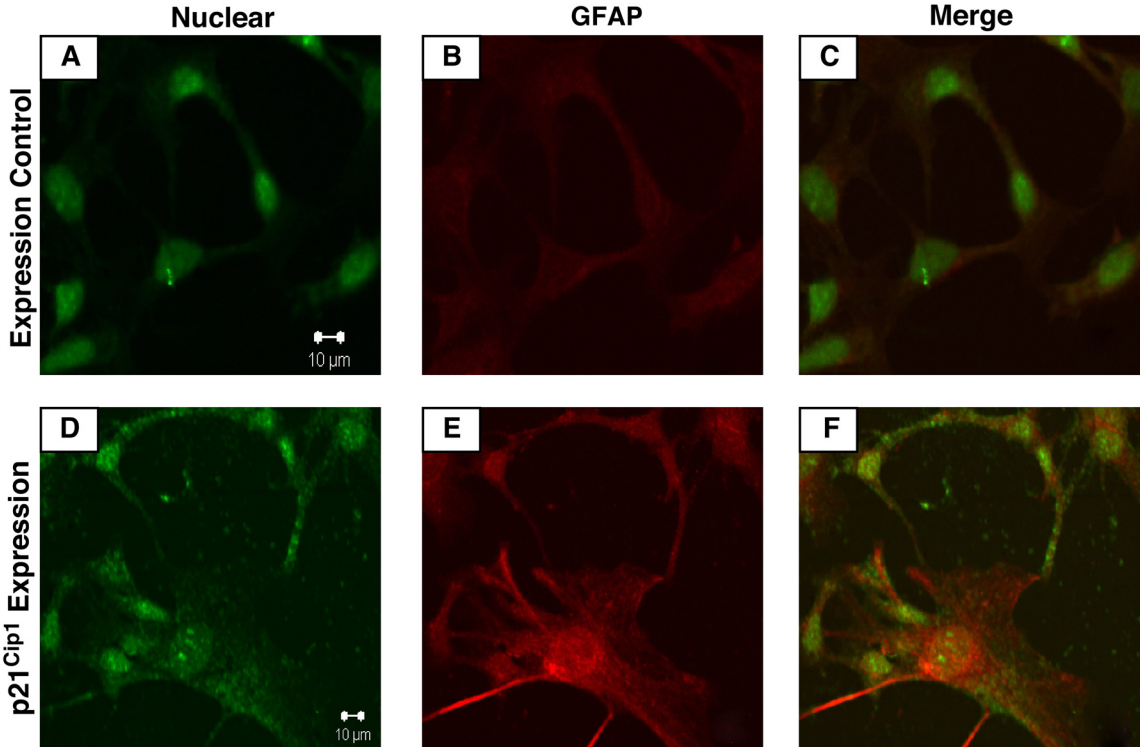

**CIV. Discussion:**

The significant increase in astrogliosis in the p44/WDR77-null mouse brain and astrocytes accompanied with increased $p21^{Cip1}$ expression led us to determine whether 44/WDR77 represses astrocyte activation through the regulation of $p21^{Cip1}$ expression. Immunostaining revealed the induction of astrogliosis by p44/WDR77 gene deletion only in astrocytes expressing high levels of $p21^{Cip1}$. Further more we confirmed the ability of $p21^{Cip1}$ to induce astrocytes activation independent of p44/WDR77 status, through over expression of human $p21^{Cip1}$ (140, 141). These results suggest that p44/WDR77 influences astrocyte activation through the regulation of $p21^{Cip1}$ expression. However, the $p21^{Cip1}$ over expression in astrocytes did not induce the level of GFAP expression generated by p44/WDR77 deletion in astrocytes. This could be due to the possibility that the p44/WDR77 controls astrocytes activation not only through $p21^{Cip1}$ but also via other factors. While there is growing evidence that cell-cycle control systems have regulatory functions in reactive gliosis, the mechanistic actions of $p21^{Cip1}$ in reactive gliosis remain incompletely characterized (246-248). $P21^{Cip1}$ has positive modulatory effects on NF-κB activation a pathway long implicated in gliosis; represent an additional possible contributing mechanism (140, 141).

## D. P21$^{Cip1}$ is a positive modulator of NF-κB during astrocyte activation induced by p44/WDR77 gene deletion.

### DI. Rationale:

A greater molecular understanding of the induction and regulatory control of the dual nature of astrogliosis as both detrimental and beneficial would vastly improve the treatment of CNS damage (50). We have observed an increase p21$^{Cip1}$ expression associated with astrocyte activation induced by the gene deletion of p44/WDR77. Upon further examination, we found that inhibition of p21$^{Cip1}$ up regulation in astrocytes after p44/WDR77 deletion inhibits astrocyte activation. From this point, we conclude that p44/WDR77 influences astrocyte activation through the regulation of p21$^{Cip1}$ expression. Recent studies implicated p21$^{Cip1}$ as a positive modulator for NF-κB, a potent inflammatory transcription factor (132, 140, 141), suggesting that the loss of p44/WDR77 in astrocytes might have deleterious effects on the CNS through the up regulation of p21$^{Cip1}$ expression and subsequent NF-κB activation (131, 140, 141).

### DII. Experimental design:

To examine p21$^{Cip1}$ regulatory effects on NF-κB activity in astrocytes activation induced by the loss of p44/WDR77, p44/WDR77$^{loxP/loxP}$ astrocytes were infected with lentivirus expressing nontargeting control or p21$^{Cip1}$ shRNA. Four days later the control and p21 shRNA-expressing astrocytes were infected with either Ad-CMV-GFP or Ad-CMV-Cre–GFP to generate 4 cell lines (WT: Control-GFP, p21$^{Cip1}$ shRNA-GFP, MT: Control-Cre, p21$^{Cip1}$ shRNA-Cre) (Figure 24A). Nine days after virus infection astrocytes were immunostained for p65.

To further explore $p21^{Cip1}$ roles on NF-κB activity in astrocyte, WT astrocytes were infected with control lentivirus or lentivirus expressing the human $p21^{Cip1}$. Nine days after infection astrocytes were immunostained for p65. Cell lysates were also prepared seven days after virus infection and subjected to western blot analysis with anti-p65.

**DIII. Results**

Immunostaining of p44/WDR77 WT (Control-GFP, $p21^{Cip1}$ shRNA-GFP) astrocytes revealed low cytoplasmic levels of p65 (Figure 32B, H). Nine days after infection, the p44/WDR77-null (Control-Cre) astrocytes expressed high nuclear levels of p65 (Figure 30E), indicative of NF-κB activation while the silencing of $p21^{Cip1}$ expression in $p21^{Cip1}$ shRNA-Cre astrocytes inhibited NF-κB activation induced by p44/WDR77 gene deletion (Figure 32K). However, Western blot analysis indicated that shRNA knockdown of $p21^{Cip1}$ failed to prevent an increase of p65 expression induced by p44/WDR77 gene deletion (Figure 28A, second panel, lane 5 versus lane 6), suggesting that p44/WDR77 can also regulate p65 expression independent of $p21^{Cip1}$.

**Figure 32. Down regulation of p21$^{Cip1}$ expression decreases p65 nuclear localization induced by p44/WDR77 deletion in astrocytes.** A-F, WT (Control-GFP) and MT (Control-Cre) astrocytes were stained for nucleus (A and D) and p65 (B and E). The p65 staining signals are merged with nuclear staining (D and F). G-L, WT (p21$^{Cip1}$ shRNA-GFP) and MT (p21$^{Cip1}$ shRNA-Cre) astrocytes were stained for nucleus (G and J) and p65 (H and K). The p65 staining signals are merged with nuclear staining (I and L).

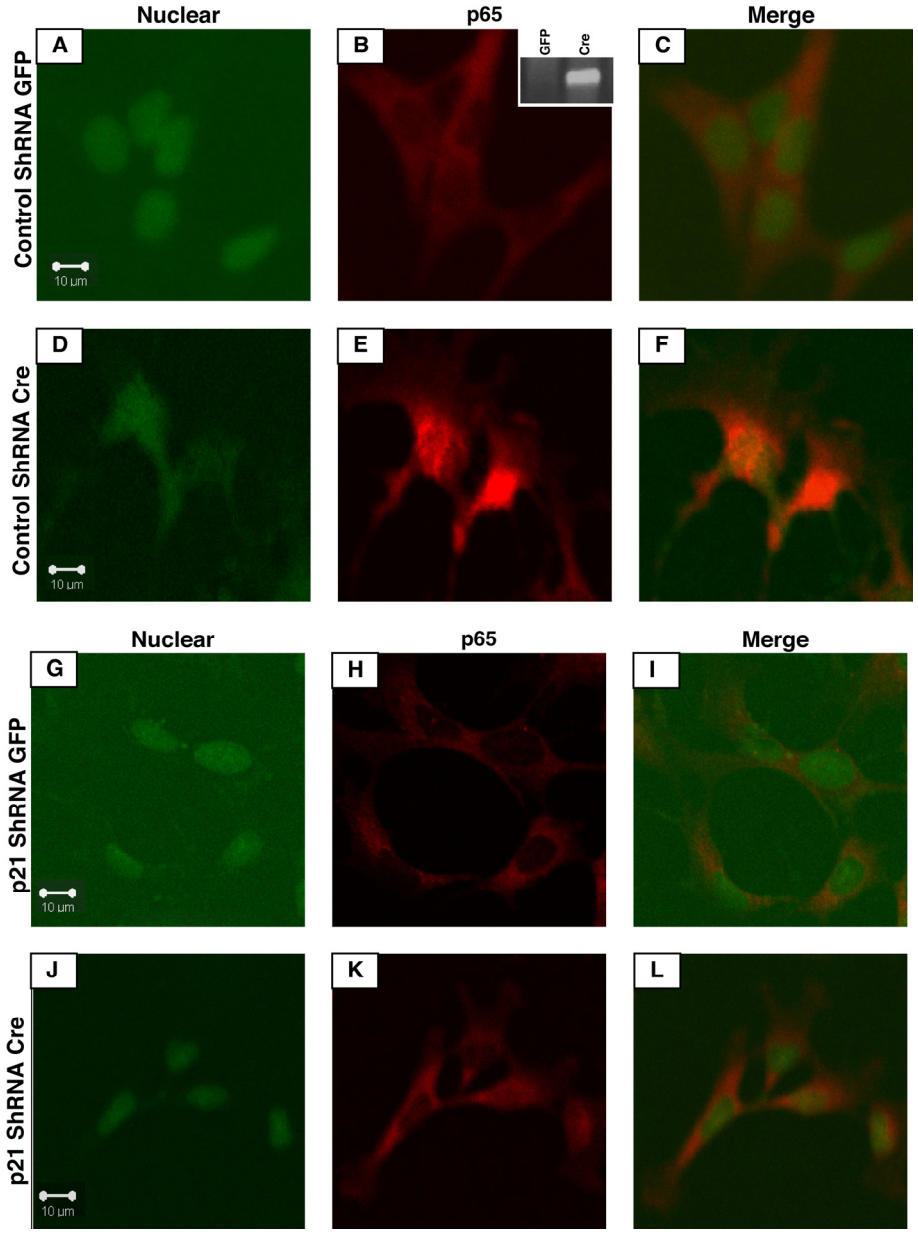

In line with studies (140, 141) that implicate $p21^{Cip1}$ as positive modulator of p65, we found that $p21^{Cip1}$ over expression increased p65 protein expression (Figure 33E), while control astrocyte maintained low levels p65 (Figure 33B). This observation was strengthened by Western blot analysis that revealed $p21^{Cip1}$ over expression increased p65 expression in astrocytes (Figure 29A, middle panel, lane 2 versus lane 1).

**Figure 33. P21$^{Cip1}$ Over expression leads to increased p65 nuclear localization and expression in astrocytes.** A-F, Control and p21$^{Cip1}$ over expression astrocytes were stained for nucleus (A and D) and p65 (B and E). The p65 staining signals are merged with nuclear staining (D and F).

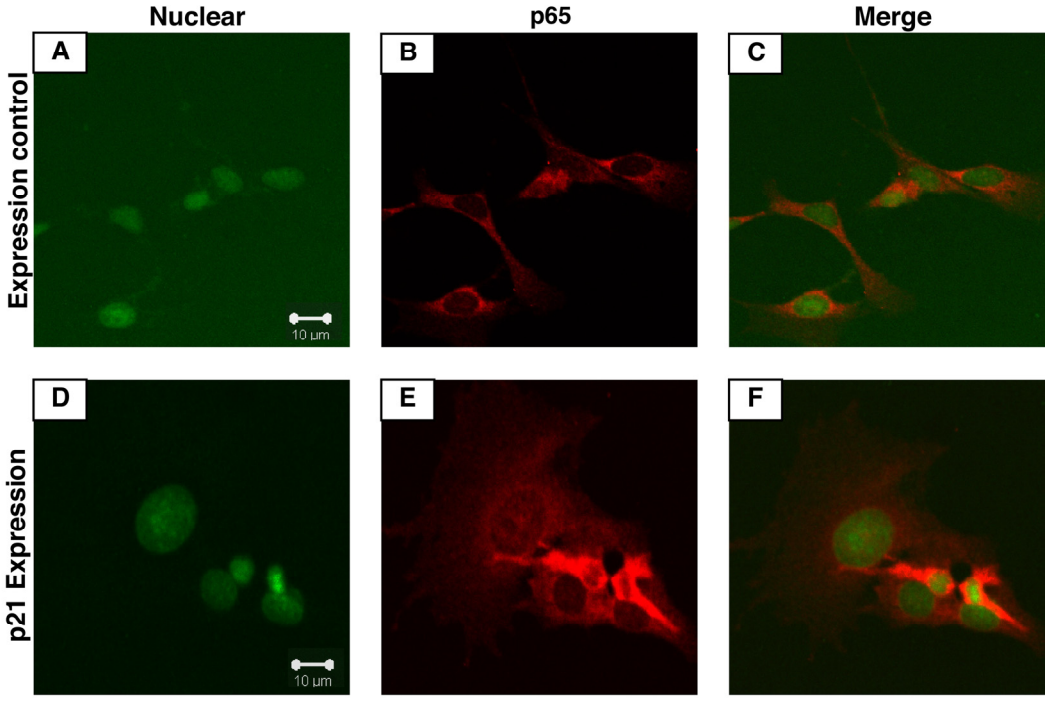

**DIV. Discussion:**

Activation of the canonical or classical NF-κB pathway has been implicated in the regulation of astrocyte activation. Activation of this pathway is characterized by nuclear localization of p65 (132, 134). Immunostaining revealed high NF-κB activation upon induction of astrogliosis by p44/WDR77 gene deletion and in astrocytes expressing high levels of $p21^{Cip1}$. P44/WDR77-null Astrocytes that had undergone silencing $p21^{Cip1}$ showed decreased NF-κB activation despite an increase in p65 expression. While the molecular mechanisms of $p21^{Cip1}$ modulation of NF-κB activity in astrocyte are not clear, this result suggests that p44/WDR77 can in part regulate NF-κB activity through modulation of $p21^{Cip1}$ expression. The growing evidence suggest that cell cycle control systems directly regulate the induction of reactive gliosis raising the possibility that signaling changes induced by astrocyte activation in cytokines such as TNF-α might induce subsequent NF-κB activation (132, 246-248). Furthermore, we demonstrated that over expression of human $p21^{Cip1}$ in astrocytes did not increase p65 expression and nuclear localization to the levels generated by p44/WDR77 gene deletion, suggesting that p44/WDR77 has additional regulatory controls over NF-κB activity.

# Chapter VII:

# Aim 4: To examine the role of NF-κB activation in astrocyte activation induced by the loss of p44/WDR77.

**A. Down regulation of NF-κB activity in astrocytes completely recovers the decrease in cell growth induced by p44/WDR77 deletion.**

**AI. Rationale:**

Astrocytic proliferation is a fundamental component in glial scar formation which can hinder patient recovery from severe astrogliosis (94, 95, 99 -103). Despite decades of research into astrocytic function the molecular mechanism of astrocytic proliferation remain unclear (50). We found that the loss p44/WDR77 in astrocytes induces a dramatic decrease in cell growth (Figure 22), and that this growth could be partially recovered through down regulation of $p21^{Cip1}$ expression (Figure 28B). Additionally the experiments depicted in Figure 29 illustrate that NF-κB, a transcription factor implicated in astrocytic proliferation, is up regulated during astrocyte activation induce by p44/WDR77 gene deletion and that NF-κB activity is positively modulated by $p21^{Cip1}$ (249, 250). While $p21^{Cip1}$ is a potent regular of cell growth and cycle, this finding also suggests p44/WDR77 might influence astrocyte growth directly through the modulation of NF-κB activity.

**AII. Experimental Design:**

To determine the roles of NF-κB in astrocytes activation induced by the loss of p44/WDR77, $p44/WDR77^{loxP/loxP}$ astrocytes were infected with lentivirus expressing (i) nontargeting control; (ii) p65 shRNA; (iii) $p21^{Cip1}$ + p65 shRNA (Figure 32A). Four day later the astrocytes were infected with either Ad-CMV-GFP or Ad-CMV-Cre–GFP to generate 6 cell lines (WT: Control-GFP, p65 shRNA-GFP, $p21^{Cip1}$ + p65 shRNA-GFP, MT: Control-Cre, p65 shRNA-Cre, $p21^{Cip1}$-Cre + p65 shRNA-Cre) (Figure 34A). Then growth of these cell lines was examined by plating the cells in a 24-well plate and cells

were counted daily from day 9 to day 13 post adenovirus infection. To confirm decreased NF-κB activity after p65 shRNA knockdown, MT (p65 shRNA-Cre, $p21^{Cip1}$-Cre + p65 shRNA-Cre) and WT (p65 shRNA-GFP, $p21^{Cip1}$ + p65 shRNA-GFP) astrocytes were subject to immunostaining for p65 nine days after adenovirus infection.

**Figure 34. Experimental design for p65 and p65 + p21$^{Cip1}$silencing and over-expressing and p44/WDR77 gene deletion in astrocytes.** A, Diagram illustrates of p65 and p65 + p21$^{Cip1}$ silencing in astrocytes. B, Diagram illustrates p65 and p65 + p21$^{Cip1}$ over-expression in astrocytes.

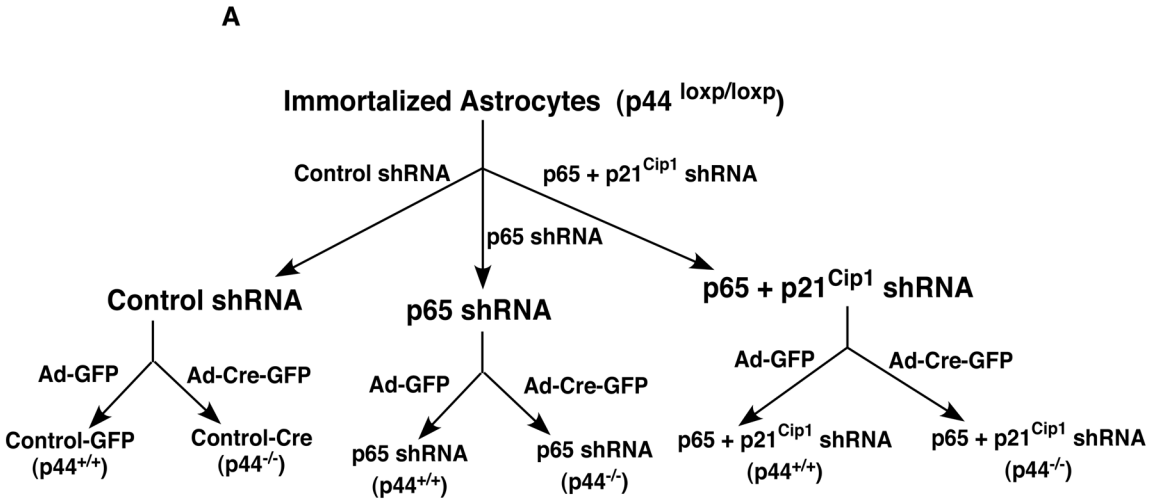


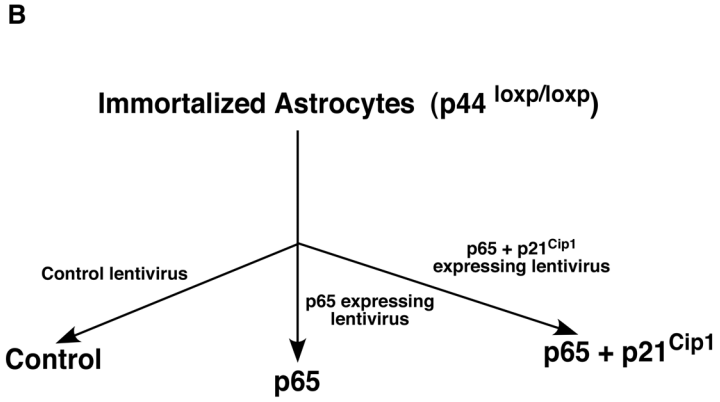

To further explore NF-κB's role in astrocytes, p44/WDR77$^{loxP/loxP}$ astrocytes were infected with control lentivirus or lentivirus expressing human p65 or human p21$^{Cip1}$ plus human p65. Then cell growth of these three lines was examined by plating the cells to a 24-well plate and counted everyday from day 9 to day 13 post infection. These astrocyte lines were subjected to immunostaining for p65 nine days after infection.

Cell lysates were collected seven days after virus infection and subjected to western blot analysis with anti- p21$^{Cip1}$, anti-p65 or anti-β-Actin antibody.

**AIII. Results:**

Consistent with the Immunostaining (Figure 32A-F) the Western blot analysis revealed increased expression of p65 associated with the loss of p44/WDR77 (Figure 28A, panel two, lane 5 versus lane 1). The Western blot assay confirmed down regulation of p65 in p65 shRNA-GFP and p21$^{Cip1}$ + p65 shRNA-GFP astrocytes (Figure 28A, second panel, lanes 3, and 4 versus lane 1). This finding was consistent with the Western blot analysis of Control-Cre, p65 shRNA-Cre and p21$^{Cip1}$ + p65 shRNA-Cre which demonstrated a decreased expression of p65 in p65 shRNA-Cre and p21$^{Cip1}$ + p65 shRNA-Cre astrocytes to basil levels (Figure 28A, second panel, lane 7 and 8 versus lane 5). The shRNA knockdown of p21$^{Cip1}$ alone did not effect p65 expression (Figure 26A second panel, lanes 2 and 6 versus lanes 1 and 5).

Immunostaining of WT astrocytes (Control-GFP) revealed low levels of p65 localized to the cytoplasm (Figure 35B and Figure 36B). The p65 silencing decreased these signals (Figure 35H, Figure 36H). Nine days after infection, the MT (Control-Cre) astrocytes expressed high nuclear levels of p65 (Figure 35E), indicative of NF-κB activation while the MT (p65 shRNA-Cre, p21$^{Cip1}$ Cre + p65 shRNA-Cre) astrocytes

showed with low cytoplasmic expression of p65 in the presence of p44/WDR77 deletion (Figures 35K, and 36K).

**Figure 35. Down regulation of p65 expression decreases p65 nuclear localization and expression induced by p44/WDR77 deletion in astrocytes.** A-F, WT (Control-GFP) and MT (Control-Cre) astrocytes were stained for nucleus (A and D) and p65 (B and E). The p65 staining signals are merged with nuclear staining (D and F). G-L, WT (p65 shRNA-GFP) and MT (p65 shRNA-Cre) astrocytes were stained for nucleus (G and J) and p65 (H and K). The p65 staining signals are merged with nuclear staining (I and L).

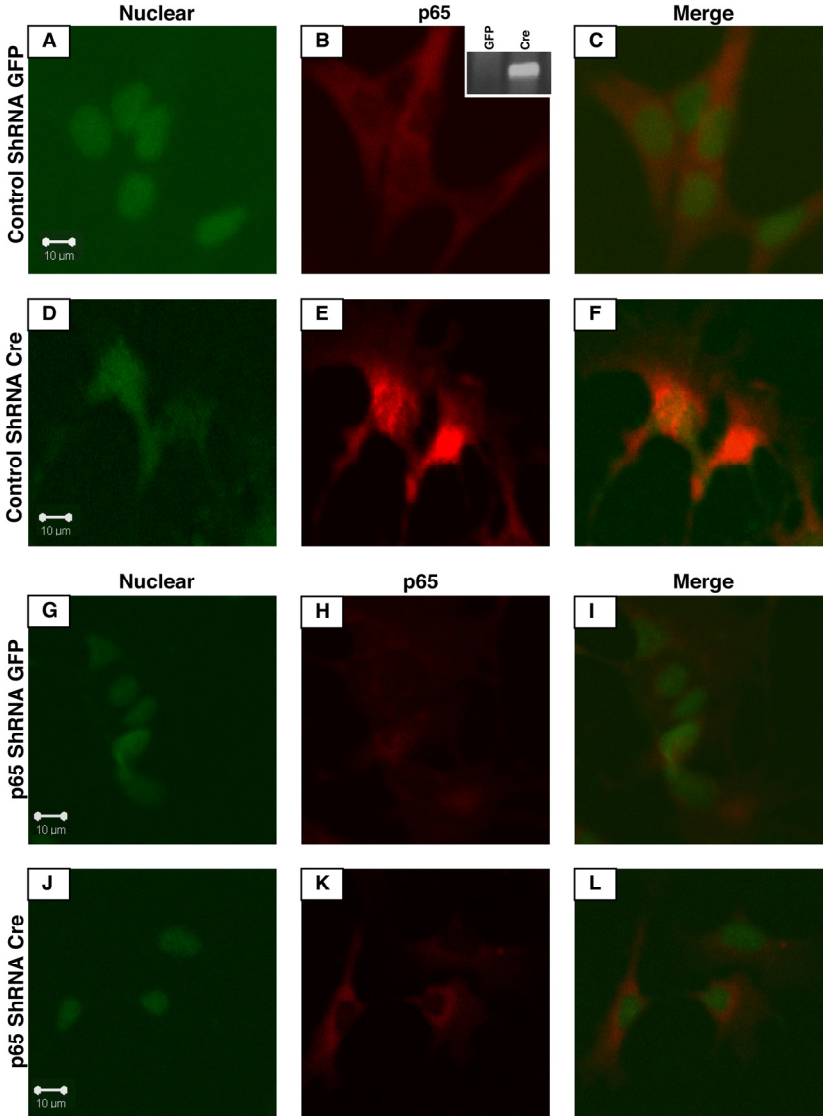

**Figure 36. Down regulation of p21$^{Cip1}$ and p65 decreases p65 nuclear localization and expression Induced by p44/WDR77 deletion in astrocytes.** A-F, WT (Control-GFP) and MT (Control-Cre) astrocytes were stained for nucleus (A and D) and p65 (B and E). The p65 staining signals are merged with nuclear staining (D and F). G-L, WT (p21$^{Cip1}$ + p65 shRNA-GFP) and MT (p21$^{Cip1}$ + p65 shRNA-Cre) astrocytes were stained for nucleus (G and J) and p65 (H and K). The p65 staining signals are merged with nuclear staining (I and L).

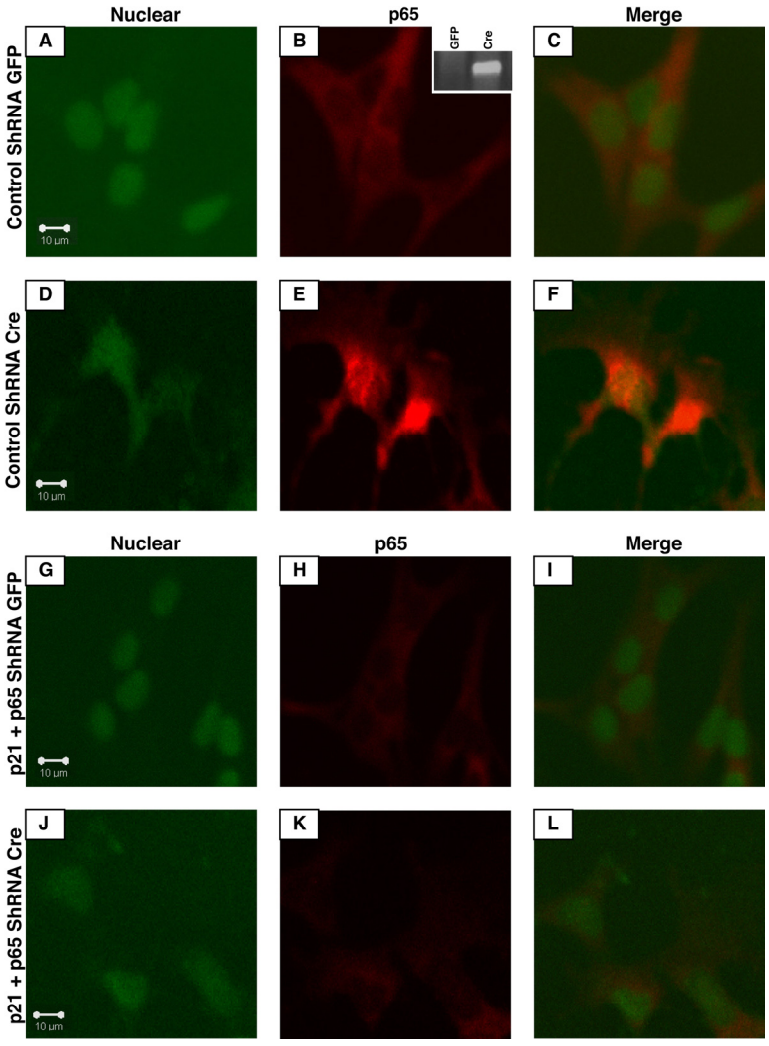

In the growth analysis WT (Control-GFP, p65 shRNA-GFP, p65 + $p21^{Cip1}$ shRNA-GFP) and MT (p65 shRNA-Cre, p65 + $p21^{Cip1}$ shRNA-Cre) astrocytes cells continued to increase in cell number until day 12 when they reach confluency. The doubling times for WT (Control-GFP, p65 shRNA-GFP, p65 + $p21^{Cip1}$ shRNA-GFP) are 26, 23, and 23 hours, respectively. The doubling times for MT (p65 shRNA-Cre, p65 + $p21^{Cip1}$ shRNA-Cre) are 23 and 26 hours, respectively. In contrast, the MT (Control-Cre) astrocytes showed only a sight increase in cell number over the course of 5 days (Figure 37).

**Figure 37. Down regulation of p65 restores growth of p44/WDR77 deficient astrocytes.** Grow curves of WT (Control-GFP, p65 shRNA-GFP, $p21^{Cip1}$ + p65 shRNA-GFP and MT (Control-Cre, p65 shRNA, $p21^{Cip1}$ + p65 shRNA-Cre) astrocytes.

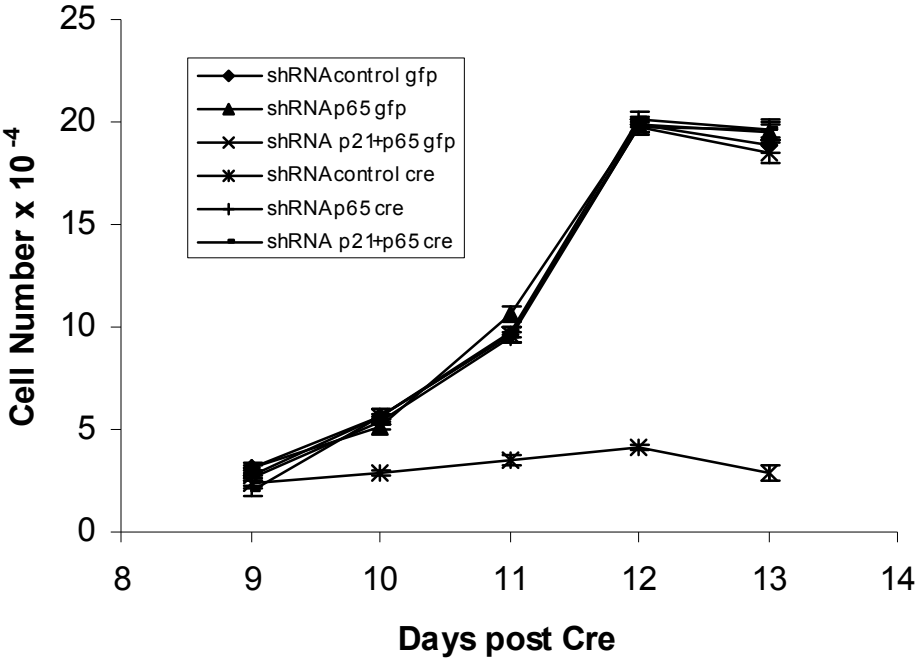

Increased p65 expression in astrocytes expressing human p65 and $p21^{Cip1}$ plus p65 was confirmed by immunostaining (Figure 38B versus Figure 38E, H). The Western blot assays using lysates from these three lines confirmed p65 over expression (Figure 29A, middle panel, lane 3 and 4 versus lane 1). Consistent with NF-κB known role as a positive modulator of $p21^{Cip1}$ (249, 250), Western blot analysis of $p21^{Cip1}$ illustrated an increase in $p21^{Cip1}$ expression after p65 over expression in astrocytes (Figure 29A, top panel, lane 3 versus lane 1).

**Figure 38. P65 over expression increases NF-κB activity.** A-I, Control, p65 and p65 + $p21^{Cip1}$ over expression astrocytes were stained for nucleus (A, D, and G) and p65 (B, E and H). The p65 staining signals are merged with nuclear staining (D, F and I).

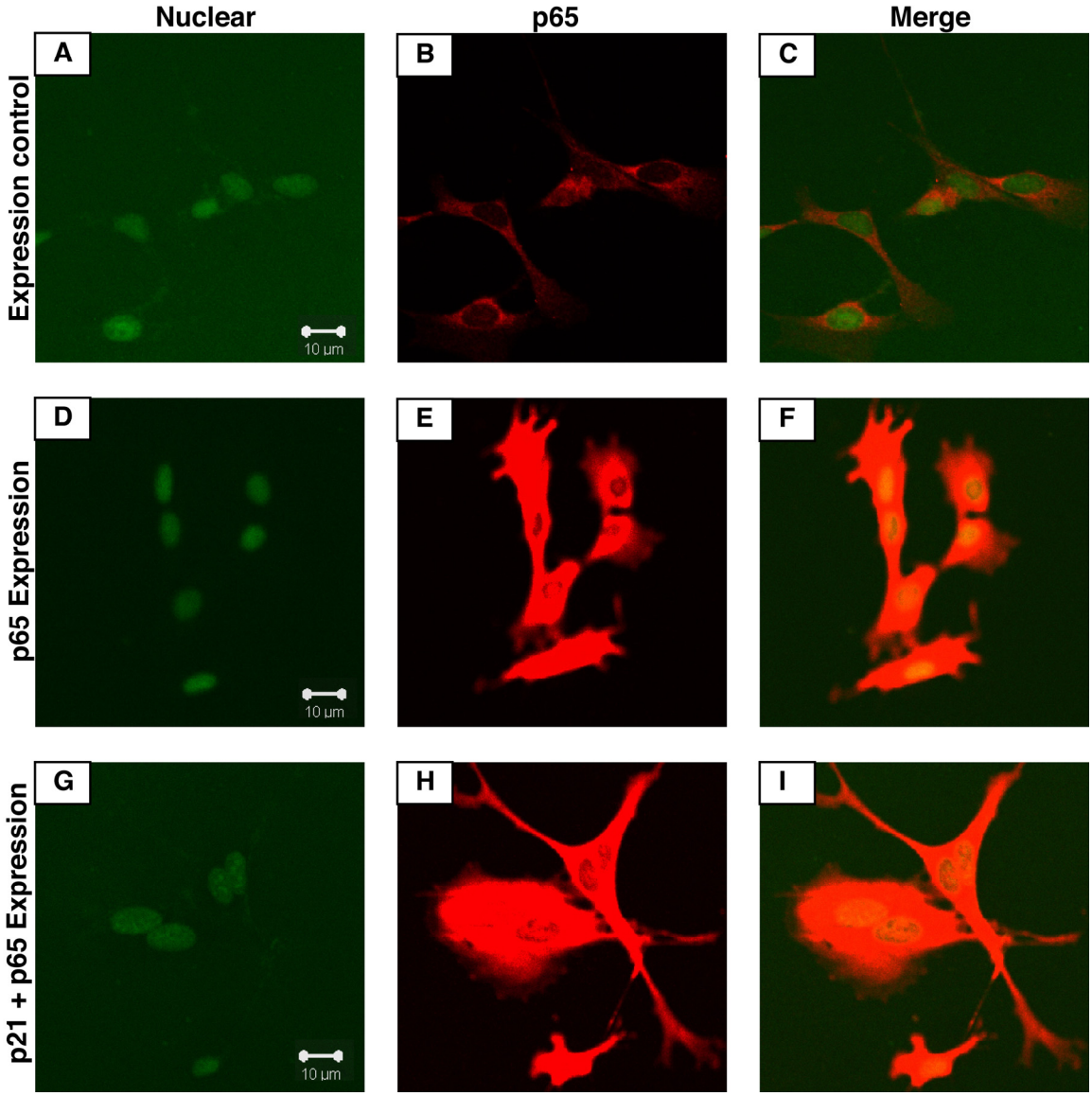

The growth analysis illustrated significantly decreased growth in p65, and p65 + $p21^{Cip1}$ expressing astrocytes. The doubling time for the control astrocytes is 24 hours. In contrast, the p65, and p65 + $p21^{Cip1}$ over expressing astrocytes showed only a sight increase in cell number over the course of 5 days (Figure 39).

**Figure 39. P65 over expression decreases growth of astrocytes**. Grow curves of Control, p65 over expression, and p65 + $p21^{Cip1}$ over expression, and p44/WDR77-null astrocytes.

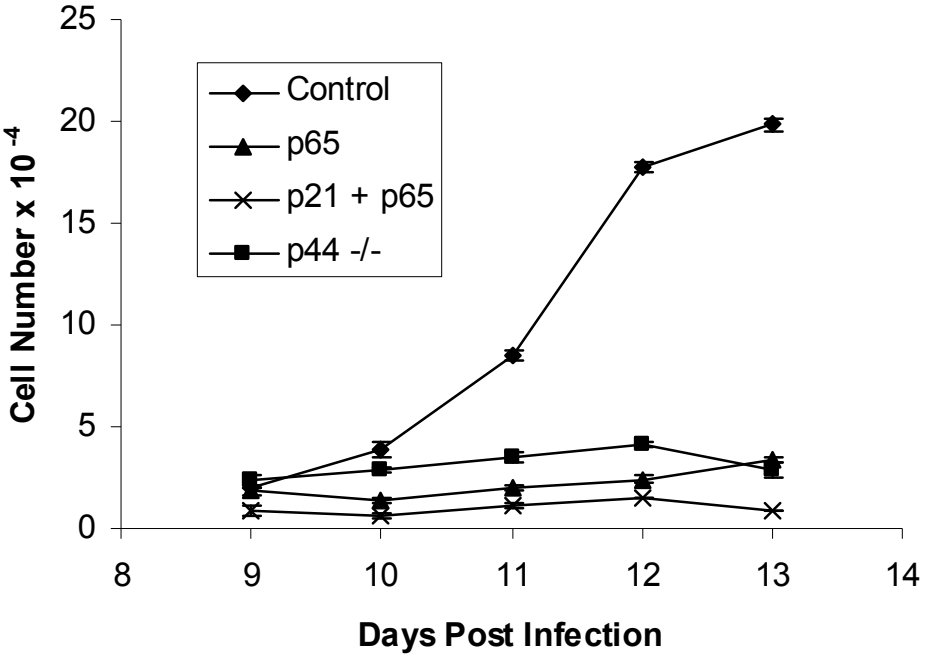

**AIV. Discussion:**

It is not surprising with NF-κB ability to influence over 150 genes that activation of the canonical or classical NF-κB pathway has been implicated in astrocyte proliferation (133, 136, 137, 249, 250). Previous experiments illustrated that the gene deletion of p44/WDR77 induces a dramatic decrease in growth of astrocytes (Figure 21). While the p65 shRNA did not completely knockdown p65 expression in the WT astrocytes, the p65 shRNA and p65 + $p21^{Cip1}$ shRNA were effective at knocking down p65 expression after astrocyte activation induced by p44/WDR77 gene deletion. We demonstrated that inhibition of the classical NF-κB pathway activity by the p65 shRNA expression can completely recover the decrease in growth of astrocytes induced by loss of p44/WDR77.

Furthermore we demonstrated that NF-κB could decrease astrocyte growth to the levels seen in p44/WDR77 deficient astrocytes. These finding suggest that p44/WDR77 regulates astrocyte proliferation through repressing p65 expression and nuclear localization. The molecular mechanisms by which NF-κB influences astrocyte proliferation still remains unclear however a number pathways including regulation of $p21^{Cip1}$ expression have been implicated in this regulatory process (138, 139). The fact that $p21^{Cip1}$ knockdown only partial recovered astrocyte growth inhibition and that no additive effect on cells growth after the knockdown of p65 and $p21^{Cip1}$ was observed infers NF-κB has regulatory roles in astrocyte growth that extend beyond $p21^{Cip1}$.

**B. The NF-κB activity is essential for astrocyte activation induced by p44/WDR77 gene deletion.**

**BI. Rationale:**

Astrocytes carry out a vast array of actions critical for healthy CNS function, thus it's not surprising that reactive astrocytes or reactive astrogliosis have primary and secondary affects on the disease pathology of the CNS with direct and even grave implications on patient outcome (39, 50, 85). We found that p44/WDR77 gene deletion in astrocytes induces astrogliosis characterized by the hallmark increase in GFAP. Analysis of p44/WDR77 regulation of astrocyte activation revealed that down regulation of $p21^{Cip1}$ expression inhibited reactive astrogliosis induced by p44/WDR77 gene deletion. Further examination of this pathway illustrated that down regulation of $p21^{Cip1}$ expression was accompanied with decreased p65 nuclear localization. These findings are consistent with studies that have implicated the canonical or classical NF-κB pathway as a regulator of both beneficial and deleterious astrocytic actions during reactive astrogliosis (50, 131, 132, 134, 143). Upon closer investigation of this phenomenon, experiments revealed that down regulation of $p21^{Cip1}$ expression only partially recovered astrocyte growth inhibition induced by p44/WDR77 gene deletion, while shRNA knockdown of p65 completely recovered the growth inhibition, suggesting NF-κB activity institutes additional regulatory actions for astrocyte activation induced by p44/WDR77 gene deletion.

**BII. Experimental Design:**

To examine roles of NF-κB in astrocytes activation induced by the loss of p44/WDR77, $p44/WDR77^{loxP/loxP}$ astrocytes were infected with lentivirus expressing (i)

nontargeting control; (ii) p65 shRNA; (iii) $p21^{Cip1}$ + p65 shRNA. Four days later astrocytes were infected with either Ad-CMV-GFP or Ad-CMV-Cre–GFP to generate 6 cell lines (WT: Control-GFP, p65 shRNA-GFP, $p21^{Cip1}$ + p65 shRNA-GFP, MT: Control-Cre, p65 shRNA-Cre, $p21^{Cip1}$ + p65 shRNA-Cre) (Figure 34A). Nine days after infection astrocytes were immunostained for GFAP. Cell lysates were also prepared from astrocytes seven days after adenovirus infection and subjected to western blot analysis with anti-GFAP.

To further explore NF-κB roles in astrocytes, WT astrocytes were infected with control lentivirus or lentivirus expressing human p65 or human $p21^{Cip1}$ plus p65 (Figure 34B). Nine days after viral infection, astrocytes were subject to immunostaining for GFAP.

**BIII. Results:**

Comparable with earlier findings WT (Control-GFP, p65 shRNA-GFP, and p65 + $p21^{Cip1}$ shRNA-GFP) astrocytes exhibited low levels GFAP and cellular structure of nonreactive astrocytes (Figure 30B, Figure 40B, and Figure 41B). Upon loss of p44/WDR77 expression (9 days post Ad-Cre infection), the MT (Control-Cre) astrocytes expressed higher levels of GFAP (Figure 30E), indicative of astrocyte reactivity. While the MT (p65 shRNA-Cre, and p65 + $p21^{Cip1}$ shRNA-Cre) astrocytes despite the loss of p44/WDR77 showed low levels GFAP and cellular structure of nonreactive astrocytes (Figure 40E, and Figure 41E). This finding was confirmed by the Western blot analysis that demonstrates a hallmark increase of GFAP in MT (Control-Cre) astrocytes while the MT (p65 shRNA-Cre, and p65 + $p21^{Cip1}$ shRNA-Cre) astrocytes maintain basil level of GFAP expression (Figure 28A, third panel, lane 5 versus lanes 7 and 8).

**Figure 40. Down regulation of p65 inhibits astrocyte activation induced by p44/WDR77 deletion in astrocytes.** A-F, WT (p65 shRNA GFP) and MT (p65 shRNA Cre) astrocytes were stained for nucleus (A and D) and GFAP (B and E). The GFAP staining signals are merged with nuclear staining (C and F).

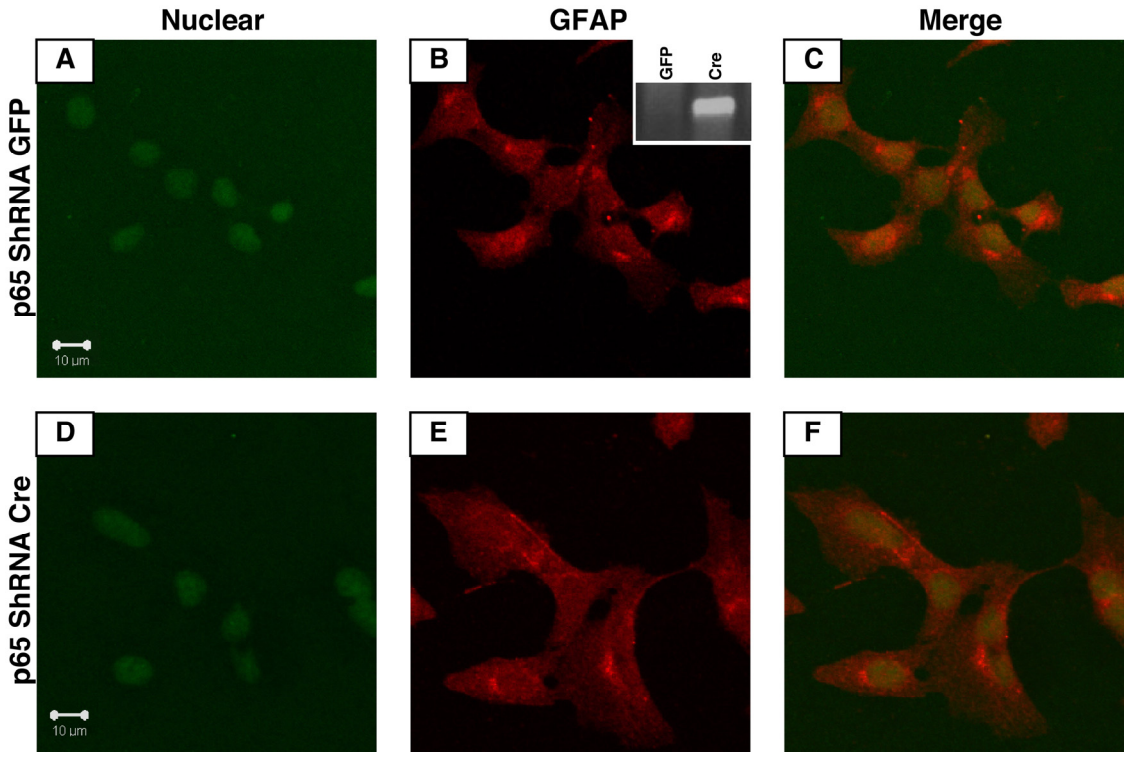

**Figure 41. Down regulation of p65 + p21$^{Cip1}$ inhibits astrocyte activation induced by p44/WDR77 deletion in astrocytes.** A-F, WT (p65 + p21$^{Cip1}$ shRNA-GFP) and MT (p65 + p21$^{Cip1}$ shRNA-Cre) astrocytes were stained for nucleus (A and D) and GFAP (B and E). The GFAP staining signals are merged with nuclear staining (D and F). The GFAP staining signals are merged with nuclear staining (C and F).

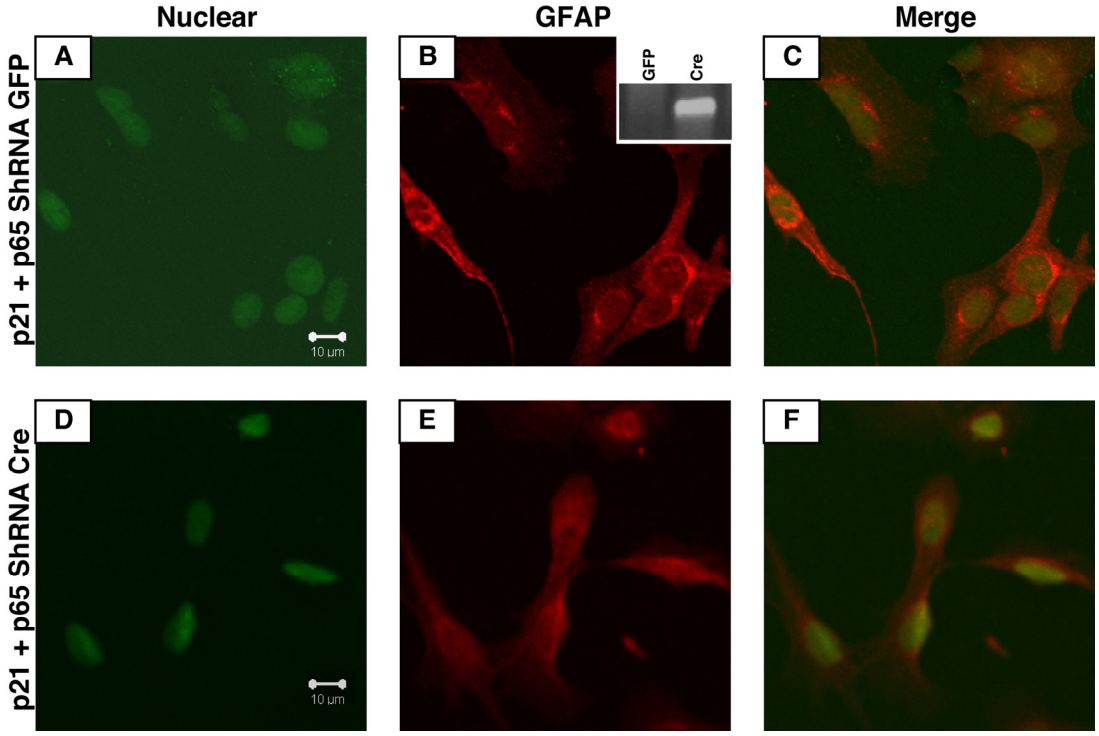

Consistent with prior studies (50, 133, 136, 137) that suggest NF-κB is a regulator of astrocyte activation, we found that p65 and p65 + $p21^{Cip1}$ over expression increased GFAP expression (Figure 42E, and Figure 43E), while the control astrocytes maintained low levels GFAP and cellular structure of nonreactive astrocytes (Figure 42B).

**Figure 42. P65 over expression leads to increased GFAP expression in astrocytes.** A-F, Control and p65 over expression astrocytes were stained for nucleus (A and D) and GFAP (B and E). The GFAP staining signals are merged with nuclear staining (C and F).

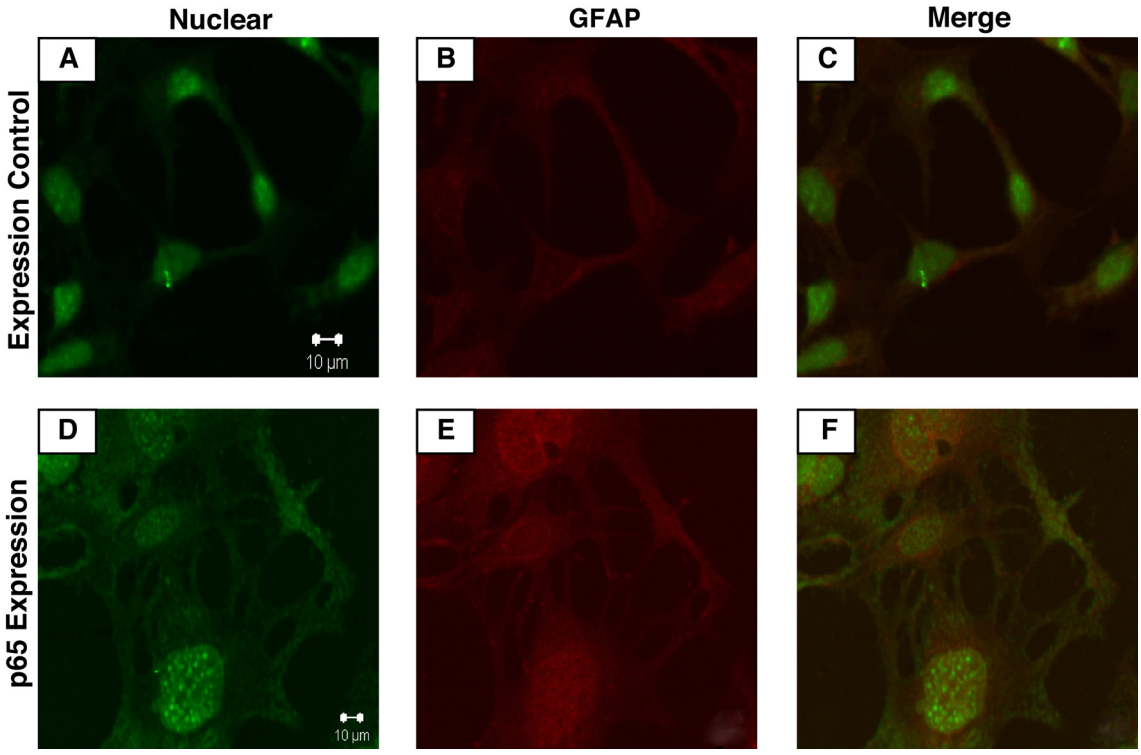

**Figure 43. P65 + p21$^{Cip1}$ over expression leads to increased GFAP expression in astrocytes.** A-F, Control and p65 + p21$^{Cip1}$ over expression astrocytes were stained for nucleus (A and D) and GFAP (B and E). The GFAP staining signals are merged with nuclear staining (C and F).

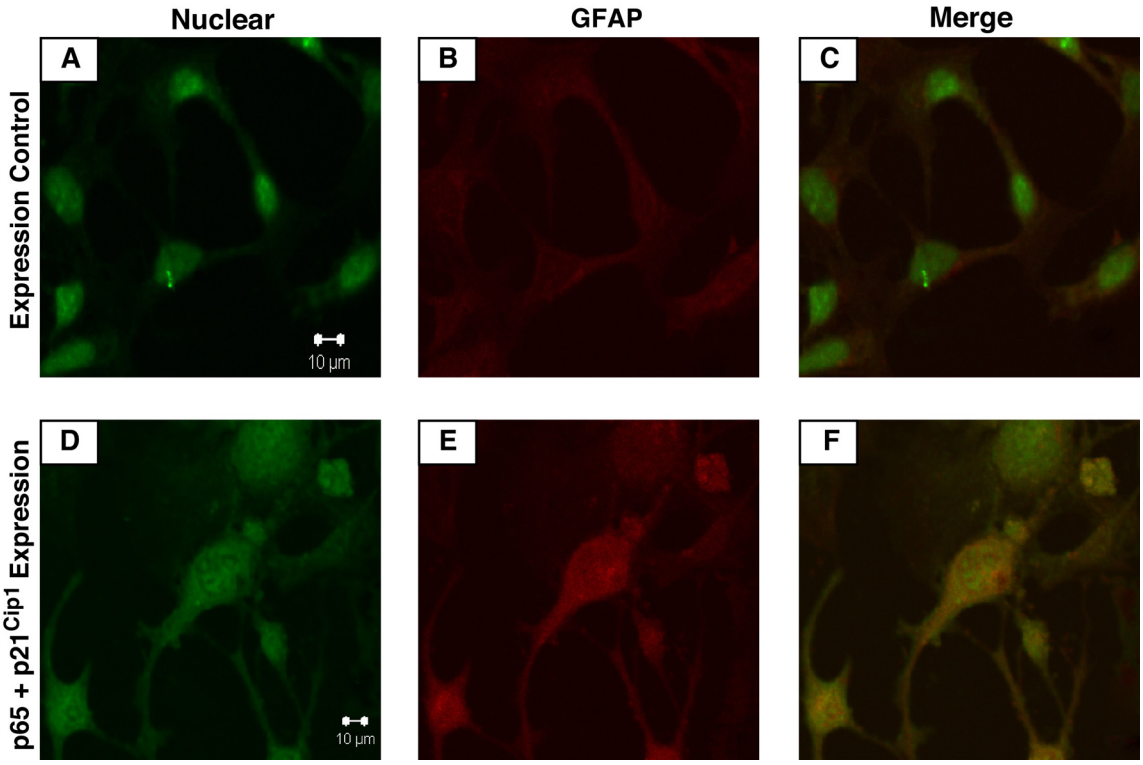

**BIV. Discussion:**

Other studies utilizing transgenic mice expressing a dominant negative (dn) form of the inhibitor of κBα driven by GFAP promoter demonstrated that the loss of NF-κB activity following spinal cord injury resulted in decreased GFAP expression and glial scaring (131). This alteration in astrocyte activation was accompanied with a reduction in astrocytic production of proinflammatory chemokines and cytokines, such as CXCL10, CCL2 (131). This study, along with a multitude other studies have suggested astrocytic NF-κB plays a role in reactive astrogliosis and neuropathology (50).

P44/WDR77 gene deletion in astrocyte induces a striking increase astrogliosis in the MT mouse brain and astrocytic culture. This induction of astrocytic activation is associated with a significant increase $p21^{Cip1}$ expression and NF-κB activation characterized by p65 nuclear localization. We found that repression of $p21^{Cip1}$ expression after p44/WDR77 deletion inhibited astrocyte activation and was accompanied with decreased p65 nuclear localization. While $p21^{Cip1}$'s role in activation of astrocyte and NF-κB is not well understood, studies of other cell cycle regulators have implicated cell cycle control systems as modulators of astrocyte activation, thus could induce secondary effects to induce p65 nuclear localization (50, 132, 246-248). Growth analysis of p44/WDR77 deficient astrocytes illustrated that NF-κB activity institutes additional regulatory actions not mediated by $p21^{Cip1}$, through completely recovered astrocyte growth after p65 knockdown, while $p21^{Cip1}$ knockdown only partially recovered astrocyte growth.

Consistent with NF-κB implications in astrocyte activation, immunostaining revealed the induction of astrogliosis by p44/WDR77 gene deletion characterized by increased GFAP expression only in astrocytes exhibiting p65 nuclear localization (50). Furthermore we confirmed NF-κB ability to induce astrocytes activation independent of

the p44/WDR77 status through the induction of over expression of human p65, suggesting that p44/WDR77 influences astrocyte activation through the regulation of p65 expression and nuclear localization. However neither p65 or p65 + $p21^{Cip1}$ over expression reached the levels of GFAP expression generated by p44/WDR77 deletion in astrocytes. This result indicates there are other changes induced by the loss p44/WDR77 in astrocytes, thus prompting further study into p44/WDR77 involvement in astrocyte activation.

# Chapter VII:

# Summary and Future Directions

## Chapter VII: Summary and Future Directions

Astrocytes, the most abundant cell type in the brain, were long underappreciated as they were thought to be merely a supportive component of the CNS, and their reactive state viewed simply as a marker for CNS disease (25, 38). The past few decades of research has drastically altered this view leading to a deepened interest on their biological importance under normal and pathologic conditions (39). Active roles for astrocytes in numerous functions essential for proper and healthy activity of the CNS have been established, some of which are providing energy metabolites to neurons, enhancing neuronal survival under stressed conditions, modulating extracellular balance of ions, and synaptic transmission (18, 40-42). Insults to the CNS initiates series of metabolic and morphological changes in astrocytes commonly referred to as reactive gliosis or astrogliosis (43-47). Despite decades of research, many of fundamental questions about the molecular mechanisms that lead to reactive astrocytes are just beginning to lead to a better understanding of overall CNS pathology (50).

Preliminary studies revealed a striking increase in reactive astrogliosis and cellular apoptosis in the brains of p44/WDR77-deficient mice. Additionally astrogliosis was only observed in astrocytes that had lost p44/WDR77 expression (Figure 12). This finding combined with prior studies in our laboratory that illustrate p44/WDR77 plays important roles in the proliferation and differentiation of prostate epithelial cells, suggest that p44/WDR77 conducts regulatory functions in cellular differentiation and possibly activation of astrocytes (181). Given astrocytes vast clinical importance this warrants farther exploration into p44/WDR77 regulatory actions in activation astrocytes. Astrocytes were isolated from mouse ($p44^{loxP/loxP}$) brain and immortalized with adenovirus E6/E7. The p44/WDR77 gene was deleted by adenovirus-mediated Cre expression. Using this cell culture system, we demonstrated p44/WRD77 is essential for growth of astrocytes and loss of p44/WDR77 expression in astrocytes leads to

dramatic changes in cellular structure and increased expression of GFAP, indicative of astrogliosis (Figure 20 – 24). Thus, p44/WDR77 prevents astrogliosis in the brain.

Recent studies have suggested that the AR-target gene $p21^{Cip1}$ directly effects astrocyte activation (140, 141, 152, 172). This finding correlated with increased $p21^{Cip1}$ expression in MT mice brains found in our gene array of whole brains from MT and WT mice. Further analysis of this pathway revealed the loss of p44/WDR77 in astrocytes generated a significant increase in $p21^{Cip1}$ expression and the inhibition of this increased expression inhibits astrocyte activation induced by p44/WDR77 gene deletion (Figure 25 – 31). While the mechanistic actions of $p21^{Cip1}$ in reactive gliosis remain incompletely characterized, there is growing evidence that cell-cycle control systems institute regulatory functions in reactive gliosis, (246-248). While a more detailed analysis is needed to confirm p44/WDR77 regulation of astrocyte cell cycle this coupled with our findings puts fourth that p44/WDR77 modulates astrocyte activation by indirectly inducing cycle changes through effecting $p21^{Cip1}$ expression (Figure 44). This doesn't preclude other modulatory actions of $p21^{Cip1}$ such as positive modulatory effects on NF-κB activation a pathway long implicated in gliosis; represent a possible contributing mechanism of action (140, 141).

Activation of the canonical or classical NF-κB pathway has been implicated in the regulation of astrocyte activation. Activation of this pathway is characterized by nuclear localization of p65 (132, 134). Examination of this pathway in astrocytes after p44/WDR77 gene deletion revealed increased activation of the classical NF-κB pathway (Figure 32). The knockdown of p65 in p44/WDR77-deficient astrocytes reduced GFAP expression to basal levels and suppressed phenotypes of activated astrocytes induced by the deletion of p4/WDR77 gene. While p44/WDR77 regulation of NF-κB activity is largely unexplored, p44/WDR77's ability to act as a cofactor for GR, a known

transrepressor of p65 activity, represents a possible mechanism of action and area that warrants further study (238).

The inhibition of increased $p21^{Cip1}$ expression decreased p65 nuclear localization. Over expression of $p21^{Cip1}$ enhanced p65 expression and over expression of p65 also increased $p21^{Cip1}$ expression. These observations suggest that $p21^{Cip1}$ and NF-kB are cross-linked. The molecular mechanisms of this cross-talk in astrocyte are not clear. This modulatory affect might be a secondary action induced by changes in cell cycle control systems that institute regulatory functions in reactive gliosis that in turn can create signaling changes in cytokines such as TNF-$\alpha$ that can invoke NF-$\kappa$B activity (132, 246-248). Other studies utilizing transgenic mice expressing a dominant negative (dn) form of the inhibitor of $\kappa B\alpha$ driven by GFAP promoter demonstrated that the loss of NF-$\kappa$B activity following spinal cord injury resulted in decreased GFAP expression and glial scarring (131). This alteration in astrocyte activation was accompanied with a reduction in astrocytic production of proinflammatory chemokines and cytokines, such as CXCL10, CCL2 (131), which might affect $p21^{Cip1}$ expression.

The data in this study puts forth the model that p44/WDR77 can influence the activational states of astrocytes through independently and jointly augmenting the expression and activity of $p21^{Cip1}$ and NF-$\kappa$B (Figure 44).

**Figure 44. Model of p44/WDR77 role is astrocyte activation.**

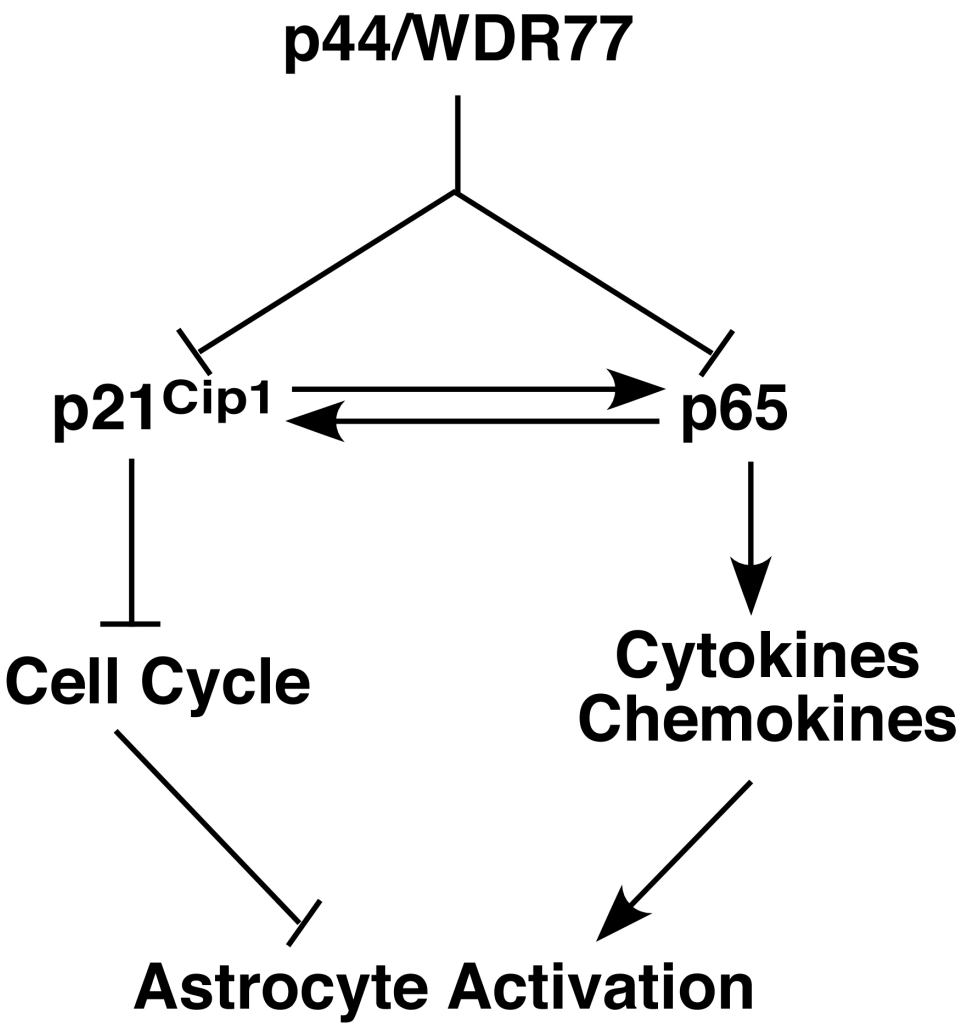

While many of detailed mechanisms of astrocyte activation remain to be eluted, a multitude of pathways have been implicated in astrocyte activation (50). Two such pathways are illustrated in androgen and glucocorticoid ability to down-regulate reactive gliosis after neural injury (227-229). P44/WDR77's gift to orchestrate modulatory effects over AR- and GR-dependent gene expression as cofactor represents a possible means to regulate astrocyte activation (180). It is also possible that p44/WDR77 might interact and function with other DNA-binding proteins in astrocytes. Further studies are needed to clarify p44/WDR77 mechanistic actions in astrocytes.

# Chapter VIII:

# References

## References

1. Olry R, Haines DE. 1998.Cerebral mythology: a skull stuffed with gods. (Neurowords 3) Hist Neurosci. 7:82-3.

2. DeFelipe J, Jones EG, Santiago RY. 1992. Cajal and methods in neurohistology. Trends Neurosci 15:237-246.

3. Colom R, Karama S, Jung RE, Haier RJ. 2010. Human intelligence and brain networks. Dialogues Clin Neurosci.12:489-501.

4. Salas C, Broglio C, Rodríguez F. 2003. Evolution of forebrain and spatial cognition in vertebrates: conservation across diversity. Brain Behav Evol 62:72–82.

5. Coote JH. 1982. Respiratory and circulatory control during sleep. J Exp Biol 100:223-44.

6. Wolf U, Rapoport MJ, Schweizer TA. 2009. Evaluating the affective component of the cerebellar cognitive affective syndrome. J Neuropsychiatry Clin Neurosci 21:245–53.

7. Fine EJ, Ionita CC, Lohr L. 2002. The history of the development of the cerebellar examination. Semin Neurol 22:375–84.

8. Frank M, Samanta J, Moustafa A, Sherman S. 2007. Hold Your Horses: Impulsivity, Deep Brain Stimulation, and Medication in Parkinsonism. Science 318:1309–12

9. Parent A, Hazrati LN. 1995. Functional anatomy of the basal ganglia: the cortico-basal ganglia-thalamo-cortical loop. Brain Res Rev 20:91-127.

10. Concha ML, Signore IA, Colombo A. 2009. Mechanisms of directional asymmetry in the zebrafish epithalamus. Semin Cell Dev Biol 20:498-509.

11. Percheron G. 2003. Thalamus. In Paxinos G, and May J. The human nervous system. 2d Ed. Elsevier. Amsterdam pp.592-675

12. Steriade M, and Llinas R. 1988. The functional states of the thalamus and the associated neuronal interplay. Physiological Reviews 68:699-742.

13. Romeo RD, Bellani R, Karatsoreos IN, Chhua N, Vernov M, Conrad CD, McEwen BS. 2006. Stress history and pubertal development interact to shape hypothalamic-pituitary-adrenal axis plasticity. Endocrinology 147:1664-74.

14. McDannald M, Kerfoot E, Gallagher M, and Holland P. 2005. Amygdala central nucleus function is necessary for learning but not expression of conditioned visual orienting. Behav Neurosci 119:202–212.

15. Killcross S, Robbins T, Everitt B. 1997. Different types of fear-conditioned behaviour mediated by separate nuclei within amygdala. Nature 388:377–80.

16. Schuurmans C, Guillemot F. 2002. Molecular mechanisms underlying cell fate specification in the developing telencephalon. Curr Opin Neurobiol.12:26-34.

17. Green TL, Hunter DD, Chan W, Merlie JP, Sanes JR. 1992. Synthesis and assembly of the synaptic cleft protein S-laminin by cultured cells. J Biol Chem 267:2014-22.

18. Nedergaard M, Ransom B, Goldman SA. 2003. New roles for astrocytes: redefining the functional architecture of the brain. Trends Neurosci 26:523-30.

19. Hansson E, Rönnbäck L. 2003. Glial neuronal signaling in the central nervous system. FASEB J 17:341-48.

20. Azevedo FA, Carvalho LR, Grinberg LT, Farfel JM, Ferretti RE, Leite RE, Jacob FW, Lent R, Herculano-Houzel S. 2009. Equal numbers of neuronal and nonneuronal cells make the human brain an isometrically scaled-up primate brain. J Comp Neurol 513:532-41.

21. Walz W. 1989. Role of glial cells in regulation of the brain ion microenvironment. Prog Neurobiol 33:309–33.

22. Vernadakis A. 1996. Glia-neuron intercommunications and synaptic plasticity. Prog Neurobiol 49:185–214.

23. Baumann N, Pham-Dinh D. 2001. Biology of Oligodendrocyte and Myelin in the Mammalian Central Nervous System. Physiological Reviews 18:871–927.

24. Kreutzberg GW. 1995. The First Line of Defense in Brain Pathologies. Drug-Research 45:357–360.

25. Ransom B, Behar T, Nedergaard M. 2003. New roles for astrocytes (stars at last). Trends Neurosci 26:520-2.

26. Vallejo R, Tilley DM, Vogel L, Benyamin R. 2010. The role of glia and the immune system in the development and maintenance of neuropathic pain. Pain Pract 10:167-84.

27. Gordon GR, Mulligan SJ, MacVicar BA. 2007. Astrocyte control of the cerebrovasculature Glia 55:1214–1221.

28. Keyser DO, Pellmar TC. 1994. Synaptic transmission in the hippocampus: critical role for glial cells. Glia 10:237–243.

29. Araque A, Parpura V, Sanzgiri R P, Haydon PG. 1999. Tripartite synapses: glia, the acknowledged partner. Trends Neurosci 22:208–215.

30. Moalem G, Tracey DJ. 2006. Immune and inflammatory mechanisms in neuropathic pain. Brain Res Rev 51:240–264.

31. Chen L, Yang P, Kijlstra A. 2002. Distribution, markers, and functions of retinal microglia. Ocul Immunol Inflamm 10:27-39.

32. Davalos D, Grutzendler J, Yang G, et al. 2005. ATP mediates rapid microglial response to local brain injury in vivo. Nat Neurosci 8:752–758.

33. Rotshenker S. 2009. The role of Galectin-3/MAC-2 in the activation of the innate-immune function of phagocytosis in microglia in injury and disease. J Mol Neurosci 39:99-103.

34. Buchanan MM, Hutchinson M, Watkins LR, Yin H. 2010. Toll-like receptor 4 in CNS pathologies. J Neurochem 114:13-27.

35. Park KM, Bowers WJ. 2010. Tumor necrosis factor-alpha mediated signaling in neuronal homeostasis and dysfunction. Cell Signal 22:977-83.

36. Klein MA, Möller JC, Jones LL, Bluethmann H, Kreutzberg GW, Raivich G. 1997. Impaired neuroglial activation in interleukin-6 deficient mice. Glia 19:227-33.

37. Stolp HB, Ek CJ, Johansson PA, Dziegielewska KM, Bethge N, Wheaton BJ, Potter AM, Saunders NR. 2009. Factors involved in inflammation-induced developmental white matter damage. Neurosci Lett. 27;451:232-6.

38. Acosta MT, Gioia GA, Silva AJ. 2006. Neurofibromatosis type 1: new insights into neurocognitive issues. Curr Neurol Neurosci Rep 6:136–14.

39. Volterra A, Meldolesi J. 2005. Astrocytes, from brain glue to communication elements: the revolution continues. Nat Rev Neurosci 6:626-40.

40. Barres BA. 2008. The mystery and magic of glia: a perspective on their roles in health and disease. Neuron 60:430–440.

41. Pellerin L, Bouzier-Sore AK, Aubert A, Serres S, Merle M, Costalat R, Magistretti PJ. 2007. Activity-dependent regulation of energy metabolism by astrocytes: an update. Glia 55:1251–1262.

42. Seifert G, Schilling K, Steinhäuser C. 2006. Astrocyte dysfunction in neurological disorders: a molecular perspective. Nat Rev Neurosci 7:194–206.

43. Correa-Cerro LS, Mandell JW. 2007. Molecular mechanisms of astrogliosis: new approaches with mouse genetics. J Neuropathol Exp Neurol 66:169-76.

44. Eddleston M, Mucke L. 1993. Molecular profile of reactive astrocytes – implications for their role in neurological disease. Neuroscience 54:15–36.

45. Pekny M, Nilsson M. 2005. Astrocyte activation and reactive gliosis. Glia 50:427–434.

46. Sofroniew MV. 2005. Reactive astrocytes in neural repair and protection. Neuroscientist 5:400–407.

47. Maragakis NJ, Rothstein JD. 2006. Mechanisms of disease: astrocytes in neurodegenerative disease. Nat Clin Pract Neurol 2:679–689.

48. Yokoyama H, Uchida H, Kuroiwa H, Kasahara J, Araki T. 2011. Role of glial cells in neurotoxin-induced animal models of Parkinson's disease. Neurol Sci. 32:1-7.

49. Schipper HM. 1996. Astrocytes, brain aging, and neurodegeneration. Neurobiol Aging 17:467-80.

50. Sofroniew MV. 2009. Molecular dissection of reactive astrogliosis and glial scar formation. Trends Neurosci 32:638-47.

51. Liem RK, Messing A. 2009. Dysfunctions of neuronal and glial intermediate filaments in disease. J Clin Invest 119:1814-24.

52. Miller RH, Raff MC. 1984. Fibrous and protoplasmic astrocytes are biochemically and developmentally distinct. J Neurosci 4:585-92.

53. Oberheim NA, Wang X, Goldman S, Nedergaard M. 2006. Astrocytic complexity distinguishes the human brain. Trends Neurosci 29:547-53.

54. Raine CS. 1984. On the association between perinodal astrocytic processes and the node of Ranvier in the CNS. J Neurocytol 13:21-7.

55. Butt AM, Colquhoun K, Berry M. 1994. Confocal imaging of glial cells in the intact rat optic nerve. Glia 10:315-22.

56. Halassa MM, Fellin T, Takano H, Dong JH, Haydon PG. 2007. Synaptic islands defined by the territory of a single astrocyte. J Neurosci 27:6473–77.

.

57. Markham JA, Greenough WT. 2004. Experience-driven brain plasticity: beyond the synapse. Neuron Glia Biol.:1(4):351-363.

58. Jessen KR. 2004. Glial cells. Int J Biochem Cell Biol 36:1861-7.

59. Powell EM, Geller HM. 1999. Dissection of astrocyte-mediated cues in neuronal guidance and process extension. Glia 26:73–83.

60. Barres BA, Smith SJ. 2001. Neurobiology. Cholesterol--making or breaking the synapse. Science. 9;294:1296-7.

61. Christopherson KS, Ullian EM, Stokes CC, Mullowney CE, Hell JW, Agah A, Lawler J, Mosher DF, Bornstein P, Barres BA. 2005. Thrombospondins are astrocyte-secreted proteins that promote CNS synaptogenesis. Cell 120:421–433.

62. Ullian EK, Sapperstein SK, Christopherson KS, Barres BA. 2001. Control of synapse number by glia. Science 291:657–661.

63. Lutz SE, Zhao Y, Gulinello M, Lee SC, Raine CS, Brosnan CF. 2009. Deletion of astrocyte connexins 43 and 30 leads to a dysmyelinating phenotype and hippocampal CA1 vacuolation.
J Neurosci 29:7743–7752.

64. Agulhon C, Petravicz J, McMullen AB, Sweger EJ, Minton SK, Taves SR, Casper KB, Fiacco TA, McCarthy KD. 2008. What is the role of astrocyte calcium in neurophysiology? Neuron:59:932-46.

65. Ladecola C, Nedergaard M. 2007. Glial regulation of the cerebral microvasculature. Nat Neurosci 10:1369–1376.

66. Fergus A, Lee KS. 1997. Regulation of cerebral microvessels by glutamatergic mechanisms. Brain Res pp. 35–45.

67. Koehler RC, Roman RJ, Harder DR. 2009. Astrocytes and the regulation of cerebral blood flow. Trends Neurosci 32:160–169.

68. Brown AM, Ransom BR. 2007. Astrocyte glycogen and brain energy metabolism. Glia 55:1263–1271.

69. Salmina AB. 2009. Neuron-glia interactions as therapeutic targets in neurodegeneration. J Alzheimers Dis 16:485-502.

70. Simard M, Nedergaard M. 2004. The neurobiology of glia in the context of water and ion homeostasis. Neuroscience 129:877–896.

71. Zador Z, Stiver S, Wang V, Manley GT. 2009. Role of aquaporin-4 in cerebral edema and stroke. Handb Exp Pharmacol 190:159–170.

72. Obara M, Szeliga M, Albrecht J. 2008. Regulation of pH in the mammalian central nervous system under normal and pathological conditions: facts and hypotheses. Neurochem Int 52:905–919.

73. Kimelberg HK. 1995. Receptors on astrocytes--what possible functions? Neurochem Int 26:27-40.

74. Anderson CM, Swanson RA. 2000. Astrocyte glutamate transport: review of properties, regulation, and physiological functions. Glia 32:1-14.

75. Bonkowski D, Katyshev V, Balabanov RD, Borisov A, Dore-Duffy P. 2011. The CNS microvascular pericyte: pericyte-astrocyte crosstalk in the regulation of tissue survival. Fluids Barriers CNS:8(1):8.

76. Halassa MM, Fellin T, Haydon PG. 2007. The tripartite synapse: roles for gliotransmission in health and disease. Trends Mol Med 13:54–63.

77. Perea G, Navarrete M, Araque A. 2009. Tripartite synapses: astrocytes process and control synaptic information. Trends Neurosci 32:t421–t431.

78. Stellwagen D, Malenka RC. 2006. Synaptic scaling mediated by glial TNF-alpha. Nature 440:1054–1059.

79. Garcia-Segura LM, Melcangi RC. 2006. Steroids and glial cell function. Glia 54:485–498.

80. Wender R, Brown AM, Fern R, Swanson RA, Farrell K, Ransom BR. 2000. Astrocytic glycogen influences axon function and survival during glucose deprivation in central white matter. J Neurosci 20:6804–6810.

81. Occhipinti R, Somersalo E, Calvetti D. 2009. Astrocytes as the glucose shunt for glutamatergic neurons at high activity: an in silico study. J Neurophysiol 101:2528–2538.

82. Magistretti PJ, Sorg O, Yu N, Martin JL, Pellerin L. 1993. Neurotransmitters regulate energy metabolism in astrocytes: implications for the metabolic trafficking between neural cells. Dev Neurosci 15:306-12.

83. Magistretti PJ, Pellerin L. 1999. Cellular mechanisms of brain energy metabolism and their relevance to functional brain imaging. Philos Trans R Soc Lond B Biol Sci 29;354:1155-63.

84. Brown AM, Sickmann HM, Fosgerau K, Lund TM, Schousboe A, Waagepetersen HS, Ransom BR. 2005. Astrocyte glycogen metabolism is required for neural activity during aglycemia or intense stimulation in mouse white matter. J Neurosci Res 79:74–80.

85. Chen Y, Swanson RA. 2003. Astrocytes and brain injury. J Cereb Blood Flow Metab 23:137–149.

86. Luna G, Lewis GP, Banna CD, Skalli O, Fisher SK. 2010. Expression profiles of nestin and synemin in reactive astrocytes and Müller cells following retinal injury: a comparison with glial fibrillar acidic protein and vimentin. Mol Vis:16:2511-23.

87. Motti D, Le Duigou C, Eugène E, Chemaly N, Wittner L, Lazarevic D, Krmac H, Marstrand T, Valen E, Sanges R, Stupka E, Sandelin A, Cherubini E, Gustincich S, Miles R. 2010. Gene expression analysis of the emergence of epileptiform activity after focal injection of kainic acid into mouse hippocampus. Eur J Neurosci 32:1364-79.

88. Norenberg MD, Rao KV, Jayakumar AR. 2005. Mechanisms of ammonia-induced astrocyte swelling. Metab Brain Dis 20:303–318.

89. Myer DJ, Gurkoff GG, Lee SM, Hovda DA, Sofroniew MV. 2006. Essential protective roles of reactive astrocytes in traumatic brain injury. Brain 129:2761-72.

90. Vijayan VK, Lee YL, Eng LF. 1990. Increase in glial fibrillary acidic protein following neural trauma. Mol Chem Neuropathol 13:107-118.

91. Pekny M, Pekna M. 2004. Astrocyte intermediate filaments in CNS pathologies and regeneration. J Pathol 204:428–437.

92. Bushong EA, Martone ME, Jones YZ, Ellisman MH. 2002. Protoplasmic astrocytes in CA1 atratum radiatum occupy separate anatomical domains. J Neurosci 22:183–192.

93. Wilhelmsson U, Bushong EA, Price DL, Smarr BL, Phung V, Terada M, Ellisman MH, Pekny M. 2006. Redefining the concept of reactive astrocytes as cells that remain within their unique domains upon reaction to injury. Proc Natl Acad Sci USA 103:17513–17518.

94. Faulkner JR, Herrmann JE, Woo MJ, Tansey KE, Doan NB, Sofroniew MV. 2004. Reactive astrocytes protect tissue and preserve function after spinal cord injury. J Neurosci 24:2143–2155.

95. Drögemüller K, Helmuth U, Brunn A, Sakowicz-Burkiewicz M, Gutmann DH, Mueller W, Deckert M, Schlüter D. 2008. Astrocyte gp130 expression is critical for the control of Toxoplasma encephalitis. J Immunol 181:2683–2693.

96. Fitch MT, Silver J. 2008. CNS injury, glial scars, and inflammation: Inhibitory extracellular matrices and regeneration failure. Exp Neurol 209:294-301.

97. Colodner KJ, Montana RA, Anthony DC, Folkerth RD, De Girolami U, Feany MB. 2005. Proliferative potential of human astrocytes. J Neuropathol Exp Neurol 64:163–169.

98. Horner PJ, Power AE, Kempermann G, Kuhn HG, Palmer TD, Winkler J, Thal LJ, Gage FH. 2000. Proliferation and differentiation of progenitor cells throughout the intact adult rat spinal cord. J Neurosci 20:2218–2228.

99. Bush TG, Puvanachandra N, Horner CH, Polito A, Ostenfeld T, Svendsen CN, Mucke L, Johnson MH, Sofroniew MV. 1999. Leukocyte infiltration, neuronal

degeneration and neurite outgrowth after ablation of scar-forming, reactive astrocytes in adult transgenic mice. Neuron 23:297–308.

100. Schachtrup C, Ryu JK, Helmrick MJ, Vagena E, Galanakis DK, Degen JL, Margolis RU, Akassoglou K. 2010. Fibrinogen triggers astrocyte scar formation by promoting the availability of active TGF-beta after vascular damage.
J Neurosci. 30:5843-54.

101. Levison SW, Jiang FJ, Stoltzfus OK, Ducceschi MH. 2000. IL-6-type cytokines enhance epidermal growth factor-stimulated astrocyte proliferation. Glia 32:328–337.

102. Herrmann JE, Shah RR, Chan AF, Zheng B. 2010. EphA4 deficient mice maintain astroglial-fibrotic scar formation after spinal cord injury. Exp Neurol. 223:582-98.

103. Liu R, Chen XP, Tao LY. 2008. Regulation of axonal regeneration following the central nervous system injury in adult mammalian. Neurosci Bull 24:395-400.

104. Rothstein JD, Dykes-Hoberg M, Pardo CA, Bristol LA, Jin L, Kunci RW, Kanai Y, Hediger MA, Wang Y, Schielke JP, Welty DF. 1996. Knockout of glutamate transporters reveals a major role for astroglial transport in excitotoxicity and clearance of glutamate. Neuron 16:675–686.

105. Swanson RA, Ying W, Kauppinen TM. 2004. Astrocyte influences on ischemic neuronal death. Curr Mol Med 4:193–205.

106. Seifert G, Carmignoto G, Steinhäuser C. 2010. Astrocyte dysfunction in epilepsy. Brain Res Rev 63:212-221.

107. Rao KV, Panickar KS, Jayakumar AR, Norenberg MD. 2005. Astrocytes protect neurons from ammonia toxicity. Neurochem Res 30:1311–1318.

108. Koistinaho M, Lin S, Wu X, Esterman M, Koger D, Hanson J, Higgs R, Liu F, Malkani S, Bales KR, Paul SM. 2004. Apolipoprotein E promotes astrocyte colocalization and degradation of deposited amyloid-beta peptides. Nat Med 10:719–726.

109. Chen Y, Vartiainen NE, Ying W, Chan PH, Koistinaho J, Swanson RA. 2001. Astrocytes protect neurons from nitric oxide toxicity by a glutathione-dependent mechanism. J Neurochem 77:1601–1610.

110. Cavaliere C, Cirillo G, Rosaria BM, Rossi F, De Novellis V, Maione S, Papa M. 2007. Gliosis alters expression and uptake of spinal glial amino acid transporters in a mouse neuropathic pain model. Neuron Glia Biol 3:141-53.

111. Takano T, Kang J, Jaiswal JK, Simon SM, Lin JH, Yu Y, Li Y, Yang J, Dienel G, Zielke HR, Nedergaard M. 2005. Receptormediated glutamate release from volume sensitive channels in astrocytes. Proc Natl Acad Sci USA 102:16466–16471.

112. Papadopoulos MC, Verkman AS. 2007. Aquaporin-4 and brain edema. Pediatr Nephrol 22:778-84.

113. Takano T, Oberheim N, Cotrina ML, Nedergaard M. 2009. Astrocytes and ischemic injury. Stroke 40:S8–12.

114. Jansen LA, Uhlmann EJ, Crino PB, Gutmann DH, Wong M. 2005. Epileptogenesis and reduced inward rectifier potassium current in tuberous sclerosis complex-1-deficient astrocytes. Epilepsia 46:1871–1880.

115. David Y, Cacheaux LP, Ivens S, Lapilover E, Heinemann U, Kaufer D, Friedman A. 2009. Astrocytic dysfunction in epileptogenesis: consequence of altered potassium and glutamate homeostasis? J Neurosci 29:10588–10599.

116. Hamby ME, Sofroniew MV. 2010. Reactive astrocytes as therapeutic targets for CNS disorders. Neurotherapeutics 7:494-506.

117. Whitney NP, Eidem TM, Peng H, Huang Y, Zheng JC. 2009. Inflammation mediates varying effects in neurogenesis: relevance to the pathogenesis of brain injury and neurodegenerative disorders. J Neurochem 108:1343-59.

118. Agostinho P, Cunha RA, Oliveira C. 2010. Neuroinflammation, oxidative stress and the pathogenesis of Alzheimer's disease. Curr Pharm Des 16:2766-78.

119. Milligan ED, Watkins LR. 2009. Pathological and protective roles of glia in chronic pain. Nat Rev Neurosci 10:23–36.

120. John GR, Lee SC, Brosnan CF. 2003. Cytokines: powerful regulators of glial cell activation. Neuroscientist 9:10–22.

121. Suh HS, Brosnan CF, Lee SC. 2009. Toll-like receptors in CNS viral infections. Curr Top Microbiol Immunol 336:63-81.

122. Park J, Choi K, Jeong E, Kwon D, Benveniste EN, Choi C. 2004. Reactive oxygen species mediate chloroquine-induced expression of chemokines by human astroglial cells. Glia 47:9-20.

123. Sastre M, Klockgether T, Heneka MT. 2006. Contribution of inflammatory processes to Alzheimer's disease: molecular mechanisms. Int J Dev Neurosci 24:167-76.

124. Norenberg MD, Rama Rao KV, Jayakumar AR. 2009. Signaling factors in the mechanism of ammonia neurotoxicity. Metab Brain Dis 24:103–117.

125. Caccamo D, Campisi A, Currò M, Li Volti G, Vanella A, Lentile R. 2004. Excitotoxic and post-ischemic neurodegeneration: Involvement of transglutaminases. Amino Acids 27:373-379.

126. Koyama Y, Takemura M, Fujiki K, Ishikawa N, Shigenaga Y, Baba A. 1999. BQ788, an endothelin ET(B) receptor antagonist, attenuates stab wound injury-induced reactive astrocytes in rat brain. Glia 26:268–271.

127. Gadea A, Schinelli S, Gallo V. 2008. Endothelin-1 regulates astrocyte proliferation and reactive gliosis via a JNK/c-Jun signaling pathway. J Neurosci 28:2394–2408.

128. Herrmann JE, Imura T, Song B, Qi J, Ao Y, Nguyen TK, Korsak RA, Takeda K, Akira S, Sofroniew MV. 2008. STAT3 is a critical regulator of astrogliosis and scar formation after spinal cord injury. J Neurosci 9:7231-7243.

129. Bundesen LQ, Scheel TA, Bregman BS, Kromer LF. 2003. Ephrin-B2 and EphB2 regulation of astrocyte-meningeal fibroblast interactions in response to spinal cord lesions in adult rats. J Neurosci 23:7789–7800.

130. Qin H, Niyongere SA, Lee SJ, Baker BJ, Benveniste EN. Qin, H. et al. 2008. Expression and functional significance of SOCS-1 and SOCS-3 in astrocytes. J Immunol 181:3167–3176.

131. Brambilla R, Bracchi-Ricard V, Hu WH, Frydel B, Bramwell A, Karmally S, Green EJ, Bethea JR. 2005. Inhibition of astroglial nuclear factor kappa B reduces inflammation and improves functional recovery after spinal cord injury. J Exp Med 202:145–156.

132. Gilmore TD. 2006. Introduction to NF-kappaB: players, pathways, perspectives. Oncogene 30; 25:6680-4.

133. O'Neill LA, Kaltschmidt C. 1997. NF-kappa B: a crucial transcription factor for glial and neuronal cell function. Trends Neurosci 20:252–258.

134. Brambilla R, Persaud T, Hu X, Karmally S, Shestopalov VI, Dvoriantchikova G, Ivanov D, Nathanson L, Barnum SR, Bethea JR. 2009. Transgenic inhibition of astroglial NF-kappa B improves functional outcome in experimental autoimmune

encephalomyelitis by suppressing chronic central nervous system inflammation. J Immunol 1;182:2628-40.

135. May MJ, Ghosh S. 1998. Signal transduction through NF-kappa B. Immunol Today 19:80-8.

136. Pahl HL. 1999. Activators and target genes of Rel/NF-kappaB transcription factors. Oncogene 22:6853-66.

137. Zaheer A., Yorek MA, and Lim R. 2001. Effects of glia maturation factor overexpression in primary astrocytes on MAP kinase activation, transcription factor activation, and neurotrophin secretion. Neurochem Res 26:1293–1299.

138. Misra UK, Kaczowka S, Pizzo SV. 2010. Inhibition of NF-kappaB1 and NF-kappaB2 activation in prostate cancer cells treated with antibody against the carboxyl terminal domain of GRP78: effect of p53 upregulation. Biochem Biophys Res Commun 19;392:538-42.

139. Saegusa M, Hashimura M, Kuwata T, Okayasu I. 2010. Transcriptional regulation of pro-apoptotic Par-4 by NF-kappaB/p65 and its function in controlling cell kinetics during early events in endometrial tumourigenesis. J Pathol 221:26-36.

140. Tusell JM, Ejarque-Ortiz A, Mancera P, Solà C, Saura J, Serratosa J. 2009. Upregulation of p21Cip1 in activated glial cells. Glia 57:524-34.

141Tusell JM, Saura J, Serratosa J. 2005. Absence of the cell cycle inhibitor p21Cip1 reduces LPS-induced NO release and activation of the transcription factor NF-kappaB in mixed glial cultures. Glia 49:52-58.

142. Seitz CS, Deng H, Hinata K, Lin Q, Khavari PA. 2000. Nuclear factor kappaB subunits induce epithelial cell growth arrest. Cancer Res 60:4085-92.

143. García-Ovejero D, Veiga S, García-Segura LM, Doncarlos LL. 2002. Glial expression of estrogen and androgen receptors after rat brain injury. J Comp Neurol. 26:256-71.

144. Craft N, Chhor C, Tran C, Belldegrun A, DeKernion J, Witte ON, Said J, Reiter RE, Sawyers CL. 1999. Evidence for clonal outgrowth of androgen-independent prostate cancer cells from androgen-dependent tumors through a two-step process. Cancer Res 59:5030-6.

145. Craft N, Sawyers CL. 1998. Mechanistic concepts in androgen-dependence of prostate cancer. Cancer Metastasis Rev 17:421-7.

146. Denmeade SR, Lin XS, Isaacs JT. 1996. Role of programmed (apoptotic) cell death during the progression and therapy for prostate cancer. Prostate 28:251-65.

147. Jenster G. 1999. The role of the androgen receptor in the development and progression of prostate cancer. Semin Oncol 26:407-21.

148. Aarnisalo P, Palvimo JJ, Janne OA. 1998. CREB-binding protein in androgen receptor-mediated signaling. Proc Natl Acad Sci USA 95:2122-7.

149. Alen P, Claessens Verhoeven G, Rombauts W, Peeters B. 1999. The androgen receptor amino-terminal domain plays a key role in p160 coactivator-stimulated gene transcription. Mol Cell Biol 19:6085-97.

150. Berrevoets CA, Doesburg P, Steketee K, Trapman J, Brinkmann AO. 1998. Functional interactions of the AF-2 activation domain core region of the human androgen receptor with the amino-terminal domain and with the transcriptional coactivator TIF2 (transcriptional intermediary factor2). Mol Endocrinol 12:1172-83.

151. Gelmann EP. 2002. Molecular biology of the androgen receptor. J Clin Oncol 20:3001-15.

152. Heinlein CA, Chang C. 2002. Androgen receptor (AR) coregulators: an overview. Endocr Rev 23:175-200.

153. Ikonen T, Palvimo JJ, Janne OA. 1997. Interaction between the amino- and carboxyl-terminal regions of the rat androgen receptor modulates transcriptional activity and is influenced by nuclear receptor coactivators. J Biol Chem 272:29821-8.

154. Janne OA, Moilanen AM, Poukka H, Rouleau N, Karvonen U, Kotaja N, Hakli M, Palvimo JJ. 2000. Androgen-receptor-interacting nuclear proteins. Biochem Soc Trans 28:401-5.

155. Kingston RE, Narlikar GJ. 1999. ATP-dependent remodeling and acetylation as regulators of chromatin fluidity. Genes Dev 13:2339-52.

156. Ma H, Hong H, Huang SM, Irvine RA, Webb P, Kushner PJ, Coetzee GA, Stallcup MR. 1999. Multiple signal input and output domains of the 160-kilodalton nuclear receptor coactivator proteins. Mol Cell Biol 19:6164-73.

157. Roeder RG. 1998. Role of general and gene-specific cofactors in the regulation of eukaryotic transcription. Cold Spring Harb Symp Quant Biol 63:201-18.

158. Workman JL, Kingston RE. 1998. Alteration of nucleosome structure as a mechanism of transcriptional regulation. Annu Rev Biochem 67:545-79.

159. Barreto G, Veiga S, Azcoitia I, Garcia-Segura LM, Garcia-Ovejero D. 2007. Testosterone decreases reactive astroglia and reactive microglia after brain injury in male rats: role of its metabolites, oestradiol and dihydrotestosterone. Eur J Neurosci 25:3039-46.

160. Coers S, Tanzer L, Jones KJ. 2002. Testosterone treatment attenuates the effects of facial nerve transection on glial fibrillary acidic protein (GFAP) levels in the hamster facial motor nucleus. Metab Brain Dis 17:55-63.

161. Pan Y, Zhang H, Acharya AB, Patrick PH, Oliver D, Morley JE. 2005. Effect of testosterone on functional recovery in a castrate male rat stroke model. Brain Res 1043:195-204.

162. Storer PD, Jones KJ. 2003. Glial fibrillary acidic protein expression in the hamster red nucleus: effects of axotomy and testosterone treatment. Exp Neurol 184:939-46.

163. McCarthy MM, Amateau SK, Mong JA. 2002. Steroid modulation of astrocytes in the neonatal brain: implications for adult reproductive function. Biol Reprod 67:691-8.

164. Bancroft J. 2005. The endocrinology of sexual arousal. J Endocrinol 186:411-27.

165. Wilson JD. 2001. Androgens, androgen receptors, and male gender role behavior. Horm Behav 40:358-66.

166. Pike CJ, Rosario ER, Nguyen TV. 2006. Androgens, aging, and Alzheimer's disease. Endocrine 29:233-41.

167. Conejo NM, Gonzalez-Pardo H, Cimadevilla JM, Arguelles JA, Diaz F, Vallejo-Seco G, Arias JL. 2005. Influence of gonadal steroids on the glial fibrillary acidic protein-immunoreactive astrocyte population in young rat hippocampus. J Neurosci Res 79:488-94.

168. Mong JA, Glaser E, McCarthy MM. 1999. Gonadal steroids promote glial differentiation and alter neuronal morphology in the developing hypothalamus in a regionally specific manner. J Neurosci 19:1464-72.

169. Mong JA, McCarthy MM. 1999. Steroid-induced developmental plasticity in hypothalamic astrocytes: implications for synaptic patterning. J Neurobiol 40:602-19.

170. Denmeade SR, Lin XS, Isaacs JT. 1996. Role of programmed (apoptotic) cell death during the progression and therapy for prostate cancer. Prostate 28:251-65.

171. Agapova OA, Malone PE, Hernandez MR. 2006. A neuroactive steroid 5alpha-androstane-3alpha,17beta-diol regulates androgen receptor level in astrocytes. J Neurochem. 98:355-63.

172. Hosohata K, Li P, Hosohata Y, Qin J, Roeder RG, Wang Z. 2003. Purification and identification of a novel complex which is involved in androgen receptor-dependent transcription. Mol Cell Biol 23:7019-29.

173. Wang DS, Shaw R, Winkelmann JC, Shaw G. 1994. Binding of PH domains of beta-adrenergic receptor kinase and beta-spectrin to WD40/beta-transducin repeat containing regions of the beta-subunit of trimeric G-proteins. Biochem Biophys Res Commun. 30:29-35.

174. Friesen WJ, Wyce A, Paushkin S, Abel L, Rappsilber J, Mann M, Dreyfuss G. 2002. A novel WD repeat protein component of the methylosome binds Sm proteins. J Biol Chem 277:8243–8247.

175. Stallcup MR, Chen D, Koh SS, Ma H, Lee YH, Li H, Schurter BT, Aswad DW. 2000. Cooperation between protein-acetylating and protein-methylating coactivators in transcriptional activation. Biochem Soc Trans 28:415–418.

176. Friesen WJ, Paushkin S, Wyce A, Massenet S, Pesiridis GS, Van Duyne G, Rappsilber J, Mann M, Dreyfuss G. 2001. The methylosome, a 20S complex containing

JBP1 and pICln, produces dimethylarginine-modified Sm proteins. Mol Cell Biol 21:8289-300.

177. Meister G, Eggert C, Buhler D, Brahms H, Kambach C, Fischer U. 2001. Methylation of Sm proteins by a complex containing PRMT5 and the putative U snRNP assembly factor pICln. Curr Biol 11:1990-4.

178. Grimmler M, Bauer L, Nousiainen M, Körner R, Meister G, Fischer U. 2005. Phosphorylation regulates the activity of the SMN complex during assembly of spliceosomal U snRNPs. EMBO Rep. 6:70–76.

179. Zhou L, Wu H, Lee P, Wang Z. 2006. Roles of the androgen receptor cofactor p44 in the growth of prostate epithelial cells. J Mol Endocrinol 37:283-300.

180. Peng Y, Chen F, Melamed J, Chiriboga L, Wei J, Kong X, McLeod M, Li Y, Li CX, Feng A, Garabedian MJ, Wang Z, Roeder RG, Lee P. 2008. Distinct nuclear and cytoplasmic functions of androgen receptor cofactor p44 and association with androgen-independent prostate cancer. Proc Natl Acad Sci USA 105:5236-41.

181. Gao S, Wu H, Wang F, Wang Z. 2010. Altered differentiation and proliferation of prostate epithelium in mice lacking the androgen receptor cofactor p44/WDR77. Endocrinology. 15:3941-53.

182. Simanainen U; McNamara K; Gao YR; Handelsman DJ. 2009. Androgen sensitivity of prostate epithelium is enhanced by postnatal androgen receptor inactivation. Am J Physiol Endocrinol Metab 296:1335-43

183. Gu X; Li C; Wei W; Lo V; Gong S; Li SH; Iwasato T; Itohara S; Li XJ; Mody I; Heintz N; Yang XW. 2005. Pathological cell-cell interactions elicited by a neuropathogenic form of mutant Huntingtin contribute to cortical pathogenesis in HD mice. Neuron 46:433-44.

184. Tchaicha JH, Mobley AK, Hossain MG, Aldape KD, McCarty JH. 2010. A mosaic mouse model of astrocytoma identifies alphavbeta8 integrin as a negative regulator of tumor angiogenesis. Oncogene 5:4460-72.

185. Sonoda Y, Ozawa T, Hirose Y, Aldape KD, McMahon M, Berger MS, Pieper RO. 2001. Formation of intracranial tumors by genetically modified human astrocytes defines four pathways critical in the development of human anaplastic astrocytoma. Cancer Res 61:4956–4960.

186. Gao S, Lee P, Wang H, Gerald W, Adler M, Zhang L, Wang YF, Wang Z. 2005. The androgen receptor directly targets the cellular Fas/FasL-associated death domain protein-like inhibitory protein gene to promote the androgen-independent growth of prostate cancer cells. Mol Endocrinol 19:1792-802.

187. Yu X, Li P, Roeder RG, Wang Z. 2001. Inhibition of androgen receptor-mediated transcription by amino-terminal enhancer of split. Mol Cell Biol 21:4614-25.

188. Reynolds AR, Kyprianou N. 2006. Growth factor signaling in prostatic growth: significance in tumour development and therapeutic targeting. Br J Pharmacol 147 Suppl 2:S144-52.

189. Simanainen U, Allan CM, Lim P, McPherson S, Jimenez M, Zajac JD, Davey RA, Handelsman DJ. 2007. Disruption of prostate epithelial androgen receptor impedes prostate lobe-specific growth and function. Endocrinology 148(5):2264-72

190. Greenberg NM, DeMayo FJ, Sheppard PC, Barrios R, Lebovitz R, Finegold M, Angelopoulou R, Dodd JG, Duckworth ML, Rosen JM, Matusik RJ. 1994. The rat probasin gene promoter directs hormonally and developmentally regulated expression of a heterologous gene specifically to the prostate in transgenic mice. Mol Endocrinol 8:230-9.

191. Jin C, McKeehan K, Wang F. 2003. Transgenic mouse with high Cre recombinase activity in all prostate lobes, seminal vesicle, and ductus deferens. Prostate 57:160-4.

192. Calleja-Agius J, Muscat-Baron Y, Brincat MP. 2007. Skin ageing. Menopause Int 13:60-4.

193. Cesta MF. 2006. Normal structure, function, and histology of the spleen. Toxicol Pathol 34:455-65.

194. Haynes L, Maue AC. 2009. Effects of aging on T cell function. Curr Opin Immunol 21:414-7.

195. Pfister G, Savino W. 2008. Can the immune system still be efficient in the elderly? An immunological and immunoendocrine therapeutic perspective. Neuroimmunomodulation 15:351-64.

196. Thoman ML, Ernst DN, Hobbs MV, Weigle WO. 1993. T cell differentiation and functional maturation in aging mice. Adv Exp Med Biol 330:93-106.

197. Cheung HT, Nadakavukaren MJ. 1983. Age-dependent changes in the cellularity and ultrastructure of the spleen of Fischer F344 rats. Mech Ageing Dev 22:23–33.

198. González-Fernández A, Gilmore D, Milstein C. 1994. Age-related decrease in the proportion of germinal center B cells from mouse Peyer's patches is accompanied by an accumulation of somatic mutations in their immunoglobulin genes. Eur J Immunol 24:2918-21.

199. Wilson A, Marlow NE, Maddern GJ, Barraclough B, Collier NA, Dickinson IC, Fawcett J, Graham JC. 2010. Radical prostatectomy: a systematic review of the impact of hospital and surgeon volume on patient outcome. ANZ J Surg 80:24-9.

200. Humphrey PA, Andriole GL. 2010. Prostate cancer diagnosis. Mo Med. 107:107-12.

201. Soriano P. 1999. Generalized lacZ expression with the ROSA26 Cre reporter strain [letter]. Nat Genet 21:70-1.

202. Di Capua Sacoto C, Lujan Marco S, Morales Solchaga G, Budía Alba A, Pontones Moreno JL, Jiménez Cruz JF. 2009. [Cancer of the penis. Our experience in 15 years] Actas Urol Esp 33:143-8.

203. Bullen K, Matthews S, Edwards S, Marke V. 2009. Exploring men's experiences of penile cancer surgery to improve rehabilitation. Nurs Times 105:20-4.

204. Obuchowska I, Mariak Z, Sherkawey N. 2005. [Clinical indications for enucleation--a review of the literature] Klin Oczna 107:159-62.

205. Shields CL, Shields JA. 2010. Retinoblastoma management: advances in enucleation, intravenous chemoreduction, and intra-arterial chemotherapy. Curr Opin Ophthalmol 21:203-12.

206. Margalit E, Sadda SR. 2003. Retinal and optic nerve diseases. Artif Organs 27:963-74.

207. Brown-Borg HM. 2009. Hormonal control of aging in rodents: the somatotropic axis. Mol Cell Endocrinol 299:64-71.

208. Guérette D, Khan PA, Savard PE, Vincent M. 2007. Molecular evolution of type VI intermediate filament proteins. BMC Evol Biol 13:164.

209. Betz UA, Vosshenrich CA, Rajewsky K, Müller W. 1996. Bypass of lethality with mosaic mice generated by Cre-loxP-mediated recombination. Curr Biol 6:1307-16.

210. Bertini G, Colavito V, Tognoli C, Etet PF, Bentivoglio M. 2010. The aging brain, neuroinflammatory signaling and sleep-wake regulation. Ital J Anat Embryol 115:31-8.

211.Shankar SK. 2010. Biology of aging brain. Indian J Pathol Microbiol 53:595-604.

212. Gontier G, Holzenberger M. 2010. IGF and insulin signaling pathways in longevity. Biol Aujourdhui 204:243-250.

213. Douglas PM, Dillin A. 2010. Protein homeostasis and aging in neurodegeneration. J Cell Biol 190:719-29.

214. Kazantsev AG. Cellular pathways leading to neuronal dysfunction and degeneration. 2007. Drug News Perspect 20:501-9.

215. Lundström L, Elmquist A, Bartfai T, Langel U. 2005. Galanin and its receptors in neurological disorders. Neuromolecular Med 7:157-80.

216. Ziv I, Melamed E. 2010. Editorial: apoptosis in the aging brain. Apoptosis 15:1285-91.

217. Pollack M, Phaneuf S, Dirks A, Leeuwenburgh C. 2002. The role of apoptosis in the normal aging brain, skeletal muscle, and heart. Ann N Y Acad Sci 959:93-107.

218. Pike CJ, Nguyen TV, Ramsden M, Yao M, Murphy MP, Rosario ER. 2008. Androgen cell signaling pathways involved in neuroprotective actions. Horm Behav 53:693-705.

219. Nichols NR, Agolley D, Zieba M, Bye N. 2005. Glucocorticoid regulation of glial responses during hippocampal neurodegeneration and regeneration. Brain Res Rev 48:287-301.

220. Felszeghy K, Banisadr G, Rostène W, Nyakas C, Haour F. 2004. Dexamethasone downregulates chemokine receptor CXCR4 and exerts neuroprotection against hypoxia/ischemia-induced brain injury in neonatal rats. Neuroimmunomodulation 11:404-13.

221. Barreto G, Veiga S, Azcoitia I, Garcia-Segura LM, Garcia-Ovejero D. 2007. Testosterone decreases reactive astroglia and reactive microglia after brain injury in male rats: role of its metabolites, oestradiol and dihydrotestosterone. Eur J Neurosci 25:3039-46.

222. Nichols NR, Day JR, Laping NJ, Johnson SA, Finch CE. 1993. GFAP mRNA increases with age in rat and human brain. Neurobiol Aging 14:421-9.

223. Nichols NR. 1999. Glial responses to steroids as markers of brain aging. J Neurobiol 40:585-601.

224. Pike CJ, Rosario ER, Nguyen TV. 2006. Androgens, aging, and Alzheimer's disease. Endocrine 29:233-41.

225. Hirsch EC, Breidert T, Rousselet E, Hunot S, Hartmann A, Michel PP. 2003. The role of glial reaction and inflammation in Parkinson's disease. Ann N Y Acad Sci 991:214-28.

226. Hsiao HY, Chern Y. 2010. Targeting glial cells to elucidate the pathogenesis of Huntington's disease. Mol Neurobiol 41:248-55.

227. Nichols NR, Agolley D, Zieba M, Bye N. 2005. Glucocorticoid regulation of glial responses during hippocampal neurodegeneration and regeneration. Brain Res Rev 48:287-301.

228. Drummond ES, Harvey AR, Martins RN. 2009. Androgens and Alzheimer's disease. Curr Opin Endocrinol Diabetes Obes 16:254-9.

229. Cheng J, Uchida M, Zhang W, Grafe MR, Herson PS, Hurn PD. 2011. Role of salt-induced kinase 1 in androgen neuroprotection against cerebral ischemia. J Cereb Blood Flow Metab 31:339-50.

230. Granchi S, Brocchi S, Bonaccorsi L, Baldi E, Vinci MC, Forti G, Serio M, Maggi M. 2001. Endothelin-1 production by prostate cancer cell lines is up-regulated by factors involved in cancer progression and down-regulated by androgens. Prostate 49:267-77.

231. Howie HL, Katzenellenbogen RA, Galloway DA. 2009. Papillomavirus E6 proteins. Virology 384:324-34.

232. Wise-Draper TM, Wells SI. 2008. Papillomavirus E6 and E7 proteins and their cellular targets. Front Biosci 13:1003-17.

233. Wang Z, Yu R, Melmed S. 2001. Mice lacking pituitary tumor transforming gene show testicular and splenic hypoplasia, thymic hyperplasia, thrombocytopenia, aberrant cell cycle progression, and premature centromere division. Mol Endocrinol 15:1870-9.

234. Tarabykin V, Britanova O, Fradkov A, Voss A, Katz LS, Lukyanov S, Gruss P. 2000. Expression of PTTG and prc1 genes during telencephalic neurogenesis. Mech Dev 92:301-4.

235. Tfelt-Hansen J, Yano S, Bandyopadhyay S, Carroll R, Brown EM, Chattopadhyay N. 2004. Expression of pituitary tumor transforming gene (PTTG) and its binding protein in human astrocytes and astrocytoma cells: function and regulation of PTTG in U87 astrocytoma cells. Endocrinology 145:4222-31.

236. Xin DQ, Zhu XH, Lai YQ, You R, Na YQ, Guo YL, Mao ZB. 2005. Regulation of expression of pituitary tumor transforming gene 1 (PTTG1) by androgen in prostate cancer. Beijing Da Xue Xue Bao 37:638-40.

237. Perng MD, Wen SF, Gibbon T, Middeldorp J, Sluijs J, Hol EM, Quinlan RA. 2008. Glial fibrillary acidic protein filaments can tolerate the incorporation of assembly-compromised GFAP-delta, but with consequences for filament organization and alphaB-crystallin association. Mol Biol Cell 19:4521-33.

238. Garside H, Stevens A, Farrow S, Normand C, Houle B, Berry A, Maschera B, Ray D. 2004. Glucocorticoid ligands specify different interactions with NF-kappaB by allosteric effects on the glucocorticoid receptor DNA binding domain. J Biol Chem 279:50050-9.

239. Gibbs SM. 2003. Regulation of neuronal proliferation and differentiation by nitric oxide. Mol Neurobiol 27:107-20.

240. Erhardt JA, Pittman RN. 1998. p21WAF1 induces permanent growth arrest and enhances differentiation, but does not alter apoptosis in PC12 cells. Oncogene 16:443-51.

241. Tanaka A, Wakita U, Kambe N, Iwasaki T, Matsuda H. 2004. An autocrine function of nerve growth factor for cell cycle regulation of vascular endothelial cells. Biochem Biophys Res Commun 313:1009-14.

242. Ravitz MJ, Wenner CE. 1997. Cyclin-dependent kinase regulation during G1 phase and cell cycle regulation by TGF-beta. Adv Cancer Res 71:165-207.

243. Besson A, Dowdy SF, Roberts JM. 2008. CDK inhibitors: cell cycle regulators and beyond. Dev Cell 14:159-69.

244. Harper JW, Adami GR, Wei N, Keyomarsi K, Elledge SJ. 1993. The p21 Cdk-interacting protein Cip1 is a potent inhibitor of G1 cyclin-dependent kinases. Cell 75:805–16.

245. Deng C, Zhang P, Harper JW, Elledge SJ, Leder P. 1995. Mice lacking p21CIP1/WAF1 undergo normal development, but are defective in G1 checkpoint control. Cell. 25:675-84.

246. Zhu Z, Zhang Q, Yu Z, Zhang L, Tian D, Zhu S, Bu B, Xie M, Wang W. 2007. Inhibiting cell cycle progression reduces reactive astrogliosis initiated by scratch injury in vitro and by cerebral ischemia in vivo. Glia 55:546-58.

247. Di Giovanni S, Movsesyan V, Ahmed F, Cernak I, Schinelli S, Stoica B, Faden AI. 2005. Cell cycle inhibition provides neuroprotection and reduces glial proliferation and scar formation after traumatic brain injury. Proc Natl Acad Sci USA 102:8333-8.

248. Koguchi K, Nakatsuji Y, Okuno T, Sawada M, Sakoda S. 2003. Microglial cell cycle-associated proteins control microglial proliferation in vivo and in vitro and are regulated by GM-CSF and density-dependent inhibition. J Neurosci Res 74:898-905.

249. Teng FY, Tang BL. 2010. NF-kappaB signaling in neurite growth and neuronal survival. Rev Neurosci 21:299-313.

250. Barca O, Devesa-Peleteiro P, Seoane M, Señarís RM, Arce VM. 2010. Bimodal effect of interferon-β on astrocyte proliferation and survival: Importance of nuclear factor-κB. J Neuroimmunol 226:73-80.

251. Belvin MP, Anderson KV. 1996. A conserved signaling pathway: the Drosophila toll-dorsal pathway. Annu Rev Cell Dev Biol 12:393-416.

252. Kuprash DV, Udalova IA, Turetskaya RL, Kwiatkowski D, Rice NR, Nedospasov SA. 1999. Similarities and differences between human and murine TNF promoters in their response to lipopolysaccharide. J Immunol 62:4045-52.

## Vita

Bryce Harvird Vincent was born in Houston, Texas on May 12, 1979, the Son of Bruce Vincent and Pamela Vincent. After completing his work at Cliffwood School, Houston, Texas in 1998, he entered Schreiner University in Kerrville, Texas. He graduated with Maxima Cum Laude, receiving the degree of Bachelor of Science with a major in biochemistry from Schreiner in May, 2003. For the next two years, he worked as a research technician in the Department of Urology at Baylor College of Medicine. In August of 2005 he entered The University of Texas Health Science Center at Houston Graduate School of Biomedical Sciences. He joined the lab of Dr. Zhengxin Wang at the University of Texas MD Anderson Cancer Center in June, 2009, where he studied the role of androgen receptor cofactor p44/WDR77 in astrocyte activation.

.